Generation of gallbladder organoids to study the genotoxic effect mediated by *Salmonella* Paratyphi A

Inaugural-Dissertation

to obtain the academic degree

Doctor rerum naturalium (Dr. rer. nat.)

submitted to the Department of Biology, Chemistry and Pharmacy

of Freie Universität Berlin

by

LUDOVICO PASQUALE SEPE

From Rome

Berlin, 2017

"I have a bad feeling about this"

Han Solo

Parts of this work have been or will be published

Ludovico Pasquale Sepe, Amina Iftekhar, Hilmar Berger, Gurumurthy Rajendra Kumar, Sascha Chopra, Sven Christian Schmidt, Thomas F. Meyer, Francesco Boccellato. Genotoxic effect of Salmonella infection of human primary gall bladder cells (*in submission*)

The present work was carried out from July 2013 to July 2017 at the Max Planck Institute for Infection Biology in the Department of Molecular Biology under the supervision of Prof. Dr. Thomas F. Meyer.

1st Reviewer: Prof. Dr. Thomas F. Meyer

2nd Reviewer: Prof. Dr. Rudolf Tauber

Date of defense: 23.03.2018

Table of contents

1. ABSTRACT

Gall bladder carcinoma is a highly deadly disease due the difficulties in its diagnosis. Observational studies found a strong correlation between the development of gall bladder cancer and *Salmonella enterica* serovar Typhi/Paratyphi A chronic carriage. If fact the CdtB subunit of its secreted typhoid toxin has DNase enzymatic activity, and is translocated to the nucleus of the host cell where it might cause DNA damage and facilitate to malignant transformation.

Current studies on *Salmonella*-induced carcinogenesis largely relies on the use of already transformed or immortalized cell lines as *in vitro* models. However, such models are not the ideal tool for investigating the initial steps of carcinogenesis. Primary cells cultured with traditional methods, on the other hand, go promptly into senescence.

Recently, the "organoid" model has been developed. This primary cell model is preferable for approximating the *in vivo* situation since it allows long term propagation of stable epithelial primary cells originating from human and murine tissue. This method relies on the maintenance of adult stemness using long-term defined culture conditions allowing the formation of 3-D structures in an extracellular matrix.

In this study, I have successfully established a corresponding model from human and murine gall bladder primary cells. The adult stemness is maintained through activation of the Wnt/β-catenin pathway by its ligands Wnt and R-spondin. In parallel, I have identified Lgr5 as a stem cell marker of the adult gall bladder. The organoids recapitulate the tissue of origin in terms of protein markers and gall bladder functionality, and their phenotype is stable in time, having the capacity to self-renew.

I subsequently infected human gall bladder organoids with the human-restricted, gall bladder cancer-linked pathogen *Salmonella* Paratyphi A. The infection leads to genotoxicity, which extends to the neighboring uninfected cells. Surprisingly, cells intoxicated with the typhoid toxin fail to arrest their cell cycle, despite harboring DNA breaks.

Human gall bladder organoids represent an unprecedented tool to study tissue physiology and pathology. In addition, for the first time it is possible to infect the human epithelium of the gall bladder *in vitro* with human restricted *Salmonellae*, and elucidate the first events of cancer initiation and bacteria induced transformation.

ZUSAMMENFASSUNG

Das Gallenblasenkarzinom ist eine oft tödlich verlaufende Krankheit, und Hauptproblem dabei ist vor allem die schwierige Diagnostik. Beobachtungsstudien ergaben eine hohe Korrelation zwischen dem Auftreten von Gallenblasenkrebs und chronischen Infektionen der Gallenblase mit Salmonellen (S. enterica Typhi bzw. S. Paratyphi A). Die CdtB-Untereinheit des von den Erregern sezernierten Typhustoxins besitzt DNase-Enzymaktivität und wird in den Kern von Wirtszelle transloziert; sie könnte dort DNA-Schäden verursachen und so die maligne Transformation begünstigen. Aktuelle Studien zur Salmonella-induzierten Karzinogenese berufen sich weitgehend auf der Verwendung bereits transformierter oder immortalisierter Zelllinien in Form von in-vitro-Modellen. Solche Modelle sind jedoch kein ideales Instrument, um den Beginn einer Karzinogenese zu untersuchen. Andererseits gestalteten sich Versuche mit Primärzellen, die mit traditionellen Methoden kultiviert wurden, bisher als schwierig, da die Zellen rasch in ein Stadium der Seneszenz übergehen.

Kürzlich wurde das so genannte "Organoid"-Modell entwickelt. Dieses Primärzellmodell ermöglicht die langfristige Vermehrung stabiler epithelialer primärer Zellen sowohl aus menschlichem als auch aus murinem Gewebe und bildet daher der in-vivo-Situation angenäherte Bedingungen. Die Methode beruht auf der Erhaltung adulter Stammzellen in der Kultur mittels bestimmter Morphogene und einer definierten extrazellulären Matrix, die die Ausbildung von 3-D-Strukturen, den Organoiden, fördert. Im Rahmen meines Dissertationsprojektes gelang es mir, ein entsprechendes Modell aus menschlichen und murinen Gallenblasenprimärzellen zu etablieren. Adulte Stammzellen werden dabei mittels Aktivierung des Wnt / β-Catenin-Signalweges in Gegenwart von Wnt und R-Spondin Liganden erhalten. In diesem Zusammenhang gelang es mir auch, Lgr5 als Stammzellmarker der adulten Gallenblase zu identifizieren. Die Organoide entsprechen dem Ursprungsgewebe hinsichtlich Proteinmarker und Gallenblasenfunktionalität; ihr Phänotyp ist zeitlich stabil und sie besitzen die Fähigkeit zur Selbsterneuerung.

Auf dieser Grundlage konnte ich menschliche Gallenblasen-Organoide mit einem humanspezifischen Salmonella-Paratyphi-A-Erregerstamm erfolgreich infizieren. Die Infektion rief deutliche Anzeichen einer Genotoxizität hervor, die sich auch auf benachbarte, nicht infizierte Zellen erstreckte. Überraschenderweise vermag das von den Erregern gebildete Typhustoxin nicht, den Zellzyklus infizierter Zellen zu stoppen, obgleich diese DNA-Brüche aufweisen.

Ein zentrales Ergebnis der vorliegenden Studie ist die Etablierung von Gallenblasenorganoiden, mittels derer die Gewebephysiologie und Pathologie untersucht werden kann. Darüber hinaus ist es mit meiner Arbeit erstmals gelungen, menschliches Epithel der Gallenblase in vitro mit humanspezifischen Salmonellen zu infizieren und so die frühen Stadien einer möglichen Bakterien-induzierten Transformation und Krebsentstehung zu erforschen..

2. INTRODUCTION

2.1 Gall bladder structure and function

The gall bladder is a hollow, blind organ situated in the abdomen between the hepatic lobes. Its function is to store and concentrate the bile, which is either produced by the liver or recycled through the enterohepatic circulation. The histological layers consists of a mucosa, a lamina propria, a single layer of innervated smooth muscle and a serosa layer (Behar 2013). The gall bladder is divided between fundus, corpus and neck. From the neck the cystic duct protrudes, which joins first the hepatic duct and then the pancreatic duct as the common bile duct. Both the cystic and the common bile duct are passive, having no peristaltic motility. At the end of the common bile duct the sphincter of Oddi penetrates the duodenal wall forming the Ampulla of Vater (Figure I - 1).

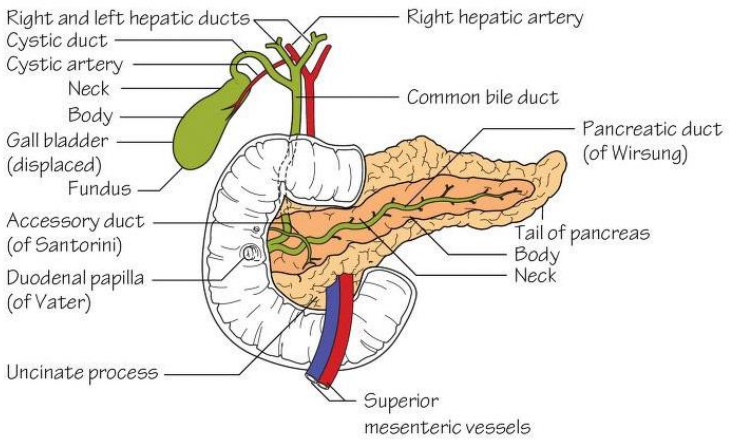

Figure I - 1 Schematic anatomy of the gall bladder and biliary tract (Faiz & Moffat 2002)

The physiological roles of the gall bladder are strictly connected with the digestive phases and regulated by neurohormonal mechanisms. The bile is continuously produced by the liver, absorbed into the intrahepatic ducts, then passively flows into the larger extrahepatic bile ducts. During the fasting phase the sphincter of Oddi helps the filling of the gall bladder, where the bile is stored and concentrated. During this period small contractions of the gall bladder avoid the precipitation of bile insoluble components (Behar et al. 1989). The strong shrinkage

of the gall bladder, however, happens during the digestive phase, when nervous and hormonal stimuli induce the contraction of the muscular layer. This leads to the release of the bile in the duodenum, where it helps the digestion of fats.

The absorptive functions of the gall bladder associated with the concentration of bile components (Pstrpw 1967; Nakanuma et al. 1997), are due to transmembrane channel proteins situated on epithelial cells. Different transport proteins exist for different molecules, for example BSEP is involved in the transport of bile acids, cMOAT/mrp2 transports non-bile acid organic anions, MDR1 hydrophobic organic cations, and MDR2 phosphatidylcholine (Gigliozzi et al. 2000; Scoazec et al. 1997; Müller & Jansen 1997). By the concomitant absorption of bile components the lumen and active secretion of water through its walls (Wood & Svanvik 1983), the gall bladder is able to reduce the volume of retained bile by 80-90% (Frizzell & Heintze 1980). As a result of it the biliary epithelium is continually exposed to a high concentrations of potentially toxic organic ions like hydrophobic organic cations. The gallbladder, however, is protected by the ATP-dependent multidrug transporter MDR1 that transports the organic cations back in the lumen (Gigliozzi et al. 2000; Pstrpw 1967; Scoazec et al. 1997)

From the cytological point of view the luminal portion of the gall bladder mucosa is constituted by a simple columnar-epithelial layer of cells, expressing high amount of keratins, in particular Cytoketatin-19 (Kuver et al. 2007), and mucins, one of the most abundant being Muc5B (Kampf et al. 2014; van Klinken et al. 1998).

The polarization of the gall bladder is ensured by tight junction proteins facing the luminal side. The most interesting one is Claudin-2, because it is highly expressed in the gall bladder epithelial cells even when compared to the highly related cholangiocytes, the epithelial cells of the bile ducts (Németh et al. 2009).

The most common pathology of the gall bladder is cholelithiasis, *i.e.* presence of gall stones, which affects an alarming 10-20% of the total European and North American population (Pak & Lindseth 2016; Stinton & Shaffer 2012). Historically gall stones were thought to form because of metabolic defects in the liver, recently, however, a crucial role of the gall bladder was highlighted. Gall bladder motility and its absorptive functions influence the formation of gall stones (Chen et al. 2015), which also represent the major risk factor for the development of gall bladder cancer (Ryu et al. 2016).

2.2 Gallbladder cancer epidemiology and risk factors

2.2.1 General risk factors

Gall bladder cancer (GBC) is a highly concerning disease due to its difficulty in diagnosis. Being the early stages asymptomatic, the tumor is found either incidentally during cholecystectomy (Basak et al. 2016), or when it is already beyond the limit of resection (Zhu et al. 2010). This results in very poor prognosis (Kanthan et al. 2015). 98% of GBCs are adenocarcinomas of epithelial origin (Kanthan et al. 2015).

Despite being the most common carcinoma of the biliary tract (Wistuba & Gazdar 2004), GBC is relatively uncommon in western countries, with an incidence of <2 in 100000, with the exception of eastern Europe: in this region the mortality peaked in Czech Republic, according to a 2013 report, touching 7.3/100000 (Ferlay et al. 2013). GBC reaches a relatively high incidence in certain regions of the world, namely south-west America and the Indian subcontinent (Randi et al. 2006). Among Chilean women GBC was found to be the deadliest carcinoma, surpassing breast, gastric, cervical and lung cancer (Andia et al. 2008). The highest incidence, however, was found in New Delhi, where 21.5 women in 100000 were found to be affected (Randi et al. 2006).

In addition to the geographical variation, strong differences in incidence are found within populations, the most consistent is that women are regularly found to be more susceptible: the female-to-male ratios is usually around 3, but reaches an alarming 5 in Colombia (Randi et al. 2006). In fact GBC is one of the few cancers whose incidence is higher in women than in men (Lowenfels & Maisonneuve 1999).

Certain ethnic groups seem also to have higher susceptibility, for example in Mexico having mixed ancestry was found to be a major risk factor (Strom et al. 1995). In the USA cancer incidence and death rates are higher among American and Alaskan natives (Henley et al., 2015).

A high body mass index (BMI) also correlates with GBC, with women with a BMI of more than 30 being at higher risk (Tan et al. 2015), as well as smoking, most probably because the bile is the main route of excretion of the carcinogens of tobacco smoke (Zatonskí et al. 1993).

The major risk factor for the development of GBC however is the presence of gall stones, cholelithiasis, which increases up to 10 fold the risk of developing the tumour (Caygill & Hill 2000; Pilgrim et al. 2013). GBC associates almost always with gall stones, up to 95% of the times in certain studies (Lazcano-Ponce et al. 2001), and cholelithiasis, like GBC, affects mostly women. In addition, some studies also suggest a link between the size and number of the stones and the risk of developing GBC (Vitetta et al., 2000), even though this association is not definite (Randi et al. 2006). Gall stones might interfere with the normal function of the gall bladder resulting in bile stasis, and, together with the continuous mechanical abrasion of the gallbladder mucosa, might induce irritation and chronic inflammation: a medical condition known as cholecystitis (discussed in section 2.4.2).

It is worth to mention that in Japan and Korea, a congenital abnormality in the development of the biliary tract can be found, the Anomalous Pancreaticobiliary Ductal Junction (APDJ) (Kimura et al. 1985). Due to this condition the pancreatic secretions regurgitate in the gall bladder, eventually causing malignant transformation. An alarming 8% to 13% (Stinton et al., 2012) of affected people will develop GBC, making this the predominant risk factor that overshadows the previously described ones: in presence of APDJ the increased risk represented by gallstones is not any more relevant, and even the gender bias disappears.

The most interesting aspect of GBC is, however, its correlation with certain bacterial infection.

2.2.2 Gallbladder cancer and non-*Salmonella* infections

Epidemiological studies frequently observed the presence of certain bacteria in connection with GBC. Beside the strong link with *Salmonella* chronic carriage, which will be discussed in detail later (section 2.2.3), some studies found bacteria of the *Helicobacter* genus in the cancerous tissue. Two studies that focused on Japanese and Thai population found *Helicobacter bilis* infection to correlate with GBC (Matsukura et al. 2002; Murata et al. 2004), and others even reported the presence of *Helicobacter pylori* DNA in the bile of diseased individuals, even though there is no final evidence of *H. pylori* colonization of the human biliary tract (Zhou et al. 2013). The most curious association comes from a study ran in Kathmandu, Nepal, where Pradhan and colleagues found that a surprising 87,5% of gallbladder neoplasms

were positive for *Helicobacter hepaticus* (Pradhan & Dali 2004). The same association was then observed by another group in Japan (Shimoyama et al. 2010).

The presence of *Helicobacter hepaticus* in the diseased gall bladder is most interesting because normally this bacterium only infects mice and it is used as a model of bacteria-induced carcinogenesis. Depending on the genetic background of the mouse the animal will develop cancer in different organs: mice knockout of Rag2 develop colitis leading to colorectal cancer (Fox et al. 2011), while in A/JCr strains *H. hepaticus* causes chronic infection of bile canaliculi that progresses to hepatitis and eventually to hepatocellular neoplasm (Ward et al. 1994).

It is worth to point out that the mentioned *H. bilis* and *H. hepaticus* have a commonality with *Salmonella* that will be discussed in section 2.6: the presence of a genotoxin which in *Helicobacter* is called the cytolethal distending toxin (CDT), and in *Salmonella* the typhoid toxin.

2.2.3 Gallbladder cancer and its link with *Salmonella* chronic carriage

The strongest evidences pointing to a link between a bacterial infection and the development of GBC come from epidemiological studies on chronic carriage of *Salmonella enterica* serovar Typhi / Paratyphi A. Even though initial clues were already suggesting a connection between *Salmonella* chronic carriage and the development of GBC (Welton et al. 1979; Mellemgaard & Gaarslev 1988; el-Zayadi et al. 1991), it was not until 1994 that a cohort study was published, which investigated the 1964 outbreak of *Salmonella enterica* serovar Typhi / Paratyphi A in the Scottish city of Aberdeen (Caygill et al. 1994). The outbreak was traced to contaminated sliced corned beef originating in South America (Brodie et al. 1970). The cohort nature of the study provided a temporal and possibly causal connection between chronic carriage and development of the tumour. It found an excess risk of 167 for the carriers to develop GBC; this result derives from the ratio observed/expected cases, but because the number of expected cases is extremely small, any additional observed case would lead to a high increase in the ratio, therefore the authors comment that they would not take 167 as the real increased risk.

Only one year after this pioneer study, an international case control study ran in Bolivia and Mexico found a similar result, showing that people with a history of typhoid diagnosis had a stunning odds ratio of 12 of developing GBC (Strom et al. 1995).

In the following years a number of observational studies, mostly case control studies, confirmed the connection between *Salmonella* Typhi / Paratyphi A chronic carriage and GBC, the link being particularly strong in geographic areas where typhoid infection is more likely to occur, like the Indian subcontinent (Nagaraja & Eslick 2014; Koshiol et al. 2016). In their meta-analysis Randi and colleagues (Randi et al. 2006) calculated the increased risk of developing GBC given the carrier status to be 5, which impressively reached 10 when self-reported diagnoses of infection were excluded.

2.3 *Salmonella* Typhi and Paratyphi A chronic carriage

2.3.1 General considerations

Clinically, a *Salmonella* chronic carrier is defined as an asymptomatic patient that intermittently sheds *Salmonella* in the feces, and has not developed symptoms of typhoid fever within the preceding year. These patients who did not completely clear the infection comprise 1-5% of the total infected individuals. The most famous case of chronic carriage is that of “Typhoid Mary”, a cook of New York, to whom are attributed around 1300 cases of infection between 1900 and 1914 (Caygill & Hill 2000) (Figure I - 2).

Because chronic carriers do not show any symptom of disease their diagnosis is rather difficult, but of central importance when struggling to decrease the burden of *Salmonella* in a certain region (Saul et al. 2013; Carvajal-Restrepo et al. 2017). Furthermore, because humans are the only hosts for *Salmonella* Typhi/Paratyphi A, carriers might represent the reservoir and the breeding ground by which new strains evolve (Roumagnac et al. 2006).

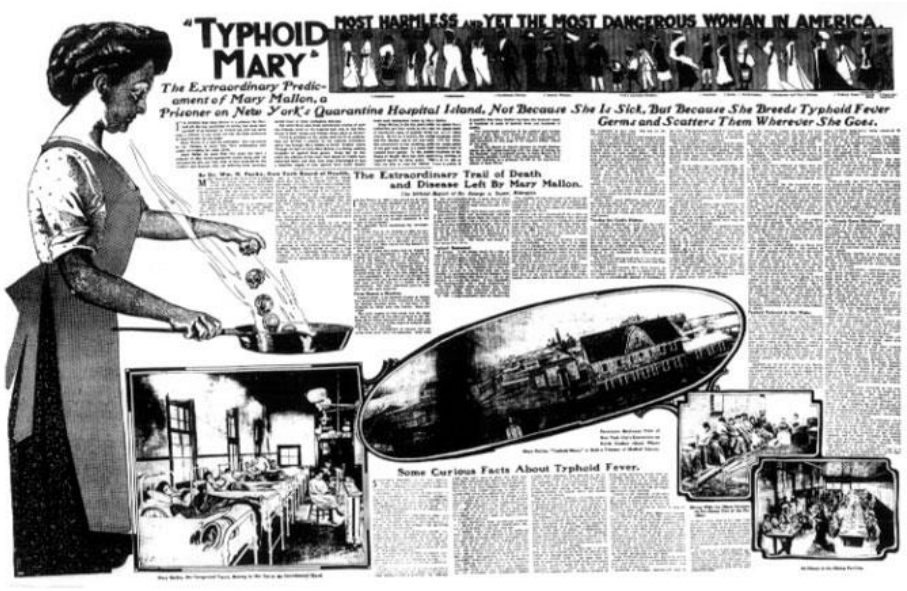

Figure I - 2 Page of the New York American which identified Mary Mallon as Typhoid Mary. The stigmatization of the cook is evident, the author referring to her as the "most harmless yet the most dangerous woman in America". It also due to media coverage that, for the sake of public health, she was quarantined on North Brother Island (New York American, June 20, 1909)

2.3.2 *Salmonella* Invasion of the gall bladder

In chronic carriers *Salmonella* resides in the gall bladder. It can reach the organ from an ascending or descending route. In the first case the bacteria would pass from the small intestine to the bile ducts in case of a malfunction of the sphincter of Oddi. They would then ascend to the lumen of the gall bladder. The more likely way to reach the gall bladder is, however, the descending route. After penetration of the intestinal epithelial barrier, the bacterium can invade immune cells (see section 2.4.2). From there, "hidden" in leukocytes to avoid immune detection, it disseminates via the blood stream in the spleen, bone marrow, and liver, which is in close contact with the gall bladder. Kupfer cells in the liver normally prevent toxic metabolites and bacteria from penetrating in intrahepatic ducts, but in case of failure *Salmonella* would easily pass in the biliary system and reach the gall bladder (Gunn et al. 2014).

In the gall bladder *Salmonella* is able to form robust biofilm on gallstones, therefore persisting extracellularly, however it is also able to invade epithelial cells (Gonzalez-Escobedo & Gunn 2013). Bacteria replicate in epithelial cells until eventually those infected cells extrude from the monolayer releasing *Salmonella* in the lumen of the gall bladder. The flow of bile can then

transport the bacterium in the gastrointestinal tract, which leads to re-infection of the gut and shedding in feces (Knodler et al. 2010).

2.3.3 Detection of chronic carriers

The clinical detection of chronic carriers is problematic, given the fact that the patients are asymptomatic and do not continuously shed the bacteria in the feces. Moreover 25% of them do not recall a history of typhoid (Gunn et al. 2014). In case of a suspect, the traditional approach is periodical cultures of *Salmonella* from the stools; the limitations are evident, especially in the impossibility to run population studies. The gold standard for clinical detection is the cultivation of *Salmonella* or PCR of *Salmonella* specific genes from bile, gallstones or gall bladder mucosa form patients that underwent cholecystectomy, but also this approach has very limited public health utility (Gunn et al. 2014).

Serological markers exist that are supposed to discriminate between carriers and people with a history of infection: in 1938 Arthur Felix demonstrated that antibodies against the Vi antigen disappeared from patients that eradicated the infection, but persisted in chronic carriers (Felix 1938). This method however is not very sensitive and might fail in detecting the chronic infection, like it happened in 1967 when it did not detect the carrier state of a 65 year old housewife from Edinburg. It was later discovered that the woman has been infected 31 years before from the husband who got typhoid in Poland (Sharp 1967). The main limitation with the use of anti-Vi antibodies for the detection of carriers, however, is in geographical areas which are endemic for *Salmonella*. A lesson from Vietnam (Gupta et al. 2006) thought us that in these settings elevated levels of anti-Vi antibodies remain even in the non-infected, non-carrier individuals with a history of infection.

New techniques to detect the asymptomatic carriers rely on the detection of immunogenic antigens expressed by *Salmonella* only during chronic infection. One of those is YncE, an uncharacterized protein with ATP and DNA-binding domains: antibodies anti YncE are found neither in acutely infected individuals nor in convalescent patients nor in healthy individuals living in endemic regions, but only in chronic carriers (Charles et al. 2013). Other research approaches are trying to find unique biomarkers other than antibodies in the blood of chronic carriers (Thompson et al. 2009; Kumar et al. 2014)

2.4.4 Treatment of chronic carriage

In terms of treatment the prolonged use of antibiotics, a standard treatment of the past, proved to be not fully efficient, and therefore is not any more recommended. This is due to the rapid emergence of multi drug resistant pathogens (resistant to ampicillin, chloramphenicol, and trimethoprim), even in Western countries (Dave et al. 2017), and to the fact that biofilm protects bacteria from the delivery of the antibiotics (Costerton et al. 1999).

Surgical removal of the gall bladder (cholecystectomy) in concomitance with antibiotic treatment is the gold standard, however sometimes it proved not to be sufficient to clear the carrier state because *Salmonella* might still persist in the biliary tree, in the liver or even in mesenteric lymph nodes (Nath et al. 2011).

2.4.5 Trends in Paratyphoid carriage

In a recent paper (Dobinson et al. 2017) Dobinson and colleagues infected human voluntaries via oral challenge with *Salmonella* Typhi or Paratyphi A, and found out that infection with the latter resulted in bacteremia (the presence of bacteria in the blood), but with limited to no clinical symptoms compared to the patients infected with Typhi.

Considering the relative mild symptoms that precede the onset of paratyphoid carriage, it is not unreasonable to speculate an increase in *Salmonella* Paratyphi chronic carriers in the near future, and possibly of GBC cases, also considering the epidemiology of the disease. Worldwide the incidence rate of paratyphoid is about 25% of the rate estimated for typhoid (Crump et al. 2004), however the burden of Paratyphi A-caused enteric fever is increasing in a number of Asian countries (Crump & Mintz 2010), in certain region accounting for 50% of all the *Salmonella*e isolated from the bloodstream, like in Nepal (Woods et al. 2006) and India (Chandel et al. 2000), a region which has also one of the highest incidence rates of GBC.

2.4 *Salmonella* acute infection

2.4.1 From ingestion to the gastrointestinal tract

Salmonella enterica related infections are supposed to cause 91 million cases of illness each year, which severity varies from asymptomatic carriage to life-threatening typhoid fever. In most of the cases however the outcome of infection is self-limiting gastroenteritis, which is mainly caused by non-typhoidal *Salmonella*e (NTS). The human restricted serovars, *Salmonella* Typhi and Paratyphi A, so called typhoidal *Salmonella*e (TS), can cause typhoid fever and paratyphoid fever respectively (Crump et al. 2004). Without treatment, the mortality of typhoid fever reaches 20% (Parry et al. 2002).

After ingestion of contaminated food, *Salmonella* passes the low pH of the stomach (Foster & Hall 1991) and colonizes the mucosa of the gastrointestinal tract. NTS express typical pathogen associated molecular patterns (PAMPs) like flagellin and lipopolysaccharide (LPS), that readily activate the immune response resulting in neutrophil recruitment and production of reactive nitrogen (RNS) and oxygen species (ROS). This leads to an efficient depletion of the pathogens at an early stage (Figure I - 3). Exception to this rule exist if NTS infects an immunocompromised individual: in certain African countries invasive NTS was observed in HIV positive patients (Gordon 2008).

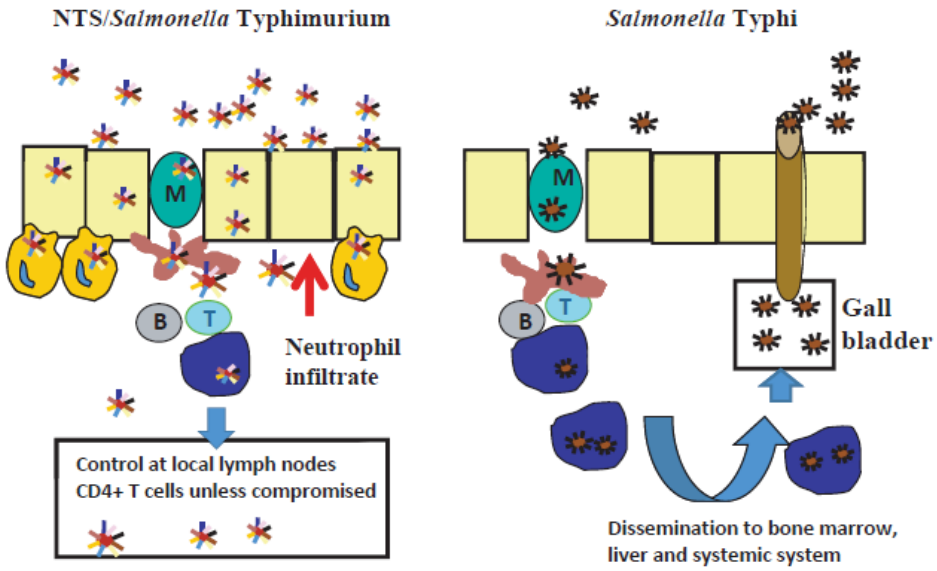

Figure I - 3 Route of infection of *Salmonella* Typhimurium and Typhi. The rectangular yellow cells is the epithelium of the gut (Dougan et al. 2011).

2.4.2 Penetration of the intestinal epithelial barrier

In the small intestine *Salmonella* invades the microfold cells (M cells) of the Payer´s patch, which normally deliver the antigens to the antigen presenting cells, and initiates mucosal immunity. In addition, *Salmonella* is able to infect enterocytes (Jepson & Clark 2001). Another way by which *Salmonella* can invade and penetrate the epithelial barrier is from the basolateral side, through disruption of the tight junctions, compromising its integrity and leading to increased permeability (Guttman & Finlay 2009). This results in the clinical symptoms of diarrhea (Förster 2008). *Salmonella* can also be uptaken directly from dendridic cells that extend their dendrites through the epithelium (Gayet et al. 2017).

Whatever the way, once *Salmonella* Typhi penetrates the epithelial barrier, is taken up by lymphoid cells like dendritic cells and macrophages of the lamina propria, remaining relatively undetected (Figure I - 3 right panel). It is interesting to note that *Salmonella* appears to kill efficiently macrophages, but it promotes the survival of infected epithelial cells inhibiting or delaying their apoptosis (Knodler et al. 2005; Wu et al. 2012).

One of the strategies by which *Salmonella* Typhi can elude immune detection (Keestra-Gounder et al. 2015) is through its Vi capsule, which prevents Toll-like receptor-4 (TLR-4) recognition (Wilson et al. 2008). In NTS, which lack the Vi antigen, bacterial components like DNA, LPS and flagella, can activate the TRLs of the host cells, resulting in a strong inflammatory response characterized by the production of various cytokines including TNF-α, INF-γ, IL-1, IL-6, IL-12, IL-18, and chemoattractors. *Salmonella* can also escape adaptive immunity by establishing itself in the epithelial cells delaying their apoptosis (Wu et al. 2012). It is also worth to mention the role of defensins: the growth of *Salmonella* is inhibited by defensins *in vivo* (Salzman et al. 2003) and *in vitro* (Wilson et al. 2014; Maiti et al. 2014).

2.5 Molecular events during invasion of *Salmonella* and its virulence factors

2.5.1 Early events: invasion and generation of SCV

In order to attach, invade host cells, disseminate and escape immune detection, *Salmonella* relies on a number of virulence factors located on the five *Salmonella* pathogenicity islands (SPI), on plasmids, or disseminated in the chromosome, like flagella, adhesins and biofilm genes. It has to be noted that most of the studies on *Salmonella* virulence factors are carried on serovar Typhimurium, a NTS which infects mice.

The initial adhesion to the host cell triggers cytoskeletal rearrangements in order to take up the bacteria into the *Salmonella* containing vacuoles (SCV). These initial invasion events are mediated by effector proteins injected in the cytoplasm of the host cell by the type III secretion system 1 (T3SS1) encoded by the *Salmonella* pathogenicity island 1 (SPI-I). Once internalized most of, but not all of, the processes, like intracellular survival and SCV biogenesis, are mediated from the type III secretion system 2 (T3SS2), encoded by the *Salmonella* pathogenicity island 2 (SPI-II) (Steele-Mortimer 2008).

Both the T3SS1 and 2 have a similar structure, comprising a basal body which extends from the inner to the outer membrane passing through the periplasm, a needle-like structure that protrudes in the extracellular space, and a translocon that effectively translocates the effector proteins in the cytosol of the host cell by forming a pore in the membrane (Ramos-Morales 2012).

Some of the T3SS1 effectors that regulate the biogenesis of SCV during the initial part of invasion are SopB, SptP and SipA (Figure I - 4). SopB ensures “to reduce the rigidity of the membrane skeleton, and to induce plasmalemmal invagination and fission”, inducing the formation of the so called membrane ruffling that help the uptake of the bacterium (Terebiznik et al. 2002). Once the bacterium is internalized, SptP reverses the actin remodeling to its original state (Fu & Galán 1999). SipA plays a role in the redistribution of the endosomes, and interacts with T3SS2 effectors, proving that an overlap exists between the expression of the two secretion systems (Brawn et al. 2007).

Early after the internalization of the bacterium, <30min p.i. (post infection), the SCV is found to be enriched of early endosome markers like SCVEEA1, Rab5 and transferrin receptor

(Steele-Mortimer et al. 1999). Those are then replaced by late lysosomal/endosomal markers (30min – 5hours p.i.), notably LAMPs, the pH drops lower than 4,5 and the SCV migrates in perinuclear position (Steele-Mortimer 2008) hijacking the microtubules motor protein kinesin and dynein (Ramsden, Holden, et al. 2007).

Phagocytes, like macrophages and dendritic cells, are able to phagocyte the bacterium by uptake into the phagosome. Its lumen rapidly acidifies and fuses with the lysosome which is filled with enzymes and anti-bacterial-proteins that help killing the bacterium (Blander & Medzhitov 2006).

Depending on the type of internalization, whether it is invasion or phagocytosis, the SCV markers and the acidification process can vary. *Salmonella* avoids the antimicrobial effects of the lysosome, even by avoiding the fusion with the lysosome altogether, or by suppressing its enzymatic effectors (Drecktrah et al. 2006).

2.5.2 Late events: formation of Sifs and intracellular replication

After the initial, events bacteria start to replicate and to form tubular irradiation from the SCV, the so-called *Salmonella* induced filaments (Sifs). These events, like the movement to the perinuclear position, cytoskeletal rearrangement and extension of Sifs, are mediated through the T3SS2 secreted proteins. SseG and SseF for example are important for redirecting exocytotic cargo vesicles from the Golgi to the SCV (Ramsden, Holden, et al. 2007; Kuhle et al. 2006), and for the maintenance of the SCV in the perinuclear position (Ramsden, Mota, et al. 2007). SifA, as the name might suggest, is important for Sif formation and it is balance by SseJ, which disrupts the Sifs (Ruiz-Albert et al. 2002). During these late events the host F-actin reorganizes itself in order to keep the stability of the SCV, an event known as the vacuole-associated actin polymerizations (Méresse et al. 2001). (Figure I - 4).

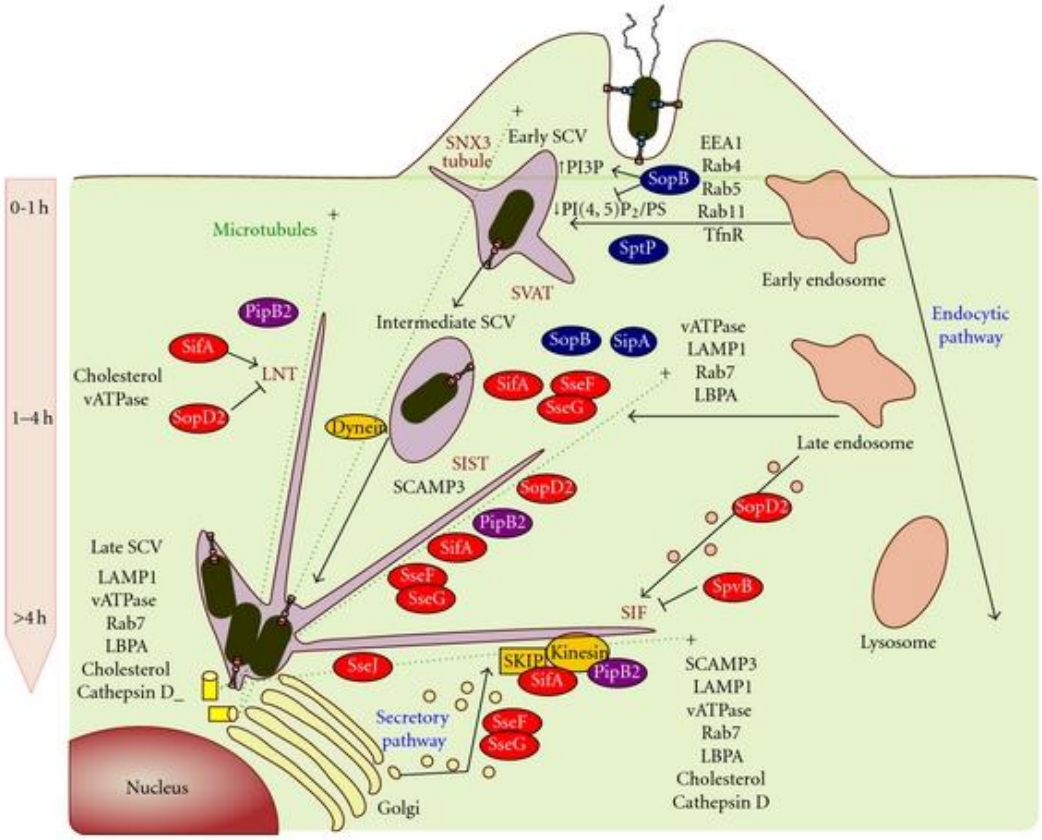

Figure I - 4 virulence factors involved in the biogenesis and maintenance of the SCV. T3SS1 effectors in blue, T3SS2 effectors in red, effectors of both the systems in purple, host proteins in orange (Ramos-Morales 2012)

2.5.3 *Salmonella* influence on the host apoptosis

One of the ways to clear the infection of the epithelial cells is for the host to activate programmed cell death: apoptosis. The release of infected dead cells, however, also results in the eventual dissemination of the bacteria (Fàbrega & Vila 2013).

SpvB and SlrP may trigger actin depolymerization as well as caspase-3 dependent apoptosis (Fink & Cookson 2007; Kurita et al. 2003). On the other hand other *Salmonella* mechanisms exist that delay or even suppress apoptosis. SigD activates Akt, a known oncogene with pro-proliferative and anti-apoptotic functions (Steele-Mortimer et al. 2000; Roppenser et al. 2013). AvrA, a T3SS1 effector, inhibits Jun N-terminal protein kinase (JNK), a host regulator of apoptosis (Jones et al. 2008). Flagellin is recognized by TLR5, which activates NFkB. This leads to a pro-inflammatory as well as anti-apoptotic signals (Vijay-Kumar et al. 2006).

For the sake of this thesis, however, I will mostly focus on another virulence factor, which might be indeed responsible for malignant transformation: the typhoid toxin and its active subunit CdtB.

2.6 The typhoid toxin

2.6.1 Genetic locus

In 2004 a genetic island of *Salmonella* Typhi was discovered which contained a homolog to *cdtB*, a gene encoding the active subunit of the cytolethal distending toxin (CDT) (Haghjoo & Galán 2004; Spanò et al. 2008). CDT is expressed by certain Gram-negative bacteria including *Escherichia coli* strains, *Campylobacter jejuni* and *Helicobacter hepaticus*. CDT is an AB_2 toxin: it is composed by an active subunit (A) and by two binding subunits (B) that help its delivery. The A subunit is called cdtB, and is a DNase delivered to the host cell, while the structural B subunits are called cdtA and cdtC, and function as shuttles. All the subunits of CDT are encoded by the same operon (Guerra et al. 2011).

In the genome of *Salmonella* Typhi / Paratyphi A the evolution, which never ceases to amaze us, led to the merge of two toxins, CDT and the pertussis toxin, to form the "chimeric" typhoid toxin. The typhoid toxin is an A_2B_5 toxin. The A subunits are cdtB and pltA, the latter being a homologue to the pertussis toxin (thus its name, pertussis-like toxin A). The B subunits form a homopentamer of the pertussis-like toxin B, pltB. The typhoid toxin lacks completely cdtA and cdtC (Figure I -5).

The typhoid toxin is found in human-restricted *Salmonella*e, Typhi and Paratyphi A, but is absent in most of the NTS, like the laboratory standard *Salmonella* Typhimurium. It can be detected in some strains belonging to the *bongori* species and the *arizonae* and *diarizonae* supspecies, which infect cold blooded hosts (Suez et al. 2013).

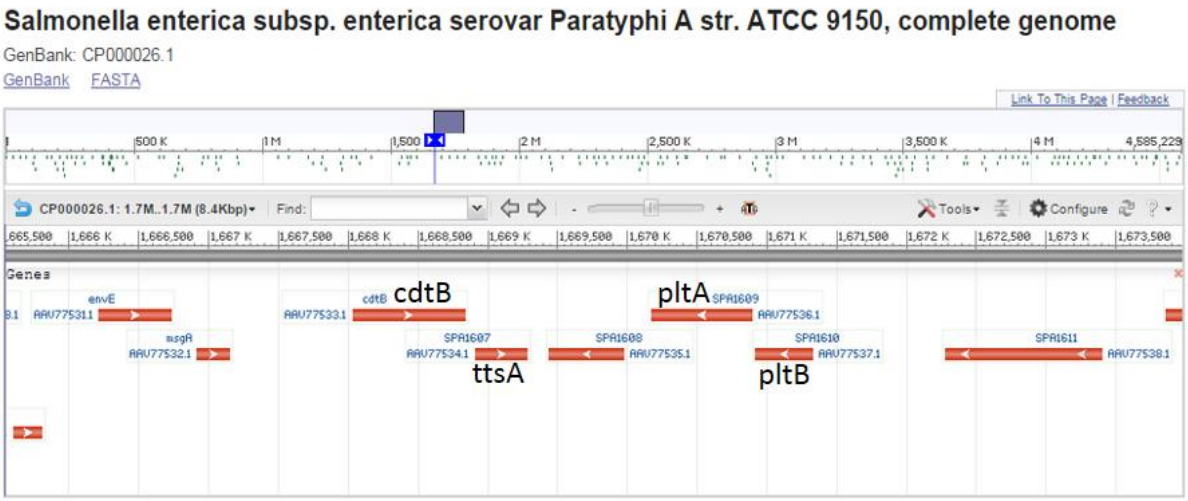

Figure I - 5 The typhoid toxin genetic locus of *Salmonella* Paratyphi A. It consists of cdtB, an operon encoding pltA (SPA1609) and pltB (SPA1610), ttsA (SPA1607) and sty1887 (SPA1608). The picture is taken from NCBI (www.ncbi.nlm.nih.gov)

2.6.2 Structure

The structure of the toxin was resolved in 2013. It appeared as a pyramidal A_2B_5 toxin, with a base of PltB pentamer, connected to one PltA subunit, and CdtB at the vertex. The α-helix at the C-terminal of PltA inserts itself in the hydrophobic pocket formed by the PltB pentamer. CdtB is anchored to PltA by a single disulfide bond between Cys269 of CdtB and Cys214 of PltA (Song et al. 2013) (Figure I - 6).

The same study which first resolved the structure of the typhoid toxin, also detected putative receptors on the host cell. It was observed that PltB binds to glycans rather than peptide motives, preferably those terminating with N-acetylneuramic acid (Neu5Ac), a sugar common in humans but not in other mammals (on a side note, the typhoid toxin produced by *Salmonella*e restricted to cold blooded lacks the Neu5Ac binding domain) (Deng et al. 2014; Song et al. 2013). Given the ubiquitous presence of glycoproteins, it is not surprising to find several protein receptors for the toxin. The study aforementioned, for example, reported Podocalyxin-like protein 1 (PODXL) as a receptor for the purified typhoid toxin on epithelial cell line Henle-407, and CD45 on hematopoietic cells (Song et al. 2013), suggesting that different receptors might be recognized on different cell types (Frisan 2015).

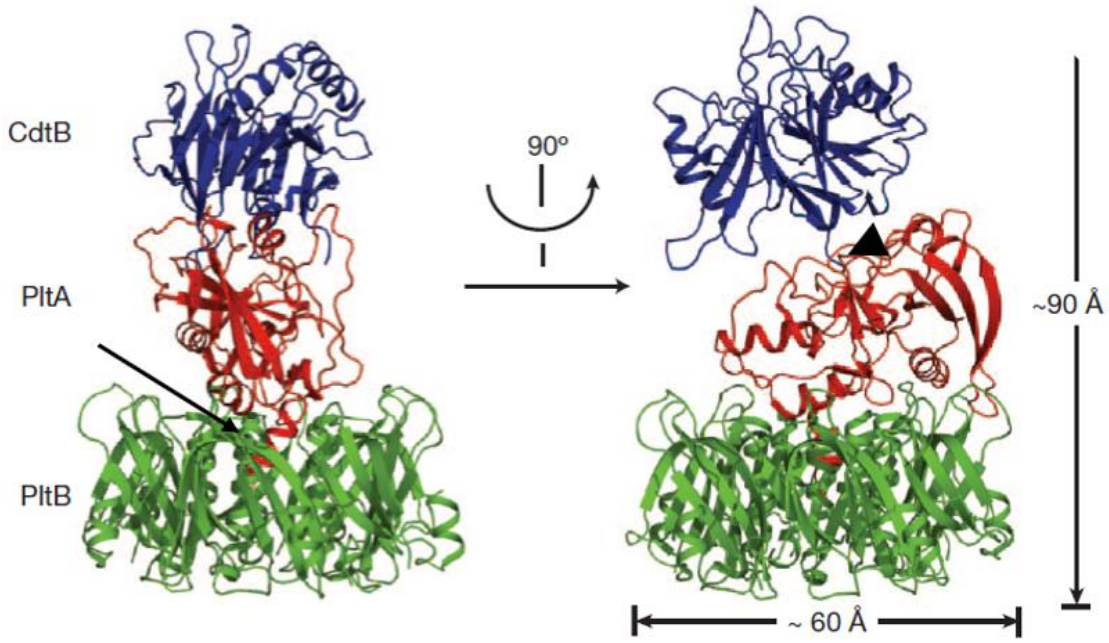

Figure I - 6 structure of the typhoid toxin. Modified by Song et al. (Song et al. 2013). Note the α-helix of PltA penetrating between the PltB pentamer (arrow). In the right panel the disulfur bond between CdtB and PltA is marked with an arrowhead.

2.6.3 Synthesis and secretion

In vitro extracellular *Salmonella* does not produce the typhoid toxin. The synthesis starts in SCV, after the bacterium has invaded the host cell (insert of Figure I – 7). The three subunits are encoded by the same genetic island, but on two different operons, one for *cdtB*, the other for *pltAB* (Figure I – 5), and they all carry a canonical secretion signal that permits their transport to the periplasm via the Sec machinery. The secretion of the toxin is therefore not directly dependent on the T3SS (Hodak & Galán 2013; Haghjoo & Galán 2004; Guidi, Levi, et al. 2013). Most likely it is the oxidative environment of the periplasm that enables the assembly of the holotoxin (Fowler et al. 2017). The toxin passes the peptidoglycan thanks to the typhoid toxin secretion A (TtsA), synthesized only by intracellular bacteria (Figure I – 7), and whose gene is found on the toxin´s genetic island (Figure I - 5). TtsA is homologue to a phage muramidase, an enzyme that lyses the bacterial wall. TtsA, however, seems to have limited lysis potential, being restricted to the peptidoglycan. The regulation of TtsA has to be carefully balanced: if it is overexpressed and granted access to the periplasm it would be able to lyse the bacterial wall as well (Hodak & Galán 2013).

The assembled typhoid toxin is now ready to be packaged in *Salmonella* outer membrane vesicles (OMVs), similarly to the CDT secretion (Frisan 2015). The OMVs bud out of the SCV, which membrane bears Neu5Ac receptors (Chang et al. 2016), and are likely to reach the host cell membrane via kinesin-dependent anterograde transport on microtubules (Figueira & Holden 2012). This process requires an intact SCV (Chang et al. 2016), in particular it seems to be dependent on the T3SS2 effector SifA (Guidi, Levi, et al. 2013).

2.6.4 Intoxication

The fusion of the SCV membrane with the cellular membrane leads to the release of the OMVs from the infected cell to the extracellular environment (Guidi, Levi, et al. 2013; Spanò & Galán 2008). It has been reported that the supernatant of infected cells is able to induce intoxication even in uninfected cells: adding a neutralizing antibody to the medium prevents intoxication (Spanò et al. 2008). Once in the extracellular environment, the OMVs are ready to be internalized. This process remains obscure, however initial data suggest that at least one possibility might be dynamin dependent endocytosis (Guidi, Levi, et al. 2013). The typhoid toxin might then follow an endocytic retrograde trafficking pathway, similarly to what happens to CDT (DiRienzo 2014), to reach the Golgi complex and the endoplasmic reticulum.

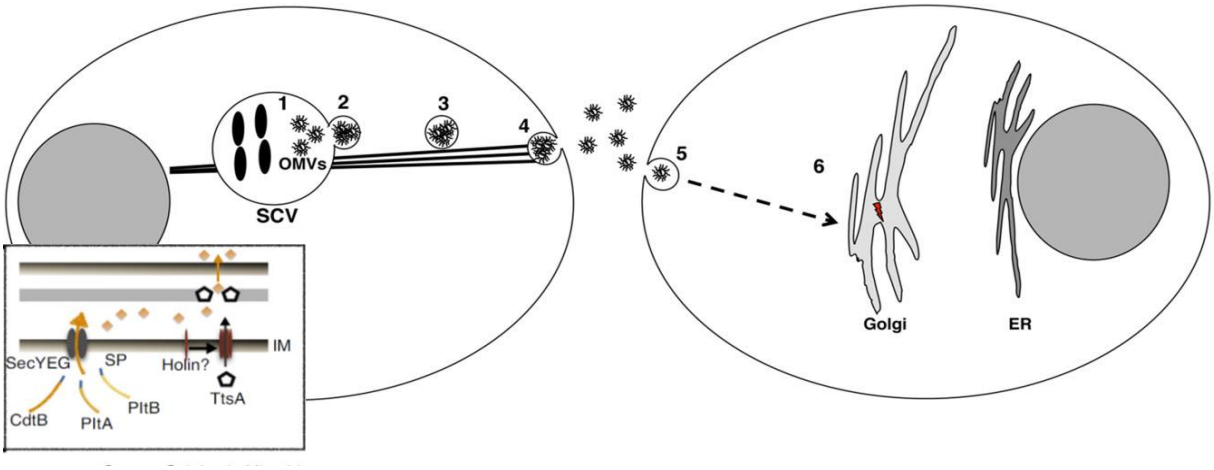

Figure I - 7 Secretion and uptake of the typhoid toxin. The insert (Fowler et al. 2017) shows the secretion of the toxin (yellow diamond) from the cytoplasm of the bacteria, through the wall (membranes in brown, peptidoglycan in grey), to the SCV. The large picture in the back is a schematic model of the OMV-containing-toxin secretion from the infected cell and uptake to a bystander (Guidi, Levi, et al. 2013)

There the host reductases might reduce the sulfur bond that keeps CdtB and PltA together (Fowler et al. 2017; Song et al. 2013; Miller & Wiedmann 2016), releasing CdtB that then shuttles to the nucleus thanks to its nuclear localization signal (Bezine et al. 2014).

2.7 CdtB – a DNase in the nucleus

2.7.1 Historical considerations

As mentioned, the typhoid toxin has two A subunits, CdtB and PltA. PltA has ADP-ribosyltransferases activity, however all phenotypes attributed to the typhoid toxin were found to be dependent on CdtB (Fowler et al. 2017).

The history of CdtB dates back to the late 80s, when Johnson and Lior observed that mammalian cultured cells exposed to the supernatant of certain bacteria (*Escherichia coli*, *Shigella dysenteriae* and *Campylobacter jejuni*) manifested cytoplasmic and nuclear distension. They called this putative toxin "cytolethal distending toxin", CLDT, later simplified in CDT (Johnson & Lior 1988b; Johnson & Lior 1988a; Johnson & Lior 1987). In the following years, reports flourished of similar phenotypes due to the infection with other bacteria, like *Aggregatibacter actinomycetemcomitans*, *Helicobacter hepaticus* (see the timeline published by Jinadasa and colleagues (Jinadasa et al. 2011)) and, more importantly, *Salmonella enterica* serovar Typhi (Lara-Tejero & Galán 2000). It was not until 2000 that this phenotype was attributed to the CdtB subunit of CDT, and that the amino acid sequence similarity of CdtB with the mammalian DNase I was reported (Elwell & Dreyfus 2000; Lara-Tejero & Galán 2000).

CdtB is indeed a DNase I. Not just the catalytic, DNA and metal binding residues have sequence homology with DNase I, but recombinant CdtB from a number of pathogens is able to digest plasmid DNA *in vitro* (Jinadasa et al. 2011). It is also reported phosphatidylinositol-3,4,5-triphosphate (PIP3) phosphatase activity of CdtB, however it seems to have little role in CdtB intoxication, the cellular toxicity being strictly dependent on its DNase activity (Jinadasa et al. 2011; Rabin et al. 2009).

Infection of cell lines with CdtB producing bacteria, like *Helicobacter hepaticus* or *Escherichia coli*, results in DNA damage seen by the phosphorylation of the histone variant H2AX at serine 139, a common marker of DNA double strand brakes, which eventually leads to ataxia telangiectasia mutated (ATM)-dependent arrest of cell cycle at the G2/M checkpoint, induction of senescence and initiation of DNA repair (Bezine et al. 2016; Jinadasa et al. 2011; Grasso & Frisan 2015). Senescent cells could then go into apoptosis, depending on the cell type (Alouf et al. 2015; Smith & Bayles 2006).

2.7.2 CdtB as a pathogenic and carcinogenic agent

How is the toxin related with malignant transformation? In 1992 James Fox witnessed an outbreak of hepatocellular carcinoma progressing to liver cancer in A/JCr mice. The etiological agent was found to be a novel *Helicobacter*, which he named *Helicobacter hepaticus* (Fox et al. 1994; Ward et al. 1994). Interestingly a *cdtb* deficient isogenic mutant was not able to induce hepatocarcinogenesis (Ge et al. 2007), providing a direct link between CdtB and carcinogenesis in an animal model. Later, it was observed that infection of 129S Rag2 knockout mice led to typhlocolitis (inflammation of the caecum and colon) eventually developing into colorectal cancer (Erdman et al. 2003).

In vitro, chronic exposure to sub-lethal doses of the recombinant *H. hepaticus* CDT, compared to a toxin lacking CdtB, provoked anchorage independent growth and impaired DNA damage response in rat fibroblasts, as well as genomic instability in a colon epithelial cell line (Guidi, Guerra, et al. 2013).

Besides having a role in malignant transformation, another interesting role of the toxin emerged from a number of *in vivo* studies suggesting that CdtB could have a crucial role in persistent colonization. In fact, different laboratories noted that mice infected with a *cdtB* knockout strain of *Helicobacter hepaticus* cleared the infection of the intestine sooner than mice infected with the w.t. strain (Ge et al. 2005; Pratt et al. 2006).

A similar conclusion was also drawn for *Salmonella* Typhi´s CdtB. Initial evidences found that the typhoid toxin was essential for the establishment of persistent infection in a mouse model of *Salmonella* Typhi (*i.e.* a Rag2 -/- mouse engrafted with human fetal liver hematopoietic stem and progenitor cells) (Song et al. 2010). To overcome the use of this highly engineered

mouse and to tackle specifically the role of CdtB, another group used a *Salmonella* Typhimurium strain transformed with the *S.* Typhi´s typhoid toxin subunits, and compared it to a control strain lacking *cdtB*. The surprising observation was that not just the *cdtB* positive strain was able to persistently colonize the mice, but that it also promoted host survival when compared the *cdtB* knockout strain. Moreover, in the intestine colitis was inhibited by the presence of the toxin at an early time point. In the liver, on the other hand, the toxin induced and low grade inflammation and persistent colonization (Del Bel Belluz et al. 2016; Guidi et al. 2016).

Interestingly, laboratory mice injected with the purified typhoid toxin exhibited many symptoms related to the acute phase of human disease, including stupor, malaise and decrease number of circulating lymphocytes. In turn, a toxin mutant in a catalytic site of CdtB failed to induce the symptoms (Song et al. 2013).

2.8 Three-dimension primary cell culture: the organoids

2.8.1 Culture of adult primary cells

Traditionally *in vitro* study of the gall bladder tumour, but then again of any other tumour, are carried out on cell lines, due to the lack of a technique to culture stable non-cancer, primary cells, *i.e.* cells derived directly from healthy human or animal tissue. Studying mutagenesis on cell lines has some major disadvantages. Above all, most of the common cell lines are derived from cancer tissue or are artificially immortalized, making studies on transformation often difficult to interpret. In addition, cell lines have been found to harbor a lot of heterogeneity because the culture itself is enough to induce mutations, implying that each research institute around the globe might be using different clones of the same cell line (Marx 2014).

To overcome this problem attempts were made to grow primary cells *in vitro*, but the traditional techniques were frustrated by fibroblast outgrowth, particularly when trying to cultivate epithelial cells (Jones 2008; Mitra et al. 2013), and by the entry of cells in irreversible

senescence (Campisi & d'Adda di Fagagna 2007). The loss of stemness was the main problem causing the limited life span of primary epithelial cells.

In recent years, however, a novel 3-dimensional culturing technique based on adult epithelial stem cells has emerged, allowing the propagation of primary cells for a long, virtually indefinite, period of time (Sato & Clevers 2013). This "organoid" technique (Figure I - 8) is already established for a number of human organs like the stomach (Schlaermann et al. 2014), the small intestine (Sato, Stange, et al. 2011), the colon (Jung et al. 2011), the fallopian tubes (Kessler et al. 2015) and the liver´s intrahepatic ducts (Huch et al. 2015). For the gall bladder, however, only a model of murine gall bladder organoids was described (Lugli et al. 2016; Scanu et al. 2015).

Organoids can be generated from the adult or embryonic tissue, embryonic stem cells (ESC), induced pluripotent stem cells (iPSC), as well as tumour biopsies and circulating tumours (Fatehullah et al. 2016). The adult stem cells of the organoids retain the potential of differentiating into different cell lineages of the same type of the tissue of origin. The primary requirement and challenge for the establishment of a long term organoid culture is finding the correct cocktail of growth factors, activators and inhibitors involved in the maintenance of the stem cell niche (Sato & Clevers 2013; Fatehullah et al. 2016).

The 3D organoids recapitulate the organ of origin from a morphological and transcriptional point of view (Schlaermann et al. 2014), can respond to stimuli normally present in the living tissue (Kessler et al. 2015), are genetically stable, and can be indefinitely expanded (Sato & Clevers 2013). An organoid derived from the human intestine, for example, is formed by a single layer of polarized cells whose basal side faces the extra cellular matrix and whose apical side faces the lumen. During its growth the organoid spontaneously organize itself forming buddings that recapitulates the crypt, which is the self-renewing unit of the intestine, with the cells differentiating into different cell lineages (including goblet cells, enterocytes, Paneth cells and enteroendocrine cells) or persisting as adult stem cell (Sato & Clevers 2013). Similarly organoids can also derive from stratified epithelia, and in that case they will retain the stratification *in vitro*.

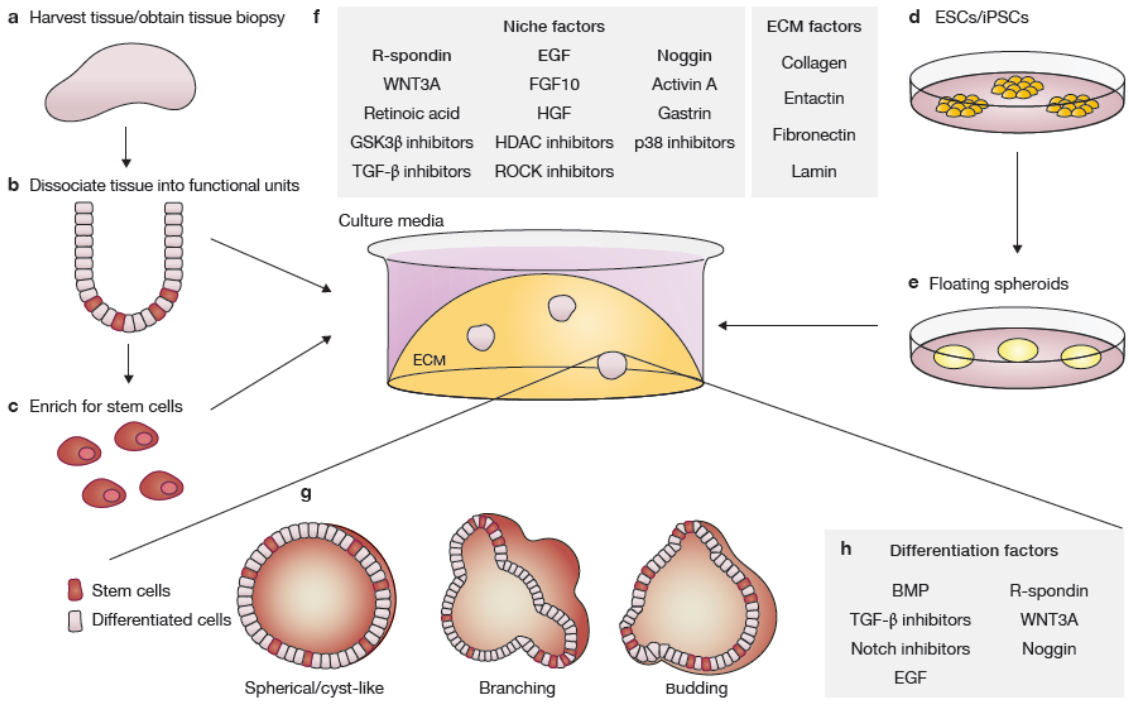

Figure I - 8 Schematic representation of organoid culture. The starting material can be tissue biopsies (a), functional units of the organ, like intestinal crypts (b), enriched adult stem cells (c) or ESC and iPSC (d) that underwent a step of *in vitro* differentiation (e). After seeding in matrigel and providing a defined cell culture medium (f), the organoids start to take their typical shapes (g). In some cases the addition of a different medium is required to achieve full differentiation (h) (Fatehullah et al. 2016)

2.8.2 Applications of organoid cultures

The possibility of growing human primary epithelial cells for an indefinite time unleashed a wide range of possible applications. First, such model is ideal to study human adult stemness (see section 2.9). Organoids are also seen as a way to join basic research with translational medicine, patients´ derived organoids are in fact used for high throughput drug screening and drug susceptibility tests, therefore providing an unprecedented tool for personalized medicine (Liu et al. 2016; Skardal et al. 2016; Huang et al. 2015). The potential use for regenerative medicine is also evident: engraftment of organoids in mice has been reported to be successful (Yui et al. 2012; Watson et al. 2014), even for genome edited organoids (Roper et al. 2017).

Organoids´ nucleic acids can be engineered (Yin et al. 2016) either using classical lentiviruses techniques (Miyoshi & Stappenbeck 2013), or by CRISPR-Cas9 editing (Driehuis & Clevers 2017). This opens the possibility to run screens, or even to model genetic diseases. Two very similar pioneering works published almost simultaneously showed that it is possible to model

colorectal cancer starting from healthy human material, and inducing serial mutations via CRISPR-Cas9 genome editing. Because organoids derived from tumours require less growing factors compared to the healthy ones, the authors could follow the steps of transformation by selection in media lacking one growing factor at a time (Matano et al. 2015; Drost et al. 2015).

2.8.3 Organoids as a model to study host-bacterial pathogen interaction

Organoids are also starting to be used as a model to investigate host-bacterial pathogen interaction (Bartfeld 2016) by combining for the first time *ex vivo* the human pathogen with the human tissue that they would naturally infect. Gastric organoids, for example, were successfully infected with *Helicobacter pylori* by injection into the lumen (Bartfeld et al. 2015), or by seeding in 2-dimensions organoid-derived primary cells, and subsequent co-cultivation with the pathogen (Schlaermann et al. 2014). The infection was verified by the successful translocation and phosphorylation of CagA, a major virulence factor that *H. pylori* injects into the host cell (Schlaermann et al. 2014). Interestingly, again thanks to gastric primary cells, the same group found that *H.* plylori is able to induce DNA damage coupled with impaired DNA damage response (DDR) (Koeppel et al. 2015). Similarly, human primary fallopian tubes epithelial cells derived from organoids have been infected with *Chlamydia trachomatis*, which resulted in DNA damage probably due to the host production of reactive oxygen species (ROS), and impaired DNA damage response. (Chumduri et al. 2013).

Intestinal organoids have also been used to model the infection with *Clostridium difficile* and the effect of its toxin (Leslie et al. 2015), and even to observe the effects of commensal bacteria like *Bacterioides thetaiotaomicron* (Engevik et al. 2013), *Lactobacillus rhamnosus* (Aoki-Yoshida et al. 2016), *Akkermansia muciniphila* and *Faecalibacterium prausnitzii* (Lukovac et al. 2014).

Initial attempts to infect intestinal organoids with *Salmonella* Typhimurium were also carried out. Zhang and colleagues simply co-cultured *Salmonella* with murine intestinal organoids and reported disruption of tight junction proteins, activation of the NFkB pathway and a general decrease in the stem cell marker Lgr5 (Zhang et al. 2014). Almost at the same time anther paper was published, in which Wilson and colleagues injected the bacteria in the lumen of

human intestinal organoids, and, while they did not observe invasive bacteria, they did report the growth of bacteria in the lumen. Moreover they found that a slight inhibition of bacterial growth was due to the host-secreted α-defensins (Wilson et al. 2014). Later Forbester and colleagues grew human intestinal organoids starting from iPSCs and, again, microinjected them with *S.* Typhimurium. They observed upregulation of genes associated with infection and inflammation as well as invasive bacteria. The invasion was found to be dependent on the bacterial invasion protein A (invA) (Forbester et al. 2015).

These early *Salmonella* infections of human and murine intestinal organoids showed that, in principle, infection of organoids is possible, but they have major disadvantages. First the method of infection is technically challenging, because of the microinjection itself and because the operator would have to microinject many organoids which hardly reach 1mm of diameter, and calculating a precise multiplicity of infection is not feasible in these settings. In addition all these studies were carried with *S.* Typhimurium that, despite being an etiological agent of gastroenteritis in humans, does not causes the severe and life-threatening typhoid fever.

A later paper partially overcame these problems. The authors infected murine gall bladder organoids originating from a mouse lacking the Arf locus (which results in inactivation of TP53) with *S.* Typhimurium. They co-cultivated in suspension the bacteria with cells deriving from organoids, and noticed that infected cells managed to reconstitute the organoid. The authors reported growth in a supplement-depleted medium which could possibly represent a hallmark of cancer (Scanu et al. 2015).

To this day this is the only paper that dealt with the *Salmonella* infection of gall bladder organoids and malignant transformation, even though using *Salmonella* Typhiumrium, which is not linked with GBC, and organoids from a mouse which was already genetically predisposed to cancer development.

2.9 The Wnt/β-catenin pathway

Organoids provided an unprecedented tool to study adult stem cells. Combining these *in vitro* tools with *in vivo* lineage tracing, it was understood that the regulation of the Wnt/β-catenin pathway plays a crucial in embryo development, as well as in the maintenance of adult stemness (Schuijers & Clevers 2012).

Multicellular organisms harbor several Wnt proteins with redundant functions: the family includes 11 members in cnidaria, and 19 in humans, but it is absent in unicellular organisms (Petersen & Reddien 2009). Wnt is produced by the stroma and by some epithelial cells, for example Paneth cells in the intestine (Kabiri et al. 2014).

Wnt is a lipid-modified-secreted protein, in which palmitoylation (the addition of a mono-unsaturated fatty acid to a serine) plays an important role in its secretion. This post translational modification occurs in the endoplasmic reticulum and is mediated by Porcupine. The modified Wnt then finds its way to the cell membrane by binding the transmembrane receptor Wntless, which is continuously recycled via endosomal vesicles.

Once secreted, Wnt works as a short-range morphogen, by binding the receptor complex formed by Frizzled (Fz) and LRP5/6 (Figure I - 9). The binding leads to the receptors´ polymerization and signal transduction by conformational change of the intracellular domains, and phosphorylation of target proteins (including LRP6 itself) (Clevers & Nusse 2012).

Wnt alone however cannot efficiently transduce the signal: the presence of the co-activator R-spondin (Rspo) is necessary. R-spondins define a family of nine proteins and are most likely produced by mesenchymal cells (Blaydon et al. 2007; de Lau et al. 2012) like intestinal myofibroblasts (Koch 2017).

R-spondin is considered as “enhancer” of the Wnt signal, as alone it cannot activate the Wnt/β-catenin pathway. Upon binding of secreted Rspo to Lgr4, 5 or 6, the receptor binds the Fz/LRP complex, thus enhancing LRP6 phosphorylation (de Lau et al. 2012) (Figure I - 9).

After the binding of Wnt and Rspo, Axin is recruited at the plasma membrane, to the intracellular domain of LRP6. Axin is a negative regulator of the Wnt/β-catenin pathway. In absence of Wnt signaling it represents the scaffold of the “destruction complex”, a protein

complex which also includes APC, two constitutively active kinases (CK1 and GSK3) and β-catenin. CK1 and GSK3 phosphorylate β-catenin, and this phosphorylated form is recognized by the E3 ubiquitinase which ubiquitinates β-catenin leading to its degradation by the proteasome (Figure I - 9 left panel). In this scenario, β-catenin cannot translocate to the nucleus to function as transcription factor.

In the presence of active Wnt signaling, however, Axin binds LRP6. This event leads to the inhibition of β-catenin ubiquitination and the saturation of its phosphorylated form, so that newly synthesized β-catenin can eventually translocate into the nucleus (Figure I - 9 right panel) (Li et al. 2012; Schuijers & Clevers 2012).

In the nucleus β-catenin replaces Groucho, which normally binds LEF1/TCF when the Wnt signal is off. At this point the β-catenin/LEF1/TCF complex, together with other transcription factors, activates the transcription of Wnt response genes (Herbst et al. 2014; Eastman & Grosschedl 1999).

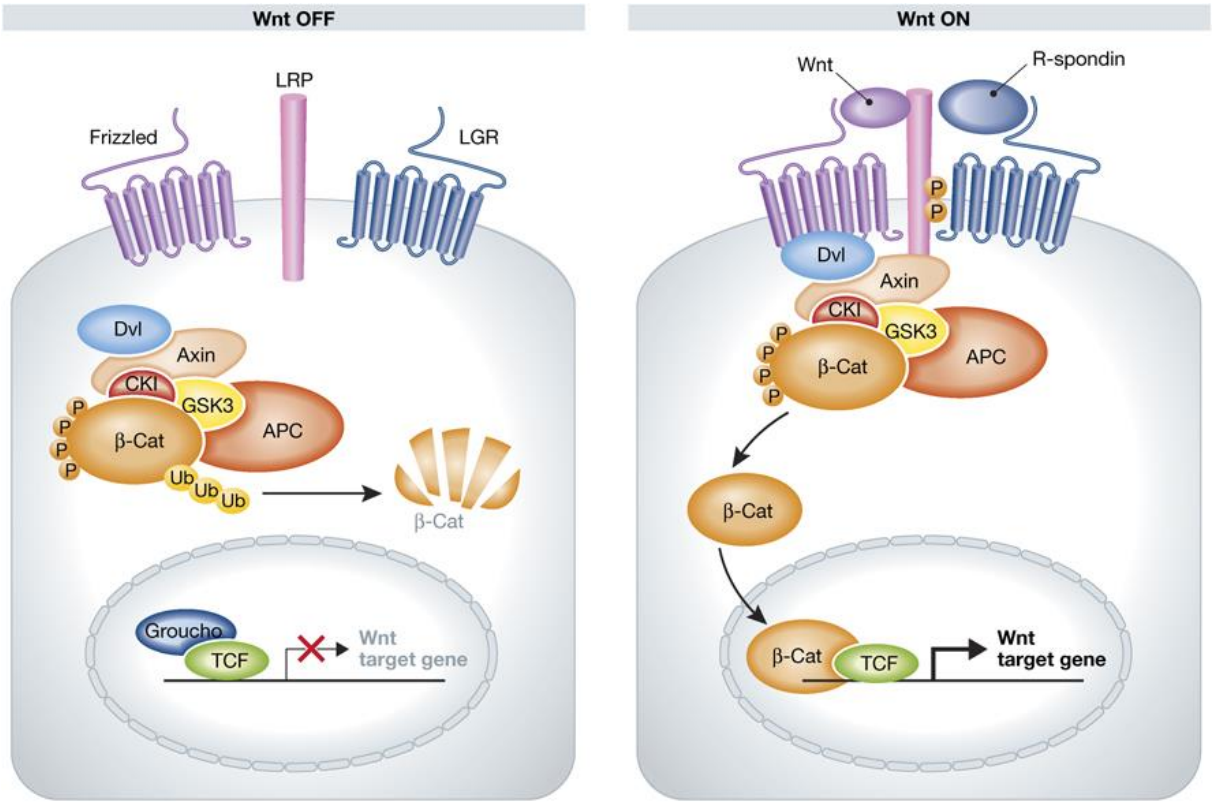

Figure I - 9 Schematic representation of Wnt and Rspo binding and signaling events mediated through the destruction complex (Schuijers & Clevers 2012)

Wnt target genes are tissue and development-specific, however one of the genes which is generally found to be activated is Axin2. Wnt therefore activates its own inhibitor as a negative feedback mechanism, ensuring a fine tuning of the Wnt/β-catenin pathway (Schuijers & Clevers 2012). Another Wnt target gene which is also an inhibitor of the pathway is Dickkopf (DKK), one of the few secreted inhibitors, that binds LRP5/6. Studies conducted on adult intestinal crypts also detected Lgr5 as a Wnt target gene (Haegebarth & Clevers 2009).

As mentioned, the Wnt/β-catenin pathway is central for the maintenance of adult stem cells, and in particular Lgr5 was found to be the stem cell marker of many epithelia including those of the gastrointestinal tract, like the small intestine, the colon (Barker et al. 2007), the liver intrahepatic ducts - though only after cellular damage - (Huch, Boj, et al. 2013), and also of certain gastrointestinal cancers (Barker et al. 2009). It is not clear whether Lrg5 represents also the adult stem cell marker of the gall bladder (Manohar et al. 2015).

2.10 Goals of the thesis

Despite the availability of organoids for most of the human gastrointestinal tract, a similar model is not available for the human gall bladder. This could serve, for example, for stem cell research, as the adult stem cells of the human gall bladder have not been clearly identified yet. In addition an organoid model reassembling the phenotypical and possibly functional features of the gall bladder could be used for modelling gall bladder pathologies like cholelithiasis, the research of which relies nowadays only on animal models.

Beside the study of physiological and pathological features of the organ, human gall bladder organoids could serve as a tool to investigate the interaction between primary human gall bladder epithelial cells and human restricted *Salmonella*e, i.e. serovars Typhi and Paratyphi A. Until now the *in vitro* study of human *Salmonella*e relied mostly on the infection of cell lines: the response of the human epithelium of the gall bladder is unknown. The outcome of the infection could provide a molecular evidences liking infection with transformation, with particular focus on the putative genotoxic effects of the typhoid toxin.

The first aim of this study was therefore to establish a human gall bladder organoid model. Then I characterized the epithelial cells of the organoids by comparing them with the tissue of origin. Some of the questions that I answered are: Am I able to grow long term organoids? Do the organoids express the same markers as the gall bladder? Is their phenotype stable in time? Do the organoids have the same absorptive proprieties of the organ? Am I be able to identify pathways and markers of adult gall bladder stem cells?

After answering these questions I focused on the infection of primary cells with the human restricted bacterium *Salmonella enterica* serovar Paratyphi A. In particular I focused on the putative genotoxic effect of the typhoid toxin. Is *Salmonella* able to infect gall bladder primary cells? Do I see any DNA damage associated with the CdtB subunit of the typhoid toxin? And, how are the cells responding to the DNA damage?

3. MATERIALS AND METHODS

3.1 Buffers, solutions, and media

10x PBS

1.36 M NaCl

27 mM KCl

14 mM KH_2PO_4

81 mM Na_2HPO_4 x 2 H_2O

adjust to pH 7.4 and autoclave

For culture application commercial PBS was used (Gibco cat. 10010023)

For washing immunostainings I used PBS-T, done by adding 0.1% [v/v] Tween 20 in 1x PBS

10x TBS

200 mM Tris base

1.4 M NaCl

adjust to pH 7.4 and autoclave

For washing western blot membranes I used TBS-T, done by adding 0.1% [v/v] Tween 20 in 1x TBS

SDS Resolving Gel Buffer

1M Tris-HCL pH8.8 (30.2g TRIS in 250ml Dis.H2O)

autoclave

SDS Staking Gel Buffer

1M Tris-HCL pH6.8 (30.2g TRIS in 250ml Dis.H2O)

autoclave

Electrophoresis Buffer

24mM Tris base

190 mM Glycine

0.1% SDS

10X Wet Blot Transfer Buffer

288g of Glycin

60g Tris

In 2l of H_20

1X Wet Blot Transfer Buffer

100ml 10X Transfer Buffer

200ml Methanol

700ml H_20

Immunoblot Blocking Buffer

3% Powder milk in TBS-T

6X Laemmli Buffer

It is a denaturing, reducing sample buffer used to load the protein samples in the SDS gel

3.0 ml Glycerol

1.5ml b-Mercaptoethanol

9.0 ml 10% SDS

3.75 ml staking gel buffer

Pinch of Bromophenol blue

Add 10 ml H2O

LB medium and plates

Lysogeny broth, a rich medium commonly used to grow *E. coli*

10 g Bacto tryptone (BD, Franklin Lakes, NJ, USA)

5 g Bacto yeast extract (BD, Franklin Lakes, NJ, USA)

5 g NaCl

In 1l ddH_2O

Adjust to pH 7.4

Autoclave

For plates add 1.5% (w/v) agar

LB 0.17M NaCl

Used to grow *Salmonella* Paratyphi A prior to *in vitro* infection. According to Elhadad et al. (Elhadad et al. 2016) this way of cultivation increases the internalization efficiency of the bacterium

Add 9.9g NaCl (0.17M) to the LB preparation before autoclaving

SOB

A rich medium used to produce chemical competent *E.coli*

2.0 % Tryptone

0.5 % Yeast extract

10 mM NaCl

2.5 mM KCl

10 mM $MgCl_2$

10 mM $MgSO_4$

In H_20

Autoclave

ITB

Buffer used to produce chemical competent *E.coli*

55 mM $MnCl_2$

15 mM $CaCl_2$

250 mM KCl

10 mM PIPES

MM5.8

A minimal medium known to stimulate the synthesis of the typhoid toxin (Guidi, Levi, et al. 2013). Traditionally *Salmonella* is grown in LB, but this prevents the production of the toxin

Prepare 10X N-minimal medium, 1l (Nelson and Kennedy, 1970):

KCl	3,72g
(NH4)2SO4	9,9g
K2SO4	0,87g
KH2PO4	1,36g

Autoclave.

Dilute the N-minimal medium to 1X in H20 and add:

100mM Bis/Tris pH 5,8

0,1% Casamino acids (Sigma 22090)

0,2% Glycerol

10uM MgCl2

Filter sterile (0,22um pores)

Blood agar plates

Standard medium used to grow *Helicobacter hepaticus*

45g Brucella Broth agar

1l ddH20

Autoclave

50ml Defibrinated Sheep Blood

0.32 ug/ul polymixinB

5 ug/ul trimethoprim

10 ug/ml vancomycin

Bacteria freezing medium

5% FBS

15% glycerol

In Brucella Broth (*Helicobacter*) or LB (*Salmonella* and *Escherichia*)

ADF++

The basal medium in which the defined medium to grow primary cells is constituted.

Advanced DMEM/F-12 (Dulbecco's Modified Eagle Medium/Ham's F-12. Thermo; Cat.: 12634010)

1% Glutamax (Thermo; Cat.: 35050061)

10mM HEPES (Thermo; Cat.: 15630080)

4% paraformaldehyde (PFA)

A chemical that allows rapid fixation of cultured cells and organs.

Dissolve 40 g PFA in 600 mL ddH_2O and heat at 60-70°C

Add concentrated NaOH dropwise until solution becomes clear

Add 100 mL 10x PBS and add ddH_2O to 1L

Adjust pH 7.4 with HCl ,sterilize the solution by filtering through 0.22 um filters and store aliquots at -20°C

Mowiol

Mounting buffer for immunofluorescence.

12 g glycerol

4.8 g Mowiol in MilliQ-H2O under constant stirring for 2 h at R

Add 24 ml Tris-HCl (0.2 M, pH 8.5)

Stir solution for 1 h at 50°C

Centrifuge 5000 g 15 min, aliquot supernatant and store at 4°C

2D immunofluorescence buffer (IFF)

Used for 2D immunofluorescence blocking (it contains BSA and FCS proteins) and washing (it contains the detergent tween)

1%BSA

2%FCS

0.1% Tween20

Diluted in PBS and filtered through 0.2um filter

Whole mount immunofluorescence buffer

Used for whole mount immunofluorescence blocking and washing. Note that compared to the 2D immunofluorescence buffer it contains a higher concentration of tween, that facilitates the penetration of antibodies into large structures like organoids.

3% BSA

1% Saponin

2% Triton X-100

0.02% Na Azide

Dilute in PBS and filter through 0.2um filter

3.2 Antibiotics

antibiotic	supplier	Stock concentration	Working concentration
Ampicillin	Sigma	100mg/ml	100ug/ml
Kanamycin	Fluka	50mg/ml	50ug/ml for high copy number plasmids; 12.5ug/ml for genomic resistance cassettes
Chloramphenicol	Sigma	10mg/ml	10ug/ml
Gentamicin	Gibco	10mg/ml	100 ug/ml or 10 ug/ml
Penicillin/Streptomycin (P/S)	Invitrogen	10000/10000 U/mL	100/100 U/mL

3.3 Plasmids

plasmid	description	source	Strain collection number
pOR25	constitutive expression of GFPmut3 / KanR	Oliver Riede dissertation, 2009	H3895
pMW788B	E.coli plasmid/CamR	Meike Soerensen	
pLS002	All the chlamydia genes were removed from the vector p2TK2--SW2, leaving in the plasmid only the Amp resistance cassette, the mCherry gene, a promoter, a terminator and an *E. coli* origin of replication	This study	H4665
pKD4	Chloramphenicol resistance cassette source for mutagenesis protocol	Datsenko, KA, BL Wanner 2000. Proc. Natl. Acad. Sci. U.S.A. 97(12):6640-5	H4659
pKD46	Temperature sensitive plasmid carrying a arabinose inducible recombinase and Ampicillin resistance cassette	Datsenko, KA, BL Wanner 2000. Proc. Natl. Acad. Sci. U.S.A. 97(12):6640-5 Kindly provided by Dr. Maria del Mar Reines, University of Balearic Islands	H3906

3.4 Oligonucleotides

All oligonucleotides (including the one used as PCR primers) were synthesized by Eurofins

3.4.1 Oligonucleotides and PCR primers for detection and cloning

oligonucleotide	Sequence (5'->3')	function
Hh_cdtbKO_PCR1_F	GGGCGTGAAATTCCTGTTAG	5' PCR primer for the upstream region of *Hh cdtB*
Hh_cdtbKO_PCR1_R	CGCGGATCCTGTCGTTGTTCGCACAGTTG	3' PCR primer for the upstream region of *Hh cdtB*, BamHI site in red
Hh_cdtbKO_PCR2_F	CGCGGATCCATATACGCGCACACCTCTCATC	5' PCR primer for the downstream region of *Hh cdtB*, BamHI site in red
Hh_cdtbKO_PCR2_R	ACGAATTTGCACCGCAGAAC	3' PCR primer for the downstream region of *Hh cdtB*
Cam-BamHI_01_F	GACTGGATCCGATATAGATTGAAAAGTGGAT	Internal to Cam cassette, used for checking the recombination in *Hh*
SPAcdtBKO_A1_F	TCTATAGTTGTCTCTTTGGTATTAAC	5' PCR primer for the upstream region of *S*PA *cdtB*
SPAcdtBKO_A1_R	CGCGGATCCACCATAAGAATATCC	3' PCR primer for the upstream region of *S*PA *cdtB*, BamHI site in red
SPAcdtBKO_A2_F	CGCGGATCCATATAAGATATATCT	5' PCR primer for the downstream region of *S*PA *cdtB*, BamHI site in red
SPAcdtBKO_A2_R	ACAGCTTCGTGCCAAAAAGG	3' PCR primer for the PAdownstream region of *S cdtB*
SPAcdtBKO_camR_F	CGCGGATCCGTGAGAAGTTCCTATTCTCTAGAAAGTA TAGGAACTTCACCCTCATCAGTGCCAACATAGT	5' PCR primer for the CamR+promoter amplification from

		pACYC177. BamHI site in red
SPAcdtBKO_camR_R	CGCGGATCCGAAGTTCCTATTCTCTAGAAAGTATAGGAACTTCTTATTCAACAAAGCCGCCGTCCC	3' PCR primer for the CamR+promoter amplification from pACYC177. BamHI site in red
SPAcdtB-gfp_PCR1_F	CTAGCTAGCCGTCCCCTCCTGCGAAAGCG	5' region homologue to upstream cdtB in green. NheI site in red
SPAcdtB-gfp_PCR1_R	CTCGAGATCCTCCTCCTCCTCCACAGCTTCGTGCCAAAAAGG	3' region homologue to downstream cdtB. XhoI site in red, 5G lnker in blue
SPAcdtB-gfp_PCR2 F: XhoI site in red, in	GAAGCTGTGGAGGAGGAGGAGGATCTCGAGGAATGAGTAAAGGAGAAGAACT	5' region homologue gfp, XhoI site in red
SPAcdtB-gfp_PCR2 R:	CCGGACGTCCGGTCCGAGCTCGGACGCGGATCCTTATTTGTATAGTTCATCCATGCCA	3' region homologue to gfp, the sites in red are respectively AatII, SacI, BamHI
SPAcdtB-gfp_PCR5 F:	CGCGGATCCTGAGTAAATAGCGTTGACGA	5' region homologue to downstream of cdtB, BamHI site in red
SPAcdtB-gfp_PCR5 R:	CGCGAGCTCATTAAGGCGTCAGGTTTTTC	3' region homologue to downstream of cdtB, SacI site in red
SPAcdtB-gfp_PCR6F	CGCGGATCCGTGTAGGCTGGAGCTGCTTC	5' homologue to KanR of plasmid pKD4, BamHI site in red
SPAcdtB-gfp_PCR6R	CGCGGATCCCCATATGAATATCCTCCTTA	3' homologue to KanR of plasmid pKD4, BamHI site in red
XhoI-flag_01_F	CCGCTCGAGGAGACTACAAAGACGATGACGACAAG	5' fragment of FLAG tag. XhoI site in red
BamHI-flag_01_R	CGCGGATCCTTACTTGTCGTCATCGTCTTTGTAGT	3' fragment of FLAG tag. BamHI site in red
SPAcdtb-flag_PCR5_R	CGCGAGCTCATTAAGGCGTCAGGTTTTTC	3' homologue to downstream sequence of

		the template. SacI site in red
Check Kan_01F	ATCGCCTTCTTGACGAGTTCTTC	5' PCR primer to check for the insertion of KanR
Check Kan_01R	GGATAAAGGAACGGGTAAGATTGTA	3' PCR primer to check for the insertion of KanR

3.4.2 Sequencing primers

oligonucleotide	Sequence (5'->3')	function
027_Seq_01_F	CAAGTGAAAGTTAAGCCAAT	Sequencing of cdtb-flag
027_seq_01R	TTTGCGCTTGCGTTTTCCCTTGTC	Sequencing of cdtb-flag
027_seq_02F	ATCCTGGTAATGAAAAATTT	Sequencing of cdtb-flag
027_Seq_03_F	ATGAATACACCTGGAATCTC	Sequencing of cdtb-flag
027_Seq_04_F	GTTGGGCTTCGGAATCGTTT	Sequencing of cdtb-flag (recombinant arm downstream)
027_seq_04_R	ACGGGTAAGATTGTAATTCCCTTA	Sequencing of cdtb-flag (recombinant arm downstream)
027_Seq_05_F	CTTGCCACTGTTCCGCGTAT	Sequencing of cdtb-flag (recombinant arm downstream)

3.5 Antibodies and dyes

Western blot: dilute primary antibodies in TBS-T 5% skim milk powder, or 5% BSA if they detect phosphorylated protein, unless not stated otherwise. Stored at -20°C for multiple uses. Freshly dilute secondary antibodies 1:250 in TBS-T 5% skim milk powder.

Immunofluorescence: Dilute primary and secondary antibodies in a buffer dependent on the assay.

antibody	Supplier	Cat.no.	source	Application and dilution
Salmonella Common Structural Antigen 1 (CSA-1)	BacTrace	01-91-99	Goat polyclonal	IF: 1:1000
Monoclonal Anti-β-Actin (Clone AC-15)	Sigma	A5441	Mouse monoclonal	WB: 1:10000
E-cadherin (clone CD324)	BD	562869	Mouse monoclonal	IF: 1:300 WB: 1:500
Ki-67 (8D5)	Cell signaling	9449	Mouse monoclonal	IF: 1:200

Ki67 (D2H10)	Cell signaling	9027	Rabbit monoclonal	IF: 1:200
Muc5AC	abcam	ab3649	Mouse monoclonal	IF: 1:200
PCNA (csPC10)	Cell signaling	2586	Mouse monoclonal	IF: 1:100
phospho-Histone H2A.X (Ser139) (clone JBW301)	millipore	05-636-I	Mouse monoclonal	IF: 1:100 WB: 1:200
phospho-Histone H2A.X (Ser139) conjugated FITCS	In house made	-	Mouse monoclonal	IF: 1:300 for standard applications, 1:100 for whole mount
β-Catenin	sigma	C2206	Rabbit polyclonal	IF: 1:300 WB: 1:500
Claudin 2	abcam	ab53032	Rabbit polyclonal	IF: 1:200 WB: 1:500
R anti Cytokeratin 19 clone EP1580Y	abcam	ab52625	Rabbit monoclonal	IF: 1:500 WB: 1:5000
Muc5B	abcam	ab87376	Rabbit polyclonal	IF: 1:300
Vimentin (D21H3)	Cell signaling	5741	Rabbit monoclonal	WB 1:1000
HRP-linked whole Ab	GE Healthcare	NA934V	Donkey	WB: 1:2500
HRP-linked whole Ab	GE Healthcare	NA931V	Sheep	WB: 1:2500
Hoechst (Bisbenzimide H 33258)	sigma	H6024	-	IF: 1:10000 for standard applications, 1:300 for whole mount
Draq5	abcam	ab108410	-	IF: 1:1000
Phalloidin 546	invitrogen	A22283	-	IF: 1:500 for standard applications, 1:200 for whole mount
Phalloidin 488	Invitrogen	A12379	-	IF: 1:500 for standard applications, 1:200 for whole mount
Phalloidin 647	invitrogen	A22287	-	IF: 1:500 for standard applications, 1:200 for whole mount

3.6 Supplements for primary cells

3.6.1 Growth factors and chemicals

Medium prepared in ADF++ (Advanced/DMEM-F12 supplemented with 1% Glutamax (Sigma), 10mM HEPES (Sigma))

Reagent	Supplier	Cat.no.	Stock concentration	Working concentration
Advanced/DMEM F12	Invitrogen	12634-010	-	-
TrypLE	Thermo Scientific	12604021	-	-
Collagenase IV	Sigma	C5138		
Matrigel, growth factor reduced, phenol red free	BD	356231	-	-
Wnt3a	In house made	-	Conditioned medium	25%
R-spondin 1	In house made	-	Conditioned medium	25%
B27	Invitrogen	17504-044	50X	1X
N2	Invitrogen	17502-048	100X	1X
human epidermal growth factor (EGF)	Invitrogen	PHG0311	200ug/ml	20ng/ml
murine epidermal growth factor (mEGF)	Invitrogen	PMG8044	500ug/ml	50ng/ml
human noggin	Peprotech	120-10C	150ug/ml	150ng/ml
murine noggin	Peprotech	250-38	100ug/ml	100ng/ml
human fibroblast growth factor (FGF)-10	Peprotech	100-26	150ug/ml	150ng/ml
Nicotinamide (NIC)	Sigma	N0636	1M	10mM
SB202190 (p38 inhibitor)	Sigma	S7067	2mM	2uM
A 83-01 (Tgf-β Type I receptor ALK-5 inhibitor)	Calbiochem	2939	1mM	1uM

Y-27632 (ROCK inhibitor)	Sigma	Y0503	3 mM	7.5uM
Forskolin (FSK)	Tocris	1099	10mM	10uM
human hepatocyte growth factor (HGF)	Peprotech	100-39	25ug/ml	25ng/ml
Fetal calf serum (FCS), heat-inactivated	Biochrom	S0415	-	-
Cryo-SFM freezing medium	PromoCell	C-29910	-	-
fluorescein isothothiocyanate-labeled dextran (4kDa)	Sigma	FD4	-	1mg/ml
EGTA	Sigma	E3889	100mM	2mM
Etoposide	Sigma	E1383	50mM	50uM
IWP-2	MerckMillipore	681671	10mM	10uM
4-hydroxytamoxifen	Sigma	T176	10mM	10uM

3.6.2 Preparation of Wnt and Rspo conditioned medium

The 293T Wnt3A cell line (ATTC CRL-2647™) and the 293T HA-Rspo1-FC cell line were kindly provided by Prof. Hans Clevers (Hubrecht Institute, Utrecht, Netherlands). Thawed and grow the cells in 100cm^2 well supplemented with 100ml DMEM 10%FCS + zeocin 300 µg/mL (Invitrogen; cat. no. 250-01) to keep the selective pressure. After around 5 days, when the cells were almost confluent, replace the medium. After 5 days collect the medium, centrifuge 3000rpm 15min to get rid of the cells and cell fragments, filter sterilize through a 0.22um pore filter and store at -20°C. It is possible to collect the supernatant for 2 more times, i.e. until 20 days after seeding.

The conditioned medium has to be tested on a 293T reporter cell line stably transduced with a construct that drives the synthesis of GFP upon activation of the Wnt pathway.

3.7 Bacteria and cells

3.7.1 Bacterial strains

strain	description	Resistance	Source or reference	Strain collection no.
Helicobacter hepaticus	Wild type	-	ATCC 51449/3B1. Kindly provided by Prof. Armelle Menard, University of Bordeaux	P557
Helicobacter hepaticus Δ*cdtB*	*cdtB* gene replaced with Chloramphenicol resistance cassette	Cam (genomic)	This study	P560
Salmonella enterica servovar Paratyphi A	Wild type	-	ATCC 9150. Purchased by ATCC	X566
Salmonella enterica servovar Paratyphi A / pOR25	*S*PA w.t. strain transformed with the plasmid pOR25 (pACYC derivative)	Kan	This study	X568
Salmonella enterica servovar Paratyphi A / pLS002	*S*PA w.t. strain transformed with the plasmid pLS002	Amp	This study	X574
Salmonella enterica servovar Paratyphi A Δ*cdtB*	*cdtB* interrupted by the Kanamycin resistance cassette	Kan (genomic)	This study	X573
Salmonella enterica servovar Paratyphi A Δ*cdtB* / pLS002	*S*PA ΔcdtB transformed with the plasmid pLS002	Amp, Kan (genomic)	This study	X575
Salmonella enterica servovar Paratyphi A / pKD46	*S*PA w.t. strain transformed with the plasmid pKD46	Amp	This study	X576
Salmonella enterica servovar Paratyphi A *cdtB-flag*	*S*PA genomic fusion of *cdtB* with flag tag	Kan (genomic)	This study	X581

3.7.2 Bacteria culture

Streak *Helicobacter hepaticus* on a blood agar plate and incubated at 37°C under microaerobic conditions (5% CO2, 4% O2). After 48h overplate the bacteria.

Streak *Salmonella enterica* on LB agar plate and incubate at 37°C. After 24h pick a single colony and use it for subsequent procedures.

If the bacteria harbor a vector, the agar plates and liquid media have to be supplemented with the antibiotics required to keep the selection pressure.

The OD to cfu curve for *Helicobacter* and *Salmonella* are found below

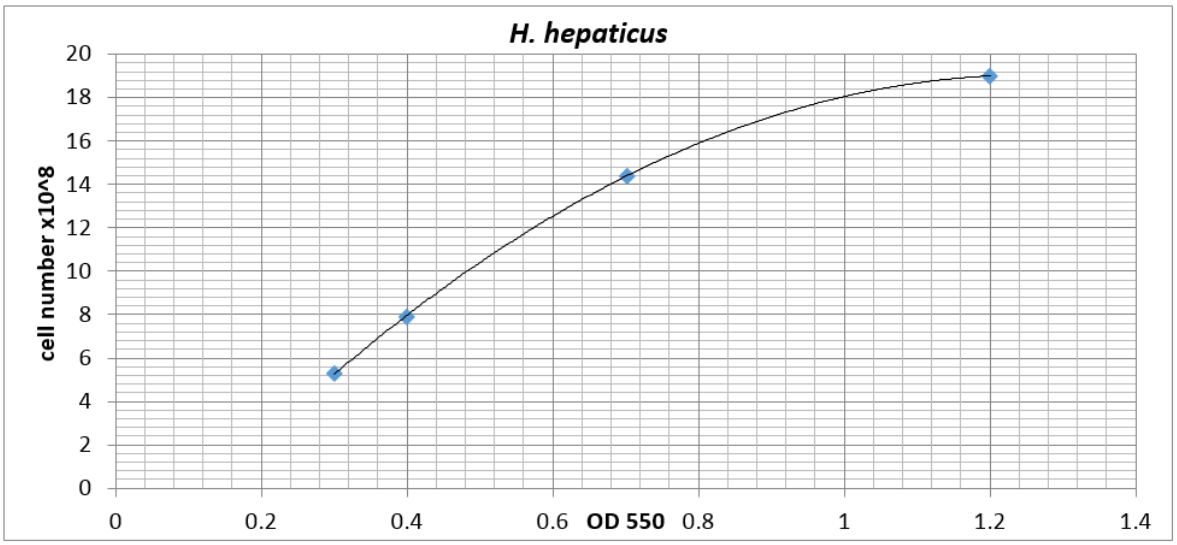

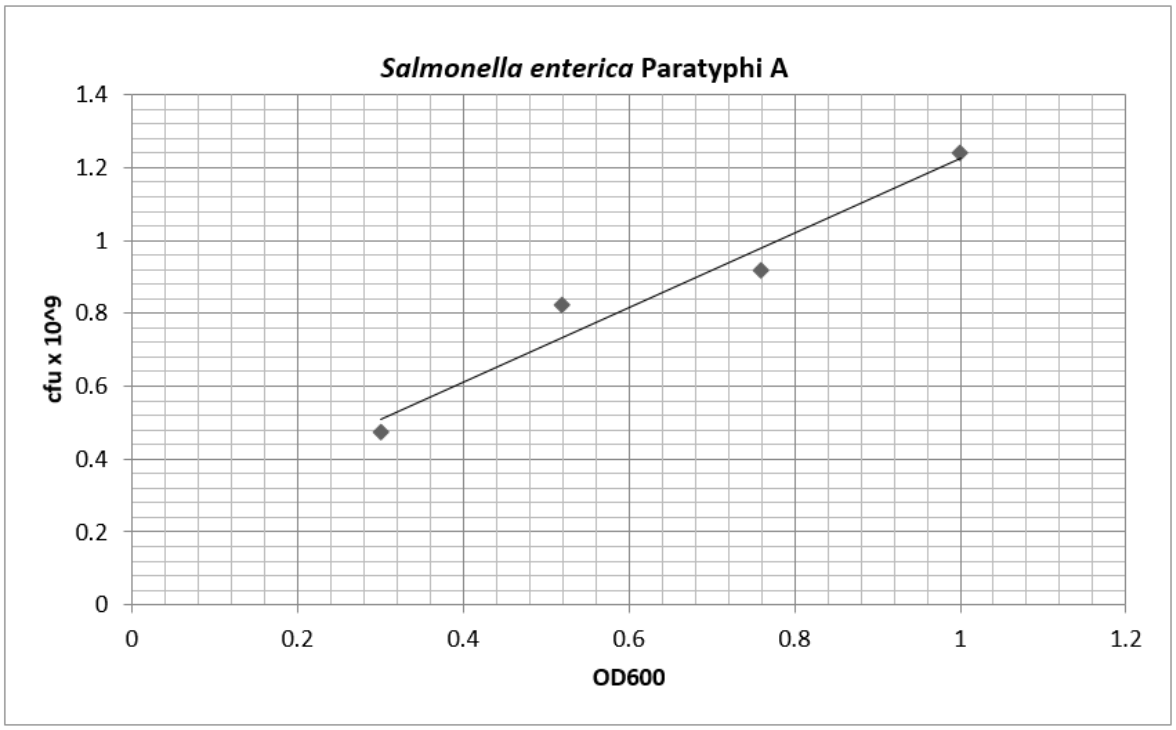

3.7.3 Freezing of bacteria

Grow bacteria originating from single colonies on blood agar plates (*Helicobacter*) or LB agar (*Salmonella*), harvest and resuspend in BB (*Helicobacter*) or LB (*Salmonella*) supplemented with 10% glycerol and 10% FCS. Store the vials at -80°C

3.7.4 Cell lines

The cell lines used are HeLa 229 and CaCo-2. They both grow in ADF++ 10%FCS if not stated otherwise.

3.8 Genetic manipulation of bacteria

3.8.1 Electroporation of *Helicobacter hepaticus*

Grow *Hh* on BB Blood agar plates supplemented with the required antibiotics for 48h. Harvest 4 dishes per construct (have at least one construct and one control) in an eppendorf containing 1ml of ice cold 10% glycerol (wash buffer), centrifuge 15000g, 3min, 4°C and resuspend the pellet in 1ml wash buffer. Repeat this washing step twice, then resuspend the pellet in 80ul ice cold wash buffer add 2ug of circular DNA. From this point on work on ice. Perform the electroporation in an *Escherichia coli* pulser: 0.2cm electroporation cuvette (Bio-Rad) at a voltage of 2.5 kV, a resistance of 200 Ohm, and a capacitance of 25uF. The time of shock should be about 4.9 ms. Immediately transfer the bacteria to an eppendorf add 100ul of 37°C BHI or BB and incubate on 2 non selective plates. After 24h harvest everything and plate on 4 selective plates. After 48h harvest the streaks and expand them to prepare stocks.

3.8.2 Transformation of H*elicobacter hepaticus* via homologous recombination

To perform homologous recombination in *Hh*, it is necessary to design a construct consisting of the fragment (including a resistance cassette) to insert in the chromosome flanked by two ~500bp sequences homologous to the genome. This construct should be cloned in an *E. coli* plasmid (pGEM-T easy is used as backbone) and can be directed electroporated in *Hh* because the bacterium will immediately loose the *E. coli* plasmid. Perform the electroporation with at least two conditions: one is the full construct and the control is the backbone only. After the selection of the positive clones it is necessary to check for the correct insertion in the genome by PCR. Furthermore, even though plasmid with the *E. coli* origin of replication should be lost in *Helicobacter*, to ensure the loss of the plasmid it is necessary to check for the sensitivity to the resistance cassette in the backbone, and the resistance to the cassette in the construct.

3.8.3 Electroporation of *Salmonella*

Dilute an overnight culture of *Salmonella* 1:100 and inoculate in two tubes of 5ml LB (one is to be electroporated with the construct, the other is the control). Incubate at 37°C shaking until the OD600 reaches 0.5. From this point on all the steps should be carried on ice. Centrifuge the bacteria 7000g, 3min, 4°C, resuspend in 1ml ice cold H_20 and spin 15000g, 1min, 4°C. Repeat the washing 4 times and the last time resuspend the pellet in 50ul ice cold H_20. Add the DNA (50ng of plasmid or 100-500ng of linear PCR product) and electroporated using 2mm cuvette, 2.5kV, 600 Ohm,25uF. Immediately recover by transferring the bacteria in an eppendorf and adding 1ml LB. Incubate at 37°C for one hour without any antibiotics, then plate 100ul on selective plates. Centrifuge the rest (7000g, 3min), resuspend the pellet it in 100ul LB and plate it on selective plates. After 24h of incubation pick single clones and streak them on new plates. Incubate for 24h and prepare stocks.

3.8.4 Transformation of *Salmonella* via homologous recombination

This protocol is based on the one published by Datsenko and Wanner (Datsenko & Wanner 2000). A linear PCR product is required consisting of the fragment to insert in the chromosome followed by a Kanamycin resistance cassette, all flanked by two ~500bp sequences homologous to the *Salmonella* chromosome. This construct is electroporated in *Salmonella enterica* servovar Paratyphi A carrying pKD46 (strain number X576 in this study), a temperature sensitive plasmid that includes an arabinose inducible recombinase and an ampicillin resistance cassette. After the recombination takes place a change in temperature will be enough to get rid of the plasmid.
In detail:
Grow *Salmonella* expressing pKD46 in 5ml LB + Amp ON at 30°C shaking. The next day dilute 1:20, grow in two tubes (one for the electroporation with the construct, the other as control) with 5ml LB + Amp + L-arabinose 1mM (SIGMA A3256) at 30°C until OD600 reaches 0.5, and then use as recipient for electroporation with the final PCR product. After the electroporation and recovery in LB, plate on LB agar + Kan (12.5ug/ml) plates overnight at 37°C. Growing the bacteria at 37°C should cause the loss of the plasmid pKD46. Pick 10 clones, expand them on LB + Kan plates and make frozen stocks.
To ensure the loss of pKD46, streak each clone on an LB+Amp 100ug/ml and LB + Kan 12.5ug/ml plate (in this exact order). Incubate at 30°C overnight to check for the sensitivity to Amp and resistance to Kan: this verifies that the clones lost the plasmid pKD46 while integrating the construct in the chromosome.

3.9 Murine material

3.9.1 Mouse strains

Mouse strain	description	reference
C57BL	Standard wild type mouse	Jackson lab # 000664
Lgr5 EGFP-IRES-CreERT2 / ROSA26 mTmG	Lgr5 promoter controls the expression of Cre recombinase which is active in the presence of 4-Hydroxytamoxifen. The constitutive ROSA26 promoter controls the mTmG locus, leading to the expression of tdTomato., which is excised when Cre is active, resulting in the expression of GFP	Barker N et al. Nature. 2007 Oct 25;449(7165):1003-7
Sox2 EGFP-IRES-CreERT2 / ROSA26 mTmG	Sox2 promoter controls the expression of Cre recombinase which is active in the presence of 4-Hydroxytamoxifen. The constitutive ROSA26 promoter controls the mTmG locus, leading to the expression of tdTomato., which is excised when Cre is active, resulting in the expression of GFP	Arnold K et al. Cell Stem Cell. 2011; 9(4):317-29
Axin2-CreERT2 / ROSA26 mTmG	Axin2 promoter controls the expression of Cre recombinase which is active in the presence of 4-Hydroxytamoxifen. The constitutive ROSA26 promoter controls the mTmG locus, leading to the expression of tdTomato., which is excised when Cre is active, resulting in the expression of GFP	Jackson lab # 018867

3.9.2 Isolation and culturing of gall bladder organoids from murine tissue

Resect the gall bladder from the abdomen and transfer in a 10cm petri dish filled with PBS. Open the tissue longitudinally to expose the mucosa and cut in 3 to 4 pieces. Now transfer the fragments in a 2ml eppendorf tube filled with 1.5ml TrypLE, and incubate in a thermo mixer, 45minutes at 37°C shaking. After the incubation pipette up and down 3 times to release the cells, and remove the pieces of tissue. Centrifuge 500g, 5min, 4°C, remove the supernatant and resuspend the pellet in 1ml ADF supplemented with 5% FCS. Wash two additional times with ADF (lacking FCS). Keeping the eppendorf on ice, resuspend the pellet in the required amount of matrigel: 50ul matrigel per well, considering that from one murine gallbladder it is possible to make 5 wells. Seed a 50ul drop of matrigel per well of a 24-well-plate. Incubate at 37°C for 10 minutes in order for the matrigel to polymerize, then add 500ul of the primary cell culture medium per well. Organoids will start to grow within three days. Replace the medium twice a week.

3.9.3 Murine primary cells culture medium

Reagent	Volume (ul) for 1ml medium
ADF++*	720
Rspo1 conditioned medium	250
P/S	10
Noggin	1
mEGF (prediluted 1:10)	1
B27	20
N2	10
NIC	10
Tgf-β inhibitor	1
P38 inhibitor	1
ROCK inhibitor**	3

*ADF++: Advanced/DMEM-F12 supplemented with 1% Glutamax (Sigma), 10mM HEPES (Sigma)

** ROCK inhibitor is added just for the first 3 days of culture

The medium can be stored at 4°C for up to one week. Replace the medium of the cell culture twice a week.

3.10 Human material

The human gall bladder material was obtained from Klinik für Allgemein-, Visceral- und Transplantationschirurgie, following the approval by the Charité University Medicine ethical committee of the application E1/238/24. The patients underwent cholecystectomy following presence of gallstones or gastric cancer. The tissue was handed to the pathology department that kept most of it for further inspection, therefore only part of it was used for experimental procedures.

The tissue was transporter to the Max Planck Institute for Infection Biology within 2 hours from the surgery in ice cold PBS. The isolation of cells was performed immediately upon arrival, however, when this was not possible, the tissue was kept in ChillProtec buffer (Biochrom) supplemented with pen/strep and gentamicin (50ug/ml) for up to 48 hours at 4°C.

ID	Date	Age	Sex	Comments
GB1	24.11.14	49	F	Diffuse gastric carcinoma, otherwise healthy GB. Patient underwent gastrectomy. Sample from the middle part of the gallbladder.
GB2	12.12.14	-	-	No information available
GB3	10.02.15	38		Cholecystectomy due to the obstruction of the bile duct (no bile flow in or out), acute inflammation of the gallbladder. I got a large piece of the GB, both fundus and corpus. Patient Hpylori positive
GB4	11.02.15			Cholelithiasis due to gallstones. Chronic infection. I got the corpus
GB5	24.02.15	46	F	Cholecystectomy due to presence of gallstones and inflammation. I got the corpus.
GB6	13.03.15	66	F	Cholecystectomy due to presence of gallstones and inflammation. I got the corpus.
GB7	30.03.15	61	F	Cholecystectomy due to cholelithiasis. I got a longitudinal section of the GB
GB8	01.04.15	73	M	Cholecystectomy after antrum carcinoma. The tissue presented gallbladder sludge
GB9	20.04.2015	79	M	Cholecystectomy after esophagus carcinoma. The gallbladder presented gallstones
GB10	18.06.2015	61	F	Cholecystectomy due to presence of gallstones and inflammation. I got the fundus.
GB11	09.07.2015	56	M	Cholecystectomy due to presence of gallstones and inflammation. I got part of the corpus
GB12	04.11.2015	37	M	Cholecystectomy due to polyps in the gall bladder. I got a healthy piece of corpus and a healthy piece of fundus.
GB13	28.01.2016	66	M	Adenocarcinoma of the gastroesophaegal junction, Type III. Patient received neoadjuvant chemotherapy before surgery
GB14	26.04.2016	29	F	Cholecystectomy due to presence of gallstone (one big gallstone of heterogeneous composition). Patient of Arab ethnicity. I got a longitudinal section of the

				GB which was divided between fundus, corpus and neck. I also got the bile.
GB15	02.09.2016	-	-	Cholecystectomy due to presence of gallstones
GB16	24.01.2017	65	F	Gastric carcinoma, otherwise healthy GB. Patient underwent gastrectomy.

3.10.1 Isolation and culturing of gall bladder organoids from human tissue

Fix part of the tissue (around 1cm2) in 3.7%PFA, 4°C ON, and then wash 3 times with PBS for eventual paraffinization. Cut 3 small pieces of the mucosa (around 0.5cm2) and snap-freeze in liquid nitrogen. Use the larger part for the isolation of epithelial cells. The protocol for the isolation cells (but not the one for the growth of the organoids) is a modified version of the one published by Auth et al. (Auth et al. 1993).

Place the tissue in a 10cm petri dish filled with PBS and scrape very gently the mucosa side in order to clean it from the residual bile and mucus. Change the PBS and repeat this step 2 or 3 times until the PBS remains clear. Place the tissue in a 10cm dish filled with Collagenase IV, with the mucosa facing the solution, and incubate at 37°C for 10 minutes. After the incubation move the tissue to a new dish and scrape the mucosa with a glass slide kept at 45° in order to release the epithelial cells. Flush the tissue with ADF++ and store the cell containing solution. Place the tissue back in the collagenase containing dish and repeat the incubation and scraping steps twice, saving the released cells in the same tube. Centrifuge the cells 1000g 3min. Resuspend the pellet in 1ml ADF++, transfer to an eppendorf and count the cells using a haemocytometer. Centrifuge again 1000g 3min. Keeping the tube on ice resuspend the pellet in the require amount of matrigel, considering 1 to 3 x10^6 cells in 50ul matrigel per well. Seed 50ul drops per well of a 24-well-plate and incubate for 10min at 37°C to let the matrigel polymerize. Add then 500ul human primary cell medium per well. This method for the isolation of cells yields 2 to 5 x 10^6 cells/cm^2 of tissue. After 5 days the first organoids will begin to form. Replace the medium twice a week.

3.10.2 Human primary cells culture medium

Reagent	Volume (ul) for 1ml medium
ADF++*	720
Rspo1 conditioned medium	250
P/S	10
Noggin	1
EGF (prediluted 1:10)	1
FGF	1
HGF	1
FSK	1
B27	20
N2	10
NIC	10
Tgf-β inhibitor	1
ROCK inhibitor**	3

*ADF++: Advanced/DMEM-F12 supplemented with 1% Glutamax (Sigma), 10mM HEPES (Sigma)

** ROCK inhibitor is added just for the first 5 days of culture

3.10.3 Splitting of organoids

After around one-two weeks of culture the organoids (either murine or human) will become big enough to necessitate shearing. This requires a mechanical and chemical treatment.

Remove the medium from the well, resuspend the matrigel drop in 500ul of ice cold ADF++ (up to four drops can be taken in 1ml of ADF++) and transfer to an eppendorf. Spin down 4500g, 3min, 4°C. Carefully remove the supernatant and matrigel, and resuspend the pellet in 1ml TypLE and incubate in a 37°C water bath for 3 to 4 minutes. During the incubation prepare the Pasteur pipette to use for the mechanical shearing: flame narrow the tip of a glass Pasteur pipette and rinse in ADF++ 5%FCS. With the narrowed pipette, pipette up and down for 7 times. Add 100ml FCS, vortex briefly and centrifuge 1000g, 3min. Wash once with 1ml ADF++ 5%FCS and twice with ADF++ lacking FCS. At this point resuspend the pellet in the required amount of matrigel, taking into consideration that generally a full matrigel drop of murine organoids can be split with a ratio 1:4, while a human with a ratio 1:3.

3.10.4 Freezing and thawing of organoids

Freeze the organoids while they are still small, usually two to three days after seeding. One full well is enough to prepare one freezing vial. Remove the medium from the well, resuspend the matrigel drop in 500ul of ice cold ADF++ (up to four drops can be taken in 1ml of ADF++) and transfer to an eppendorf. Spin down 4500g, 3min, 4°C. Carefully remove the supernatant and matrigel, and resuspend the pellet in 500ul (per starting well) of Cryo-SFM freezing medium (VWR; cat. 10172-414). Transfer the vial in an isopropanol containing freezing container and put at -80°C where it can be kept up to three months. Transfer the vial into liquid nitrogen for long term storage.

For thawing, place the frozen vial in 37°C water bath briefly, until thawed. Transfer the cells containing buffer in an eppendorf tube and spin 100g 3min. Wash once with ADF++, discard the supernatant and resuspend the pellet in the required amount of matrigel.

3.10.5 3D to 2D seeding

Primary GB cells can be grown in 2D on a plastic surface. It is not possible to passage them and the cells lose the polarity, however it can be useful for certain application, for example infection.

Before the procedure collagen coat the required number of wells: add 400ul per well (24-well format) of a solution consisting of 0.02M acetic acid supplemented with bovine collagen type I (GIBCO; cat.: A1064401) 10 µg/cm2 for plastic or 15 µg/cm2 for glass. Incubate the plate for 1h at 37°C, then wash twice with warm PBS.

Two full drops of matrigel are enough to get an almost confluent (~90%) well of a 24-well-plate in 24h. Use the "splitting of organoids" protocol, with the difference that the TrypLE treatment shall last 15 minutes. Seed the resulting single cells on the previously collagen coated plate in the primary cells medium (the medium for the 2D culture is the same as the 3D culture).

3.11 Functional assays

3.11.1 Epithelial barrier functionality assay

Modified version of the protocol described by Elamin (Elamin et al. 2013)

Split a well of organoids and resuspend GB cells in 80ul ice-cold matrigel. Spread the matrigel at the bottom of a 24-well MatTek plate. After 5 days of growing add 1mg/ml FITC-labeled dextran (mw 4kDa. Sigma; cat.: 46944) to the medium for 1h and take a picture (Axiovert35 GFP + spin disc, 15msec exposure). Add 2mM EGTA and take a picture every 1 minutes. EGTA will chelate the Ca^{++} ions used for the tight junction functionality enabling the flow of the dye in the lumen of the organoids.

Measure the FITC signal intensity with the software ImageJ and make a dot plot showing luminal relative fluorescence in time using Microsoft Excel

3.11.2 Organoids' functional assay

This protocol is based on the one described by Tanimizu et al. (Tanimizu et al. 2007). Two wells of GB organoids and one of gastric organoids are necessary. The gastric organoids are grown as described by Schlearmann et al. (Schlaermann et al. 2014). 7 days post seeding incubate the GB and the gastric cells with DMEM/F-12 containing 100 uM rhodamine-123 (Sigma-Aldrich, cat.R8004) for 5 min and wash with three times with PBS.

To show that transport of rhodamine-123 depends on activity of multidrug resistance gene products (mdr), incubated the spheroids with 10 µM R-(+)-verapamil (Sigma-Aldrich, cat. V4629), an mdr inhibitor, for 30 min before adding rhodamine-123.

Place the chamber on the stage of the Leica SP-E confocal microscope, and acquire the images every minute for 30 min. Keep the temperature and CO2 concentration at 37°C and 5%, respectively.

3.12 Infection experiments

3.12.1 Infection and intoxication of cell lines with *Helicobacter hepaticus*

Plate *Hh* on blood agar plates with the required antibiotics (Cam when using the *ΔcdtB* strain), incubate in microaerobic condition at 37°C for 48h, overplate on a new plate and incubate again for 48h.
The day of the overplate (i.e. 2 days before the infection) seed the cells on a 12-well-plate: For HeLa cells the seeding density should be about half of the density required the day of infection. Seed 10x10^4 cells/ml for HeLa cells, 3x10^4 cells/ml for CaCo-2. One day after seeding replace the medium with one lacking FCS. After 24h (i.e. 2 days after overplating the bacteria and seeding the cells) it is possible to infect the cells. Aliquot 1 ml PBS into a sterile microcentrifuge tube and inoculate a small amount of Hh. Wash the bacteria twice by centrifuging 7000g 3 min, discarding the supernatant and resuspending in 1 ml PBS. The last wash resuspend the bacteria in ADF++. Determine the OD at 550nm in order to have a MOI of 100 (see the OD to cfu curve) in the required volume of ADF++. Add the bacteria suspension to the cells and incubate plates at 37°C for 72h to see the cytopathic effect.

To prepare *Hh* supernatant grow the bacteria on a blood agar plate for 24h, harvest with a cotton swab in DMEM, spin down (6000g, 1min), take up the supernatant without disturbing the bacteria and filter it through a 0,45um-pore filter. Apply on cells 100ul supernatant per 1ml of medium, and incubate for 72h

3.12.2 *Salmonella* infection of 2D primary cells

The infection shall be performed when the cells are ~70% confluent.

Grow *Salmonella* enterica Paratyphi A for 8h in 5ml LB (add antibiotics if necessary) with aeration (i.e. 37°C shaking 180rpm). Dilute 1:100 in a tube containing 10ml LB NaCl 0,17M. (add antibiotics if necessary), in microaerobic environment, without shaking for 16h at 37°C (as suggested by Elhadad et al. (Elhadad et al. 2016)). Wash the bacteria twice by centrifuging 7000g, 3min and resuspend the pellet in PBS. The last wash resuspend in 1ml infection medium, then determine the OD600, calculate the cfu to MOI 100 and add the required volume to infection medium (5000ul per 12-well plate; 200ul per 24well plate).

Add the bacteria-containing medium to the cells and spin the plate down 1000g, 5min, RT. Incubate at 37°C for 2h, then perform the gentamycin protection assay: wash the cells twice with 37°C PBS, add 500ul of medium supplemented with 100ug/ml gentamycin to kill the extracellular bacteria and incubate at 37°C 1h.Wash twice with 37°C PBS, use one well to determine the invasion rate of the bacteria, and add to the other wells the infection medium supplemented with 10ug/ml gentamicin for the duration of the experiment (3 days, except for the microarray for which the infection lasted 5 days).

To calculate the invasion rate, 3h after infection (i.e. 1 hour after adding the 100ug/ml Gentamycin for the protection assay) remove the medium to one well and wash twice with 37°C PBS. Add to the cells 1ml 1% TritonX in order to permeabilize the membrane and release the intracellular bacteria. Incubate at room temperature for 2 minutes and plate immediately on LB agar dishes sequential dilutions. Incubate ON at 37°C and calculate the invasion rate as: cfu recovered/cfu used for the infection.

3.12.3 Primary cells infection medium

The primary cells infection medium is like the normal medium, but it lacks P/S (which is replaced by ADF++) and it is supplemented with antibiotics to keep the plasmid selection pressure if needed (e.g. 100ug/ml Amp in case of pOR25)

Reagent	Volume (ul) for 1ml medium
ADF++*	730
Wnt3a 25%	250
Noggin	1
EGF (prediluted 1:10)	1
FGF	1
HGF	1
FSK	1
B27	20
N2	10
NIC	10
Tgf-β inhibitor	1

*ADF++: Advanced/DMEM-F12 supplemented with 1% Glutamax (Sigma), 10mM HEPES (Sigma)

3.12.4 Infection for the microarray comparing w.t. infection, *ΔcdtB* infection and non-infection

Prepare 14 25 cm^2 T-25 flask by collagen coating and seed 0,5x10^6 cells in each.

After 3 days infect 6 flasks with mCherry *Salmonella* w.t. (strain collection X574); 6 flasks with mCherry *Salmonella ΔcdtB* (strain collection X575); one flask with the non fluorescent w.t. bacterium and leave one uninfected.

Do not changed the medium for the whole duration of the infection to avoid losing the toxin which is secreted in the medium. 5 days after the infection perform a FACS sorting in order to isolate the infected cells from the non infected ones.

The infection was performed with organoids form patient hGB13 at passage 10, and repeated at passage 11

3.12.5 *Salmonella* infection of 3D organoids

Start with 2 full wells per condition (around one week post seeding). The day before the infection grow *Salmonella* in 5ml LB + antibiotics (if needed) overnight at 37°C shaking (180 rpm). Dilute the overnight culture 1:33 in fresh LB and incubate for 3.5h (37°C shaking). Shear a well of organoids following the "splitting of organoids" protocol, but with the following modifications: take up to 4 wells in 1ml ice cold ADF++ and transfer to an Eppendorf, spin 4500g 3min 4°C, remove matrigel and resuspend in 1ml ice cold ADF++, shear 5 times with a flame-narrowed Pasteur pipette (without TrypLE treatment). Centrifuge 1000g 3min. Resuspend pellet in the required amount of ADF++ in order to have 200ul of final volume per condition and transfer 200ul of cells in one Eppendorf per condition. To estimate the number of cells take part of the solution, incubate it 15 min with Trypsin 37°C, then pipette up/down 10 times with a flame-narrowed Pasteur pipette in order to get single cells. Calculate the cell concentration counting with a haemocytometer.

Pellet 2ml of bacteria the culture (7000g, 3min) which by now should have reached late log phase and wash pellet twice with 37°C warm PBS. After the last centrifugation resuspend the pellet in 1ml ADF++.

Determine the OD600 and calculate the bacteria dilution to obtain MOI 100. Add the bacteria to the sheared organoids in order to have max 300ul ADF++ of cell suspension + bacteria and incubate in an eppendorf 1h at 37°C (the Eppendorf should be kept horizontal during the infection time to maximize the surface).

After the infection spin down (1000g, 3min), remove the medium and wash twice with warm PBS centrifuging 1000g 3min. Seed in the required volume of matrigel (50ul per well) and incubate at 37°C until the polymerization of matrigel (~10min). Now perform the gentamycin protection assay: kill the remaining extracellular bacteria by adding 500ul of killing medium (infection medium + 100 ug/ml gentamicin) and incubate for 1h at 37°C. Wash with warm PBS, use one well to calculate the invasion rate, and add to the other wells the infection medium supplemented with 10ug/ml Gentamicin for the duration of the experiment.

Calculate the invasion rate with one well: after gentamycin assay break the matrigel with ice cold ADF++, spin (4500g, 3min, 4°C), remove the supernatant and the matrigel, and resuspend in ice cold ADF++. Centrifuge 1000g, 3min, 4°C and discard the supernatant to get rid of the residual matrigel and bacteria. Resuspend the pellet in 1 ml 1% Triton X100 by vortexing and incubate 2 min at RT. Immediately plate different dilutions on LB plates, incubate at 37°C and count the cfu the following day. The invasion rate will be cfu recovered/cfu used for the infection.

3.13 Intoxication experiments

3.13.1 Intoxication of 2D cells with *Salmonella* supernatant

Grow *Salmonella* Paratyphi A from a single colony in 5ml LB overnight, 37°C, 180rpm. Take 200ul of bacteria, spin down (7000g, 3min), resuspended in 10ml MM5.8 and incubate overnight 37°C shaking 180rpm. After the incubation check that the OD600 is 0.4-0.5. If it did not get to that point keep growing the bacteria, but do not

let them reach the lag phase. Spin down 7000g, 5min, 4°C and filter sterile the supernatant (0,22um pores-filter). Concentrate the supernatant 20 folds using the columns Amicon Ultra-15 (Millipore cat.: UFC903024) by spinning 2000g, 4°C for as long as needed (start with 5min). If needed adjust the volume with sterile MM5.8. Dilute the supernatant in the standard primary medium 1:20 and add to the cells. Incubate for 24h (unless stated otherwise). As a positive control 24 hours before harvesting treat one well with 50uM etoposide.

3.14 FACS sorting experiments

3.14.1 Sorting of infected cells for the microarray comparing w.t. infection with non-infection and w.t. infection with *ΔcdtB* infection

After 5 day-infection with mCherry expressing bacteria, wash the flask with 3ml 37°C PBS, add 2ml Trypsin-EDTA and incubate at 37°C for 10 min. Harvest the detached cells in a falcon tube. Add 5ml DMEM 5%FCS to inactivate the trypsin, spin 4°C, 1000g, 3min and discard the supernatant. Resuspend the pellet in 500ul Sorting buffer (1X PBS without Ca, Mg; 1% FCS; 10mM HEPES, pH 7.2; 10ug/ml DNAse I (corresponds to 10U/ml)) and pass the cells through the strainer on the cap of the sorting tube (Falcon 352235). Put the tubes on ice and run the sorting.

The FACS sorting was performed by the FACS core facility of the DRFZ, using the FACS ARIA (BD biosciences).

Cells infected with the bacteria were sorted according to the fluorescence given by the intracellular *Salmonella* expressing mCherry. At the beginning of the sorting the tube with the cells infected with the non-fluorescent bacteria was used as a control to check the size of the cells and set the gating.

3.15 Protein techniques

3.15.1 SDS-polyacrylamide gel electrophoresis (SDS-PAGE) and Western blot

Prepare the solutions and pour the Running Gel. Wait for 20min for it to polymerize, add the Staking Gel on top, the comb and wait 10min for the polymerization

Running Gel (for 2 gels)

	12% Acrylamide	15% Acrylamide
Acrylamide/Bis-acrylamide 30%/0.8%	3.9ml	4.95ml
Resolving Gel Buffer	3.76ml	3.76ml
H_2O	2.46ml	1.31ml
10% SDS	100ul	100ul
10% APS	80ul	80ul
TEMED	8ul	8ul

Staking Gel (for 2 gels)

Acrylamide/Bis-acrylamide 30%/0.8%	1ml
Staking Gel Buffer	500ul
H_2O	2.4 ml
10% SDS	40ul
10% APS	40ul
TEMED	5ul

After the gel is ready, place it in the running apparatus, pour the running buffer in both the chambers and load the samples.

Run the gel at 70V until the front reaches the running gel, then increase the voltage up to 120V.

Once the running is complete, disassemble the cast and soak the gel in the wet-blot-transfer buffer. Activate the PVDF membrane in methanol 2min, then store it in wet-blot-transfer buffer for at least 5min.

Prepare the transfer sandwich (make sure everything is wet in the buffer) in the cassette in this order: + (transparent side), sponge, whatman paper, membrane, gel, whatman paper, sponge, - (black side). Transfer it to the transfer apparatus, fill it with wet-blot-transfer buffer and run it at 4°C 250mA, 2.5h.

After the transfer block the membrane with 5% Milk in TBS-T for 1h, RT, shaking, then soak it in the primary antibody and incubate 4°C ON rolling. The following day wash 3 times 5min in TBS-T, incubate it in secondary antibody (HRP conjugated) 1h, RT, shaking and wash it once more 3 times 5min in TBS-T. Develop the membrane using the ECL detection system

3.15.2 Manual paraffinization of organoids

Break up the matrigel with ice cold ADF++, transfer in a glass tube on ice and wait for the organoids to settle down by gravity. Wash in this way two more times, then bring to RT and fix with pre-warmed (37°C) 3.7%PFA 1h RT. Wash with PBS twice always letting the organoids settle by gravity in order to keep the structure.

Now it is necessary to dehydrate. Wash the organoids in this sequence: 70% EtOH, 80% EtOH, 90% EtOH, absolute EtOH, 100% isopropanol, 100% acetone, and again 100% acetone. Each wash should last 20 minutes. Carefully transfer the organoids in acetone into a paraffin embedding jar (metal), remove almost all the acetone, transfer metal jar with organoids to 60°C heating plate, add molten paraffin and let stand for 10min at 60°C. Transfer to cooling plate, add a labeled lid of a plastic embedding cassette and incubate for 1h to get solid. Specimen are now ready for microtome sectioning.

3.15.3 Paraffinization of tissue

After fixation of the tissue (3.7% PFA, 4°C ON), place it in an embedding cassette and transfer it to a Leica TP1020 tissue processor set to wash the tissue in this order, each wash lasting 1h: 70% EtOH, 80% EtOH, 90% EtOH, absolute EtOH, 100% isopropanol, 100% acetone, again 100% acetone, paraffin and again paraffin. When the cycle is finished transfer the tissue to a metal jar placed on a 60°C heating plate, add molten paraffin and transfer to cooling plate, add a labeled lid of a plastic embedding cassette and incubate for 1h to get solid. Specimen are now ready for microtome sectioning.

3.15.4 Immunofluorescence of paraffin sections

With a microtome make 5um sections and transfer them to HistoBond slides (Marienfeld, cat. 0810000). Rehydrate the sections washing them in this order: twice with xylene, 10 min each time, then 100% EtOH, 90% EtOH, 70% EtOH, 50% EtOH, H_20 and again H_2O. Each wash should last 2 min. Now transfer the slide to pre-

warmed 95°C antigen retrieval solution (Dako, cat. S1699) and incubate for 30min. After the incubation let cool down at RT, wash 10 times with running water and a final time with ddH_20. Carefully wipe the water around the organ piece and circle around it with a Pap pen (Biozol, cat. CED-MU12). Add 50ul IFF and block by incubating 60min in a moisten chamber. Remove the IFF, add the primary antibodies previously diluted in IFF and incubate ON in a moisten chamber. The following day wash with PBS-T 3 times, 2min and then add the fluorochrome linked secondary antibodies together with the required dyes diluted in IFF. Incubate 60min in a moisten chamber in the dark. After the incubation wash 3 times, 3min with PBS-T and one time with water. Mount the slide with mowiol, place on top a coverslip, let dry and acquire images at a confocal microscope.

3.15.5 Immunofluorescence of 2D cells

After performing the experiment (cells should be grown on a glass coverslip), wash the cells twice with PBS, fix in PFA 3.7%, 30min, RT and wash twice with PBS. Add 50ul IFF on top of the coverslip and block for 1h RT in a moisten chamber. Dilute the primary antibodies in IFF, add a 50ul drop on the coverslip and incubate 90min RT. Wash 5 times 3 min with PBS-T and add the fluorochrome-linked secondary antibodies and the other dyes diluted in IFF. Incubate 60min in the dark, wash 3 times 5min with PBS-T and once with H_20. Mount the coverslip with mowiol on a glass slide, let it dry and acquire the picture at the confocal microscope.

3.15.6 Whole mount immunofluorescence of organoids

After performing the experiment, block the organoids with 1ml of 3.7% PFA without disrupting the matrigel drop. Incubate 30min RT, then wash with PBS 1h, 3 times. Block in 3D blocking buffer ON at RT. Dilute the fluorochrome-linked antibodies and the dyes in the 3D blocking buffer and incubate ON at RT in the dark. Wash with blocking solution 1h 3 times, mount the matrigel drop with Vectashield (Vecta cat. H-12000) on a glass slide and acquire the images at the confocal microscope.

3.17 RNA techniques

3.17.1 RNA isolation

Total RNA was Isolated with Trizol (Invitrogen cat.: 15596026) following the manufacturer´s protocol using Glycogen as co-precipitant. Quality control and quantification of total RNA was assessed using an Agilent 2100 Bioanalyzer (Agilent Technologies) and a NanoDrop 1000 UV-Vis spectrophotometer (Kisker).

3.17.2 Microarray

The microarray was performed by the Microarray core facility of the MPIIB (Dr. Hans-Joachim Mollenkopf), and the extraction of the data was performed by Dr. Hilmar Berger (bioinformatician of the MPIIB, department of molecular biology). Microarray experiments were performed as independent dual-color dye-reversal color-swap hybridizations using two biological replicates, each. Total RNA was amplified and labeled with the dual-color Quick-Amp Labeling Kit (Agilent Technologies). In brief, mRNA was reverse transcribed and amplified using an oligo-dT-T7 promoter primer and labeled with cyanine 3-CTP or cyanine 5-CTP. After precipitation, purification, and quantification, 0.75 µg of each labeled cRNA was fragmented and hybridized to custom whole genome human 8 × 60k multipack microarrays (Agilent-048908) according to the supplier's protocol (Agilent Technologies). Scanning of microarrays was performed with 3 µm resolution using a G2565CA high-resolution laser microarray scanner (Agilent Technologies). Microarray image data were processed with the Image Analysis/Feature Extraction software G2567AA v. A.11.5.1.1 (Agilent Technologies) using default settings and the GE2_1105_Oct12 extraction protocol. The extracted dual-color raw data txt files were further analyzed using R and the associated BioConductor package limma (Ritchie et al. 2015). Microarray data have been deposited in the Gene Expression Omnibus (GEO; www.ncbi.nlm.nih.gov/geo/) of the National Center for Biotechnology Information and can be assessed with the GEO accession number GSE100656.

The analysis of the results was done using Microsoft Excel, the software TIBCO Spotfire was used to create volcano plots.

The “average expression” of each gene is given as log2 intensity. It was calculated as the average of the individual dye-swap, which was then averaged between replicates.

3.18 DNA techniques

3.18.1 PCR for detection

For the detection of the presence and length of a particular DNA fragment, use GoTaq polymerase kit (Promega, M7122).

Prepare the PCR reaction mix on ice,

component	Final concentration	Volume for 50ul final volume
5X green GoTaq Flexi buffer	1x	10ul
$MgCl_2$ solution, 25mM	1mM	2.5ul
dNTP mix 10mM each	0.2mM each	1ul
Upstream primer, 10uM	0.5uM	2.5ul
Downstream primer, 10uM	0.5uM	2.5ul
GoTaq polymerase	1.25U	0.25ul
Template DNA	0.5ug genomic, 10ng plasmid	Variable
H_20	-	To 50ul

Transfer the tubes to a thermocycler with the following settings:

step	temperature	time	Number of cycles
Initial denaturation	95°C	2min	1
Denaturation	95°C	1min	35
Annealing	42-65°C dependent on primers' Tm	1min	
Extension	72°C	1min/kb	
Final extension	72°C	5min	1
Keep	4°C	forever	1

Run 5-10ul on an agarose gel to check for the size of the fragment

3.18.2 PCR for cloning

For cloning applications there is the need of a polymerase with proofreading activity. Usedthe Phusion High-Fidelity PCR kit (NEB, cat. E0553).

Prepare the PCR mix on ice

component	Final concentration	Volume for 50ul final volume
5X HF buffer	1x	10ul
dNTP mix 10mM each	0.2mM each	1ul

Upstream primer, 10uM	0.5uM	2.5ul
Downstream primer, 10uM	0.5uM	2.5ul
Phusion HF polymerase	1U	0.5ul
Template DNA	0.5ug genomic, 10ng plasmid	Variable
H_20	-	To 50ul

Transfer the tubes to a thermocycler with the following settings:

step	temperature	time	Number of cycles
Initial denaturation	98°C	30sec	1
Denaturation	98°C	10sec	35
Annealing	45-72°C dependent on primers' Tm	30sec	
Extension	72°C	30sec/kb	
Final extension	72°C	10min	1
Keep	4°C	forever	1

Dilute 2ul of product with 8ul H20 + 1ul of 10x loading dye (promega G1881) and run on an agarose gel to check for the size of the fragment. If needed purify the rest with GeneJET PCR purification kit (Thermo Scientific, cat. K0701) following manufacture's protocol.

3.18.3 Agarose gel electrophoresis

To check for the quality and size of the fragment, run the PCR product (or other DNA probes) on a 1 to 5% agarose gel (low melting LE agarose (Biozym, cat. 840000) in 0.5x TAE buffer) at 100V, until the front of the buffer reached the bottom of the gel. Purify it with with GeneJET gel extraction kit (Thermo Scientific, cat. K0691) following manufacture's protocol.

3.18.4 Restriction cut and ligation

All the restrictions were performed with FastDigest enzymes produced by Thermo Scientific.

In a 0.5ml PCR tube add 1u of enzyme per 1ug of template DNA + 3ul 10x FastDigest buffer (Thermo Scientific, cat. B64) + H20 to 30ul.

If a plasmid backbone has to be cut for cloning procedures, add in the mixture 1ul of Thermosensitive Alkaline Phosphatase FastAP (Thermo Scientific, cat. F0652) per 1ug of template DNA. The phosphatase removes the phosphate group from the 5' of the DNA in order to prevent the re-circularization of the plasmid. Cut also the insert with the same restriction enzyme(s), but there is no need not add FastAP. Incubate the two tubes in a 37°C water bath for 30min.

To ensure that the cut took place, run the product on agarose gel and check the size. Purify the desired band with GeneJET PCR purification kit (Thermo Scientific, cat. K0701), or, if only one band is observed, with GeneJET gel extraction kit (Thermo Scientific, cat. K0691) following manufacture's protocol.

After the purification, ligate the insert to the backbone using T4 ligase kit (NEB, cat. 0202). Prepare the mix: 1ul T4 ligase + 2ul 10X T4 DNA Ligase Reaction Buffer + Insert DNA + backbone DNA + H_20 to 20ul. The molar ratio backbone : insert should be 1:3, with 50ng of backbone. Incubate at 16°C ON. The following day transform *E. coli*

to produce the plasmid. The molar ratio calculator used was the one of the "in silico" website: http://www.insilico.uni-duesseldorf.de/Lig_Input.html

3.18.5 Transformation of *E.coli* and selection of positive clones

Chemical competent *E.coli* TOP10F were prepared as described by Inoue et al. (Inoue et al. 1990). Briefly, bacteria were grown in 250ml SOB medium at 18°C to OD550 of 0.5. They were centrifuged 2000g, 20min, 4°C, and the pellet was resuspended in ice-cold ITB. The bacteria were washed twice more in this way, then the pellet was resuspended in 20ml ITB + 1.5ml DMSO. 50ul aliquots were prepared on ice and stored at -80°C.

For the transformation, thaw a vial of competent *E. coli* keeping it on ice for 10min, then add the DNA (1ng of plasmid, or 3ul of the ligated product) and incubate 30min on ice. Heath shock by transferring the tube in a 42°C water bath for 42sec, then put on ice for 2min. Add 1ml of 37°C LB (without selection) and incubate at 37°C for 1h with aeration: this will lead to the expression of the resistance harbored in the vector. Plate 100ul on an LB agar plate with the required antibody added. Spin the rest of the tube 7000g, 3min, remove the supernatant, resuspend the pellet in 100ul LB and plate it. Incubate the two plates at 37°C ON. The following day select 5 colonies to be tested by picking them with a tip, incubating them in 5ml LB + antibody and growing them at 37°C, shaking, for 8h. Extract the DNA using the kit QIAprep Spin Miniprep Kit (Qiagen, cat. 27104) following manufacture's protocol. Select the correct transformant by PCR and/or enzymatic cut. Grow the positive clone in 100ml LB + required antibody 37°C ON shaking. The following day prepare a frozen stock in LB supplemented with 5%FCS and 15% glycerol and purify the vector using QIAGEN Plasmid Midi Kit (Qiagen, cat. 12125).

3.19 *in vitro* analyses

3.19.1 Statistical analysis

Statistical analyses were performed with the software Graphpad Prism 7. P values were calculated using Student´s t test. A result is considered significant when the p value was <0.05. The asterisks represent the following p values:

P value	Summary
< 0.0001	****
0.0001 to 0.001	***
0.001 to 0.01	**
0.01 to 0.05	*
≥ 0.05	ns

3.17.3 Gene Set Enrichment Analysis (GSEA)

The GSEA was performed by Dr. Hilmar Berger (bioinformatician of the MPIIB, department of molecular biology).

For the first analysis we used a gene set of β-catenin target genes published previously (Herbst et al. 2014) and performed GSEA on genes pre-ranked by gene expression-based t-score between early and differentiated organoids, using the fgsea R package (Sergushichev 2016) with 5,000 permutations.

For subsequent analysis I used the list GO_INFLAMMATORY_RESPONSE from the gene set enrichment analysis database (http://software.broadinstitute.org/gsea/msigdb/geneset_page.jsp?geneSetName=GO_INFLAMMATORY_RESPONSE) and performed GSEA on genes pre-ranked by gene expression-based t-score between infected and uninfected 2D primary cells, using the fgsea R package (Sergushichev 2016) with 5,000 permutations.

4. RESULTS

4.1 Establishment and characterization of murine gall bladder organoids

4.1.1 Establishment of murine gall bladder organoids

At the start of this study no murine gall bladder organoid model was yet described in the literature. In addition, murine primary material was more easily available compared to human, therefore the establishment of a murine organoid model was regarded as a starting point, to then turn to human organoids.

Gall bladders from C57BL mice (Figure II - 1 A) were obtained following sacrifice of the animals by cervical dislocation. The gall bladders were emptied of bile (if present), cut into small pieces and cells were isolated following enzymatic and mechanical treatment. Isolated cells were seeded in matrigel and provided with a defined medium based on the one previously used to grow small intestine primary cells (Sato & Clevers 2013). Briefly, it contained DMEM-F12 and included 25% R-spondin 1 conditioned medium, B27, N2, noggin, murine epidermal growth factor (mEGF), nicotinamide (NIC), A 83-01 (a TGF-β Type I receptor ALK-5 inhibitor) and Y-27632 (inhibitor of the kinase ROCK).

After 2 to 4 days some isolated cells started to give rise to hollow 3-dimensional structures (Figure II - 1 B arrowhead). The medium was changed twice per week, and once per 7-10 days the culture was split. The splitting process consisted in separating the fully grown organoids from the matrigel and breaking them to fragments or single cells by enzymatic and mechanical dissociation. After re-seeding in matrigel and supplementing with the defined medium, organoids re-formed within 2/3 days. In this way it was possible to keep the culture for an indefinite time, without any apparent phenotypical change (Figure II - 1 B).

To check the organoid forming efficiency, that is the ratio of seeded cells giving rise to an organoid, organoids at passage 0 (the ones originating from the isolated cells) were split to single cells, and 500 to 800 cells were seeded in a matrigel drop. After one week the number of resulting organoids was counted. After 18 passages, which corresponds to 6 months, the procedure was repeated (Figure II - 1 C).

The organoid forming efficiency remained stable over time: 8-10% of the seeded cells gave rise to organoids, meaning that the primary medium, together with the support given by the matrigel, is able to maintain the adult stem cell potential over time.

Another proof of the stability of murine organoids was given by the expression of the proliferation marker PCNA. The murine organoids were fixed, paraffinized and immunostained with an antibody recognizing PCNA at passage 1 and 19 (Figure II - 1 D). The quantification of PCNA positive cells (Figure II - 1 E) verified that there is no senescence associated with the long term cultivation of murine gall bladder epithelial cells in the form of organoids: 35% of the cells were in active state of proliferation regardless of the age of the organoid.

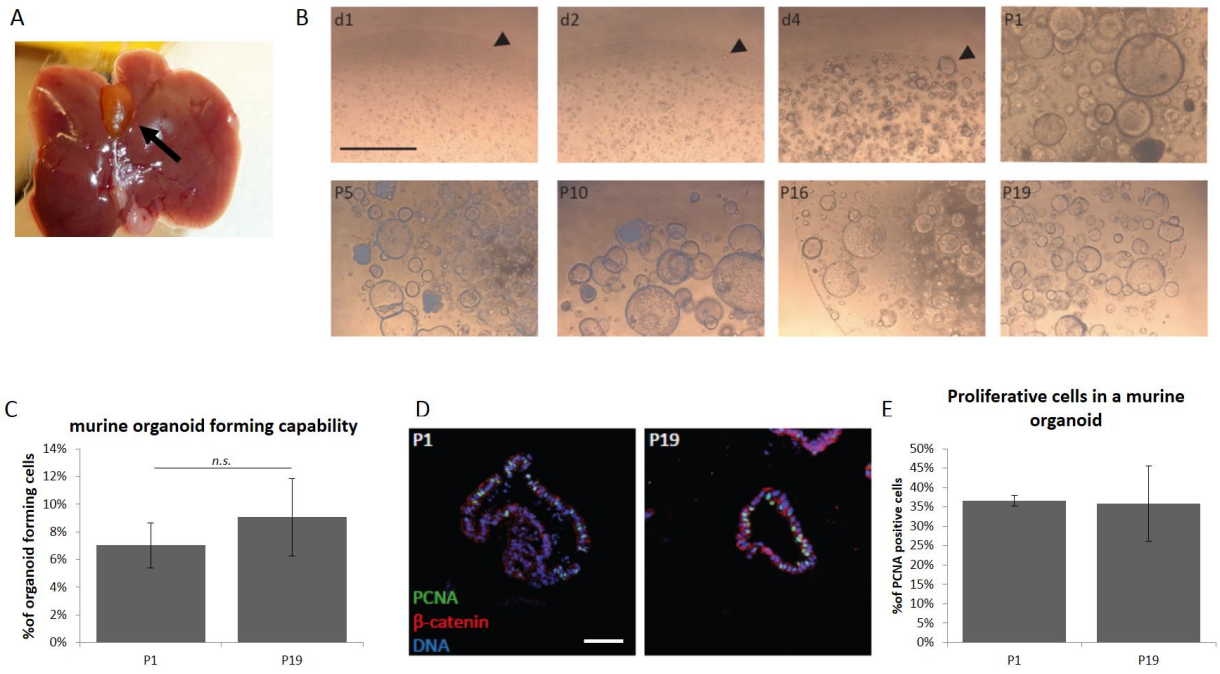

Figure II - 1 Generation and stability of murine gall bladder organoids. (A) The murine gall bladder is visible between the two lobes of the liver (arrow). (B) Pictures taken at different days after seeding and at different passages. Passage 19 is 6 months after initial isolation. Arrowhead points to a single isolated cell growing into an organoid. Scale bar is 1mm. (C) Quantification of organoid forming cells confirming the stability of the model. Bars indicate SD. (D) Paraffinized section of murine organoids at passage 1 and 19 immunostained for PCNA (green), β-catenin (red) and DRAQ5 to stain the DNA (blue). Scale bar is 50um. (E) Quantification of PCNA positive cells at passage 1 and 19. Bars indicate SD.

4.1.2 Phenotypical characterization and stability of murine gall bladder organoids

After successful establishment of the culturing protocol, the organoids were characterized in terms of protein markers to ensure the epithelial and gall bladder identity. Because no univocal marker exists for the gall bladder, a combination was selected: all markers are overexpressed in the gall bladder compared to other organs (Kampf et al. 2014; van Klinken et al. 1998; Kuver et al. 2007).

Paraffinized sections of the gall bladder were compared to organoids´ sections. They were stained with one gall bladder marker at a time (in red), together with the epithelial marker E-cadherin (in green), and DRAQ5 to stain the nucleus (in blue) (Figure II - 2 A).

The luminal portion of the gall bladder mucosa consists of a simple columnar-epithelial layer of cells. Similarly gall bladder organoids were found be formed by a single layer of purely epithelial cells, as seen by the expression of E-cadherin by all of the cells (Figure II - 2 A). Like the organ, the cells were polarized, shown by the basolateral staining of E-cadherin and by the slightly eccentric nuclei.

Gall bladder typically expresses Cytokeratin-19 (CK-19) (Kuver et al. 2007), and this marker was also found in the cytoplasm of organoids´ cells, localized particularly on the apical side (Figure II - 2 A, left column). Claudin-2 (Cla-2) is a tight junction protein highly expressed in the gall bladder if compared to other organs, including the highly similar bile ducts´ cholangiocytes (Németh et al. 2009). Its localization confirmed not only the identity of the primary cells, but also their polarity (Figure II - 2 A, central column), the apical side of the cells facing the lumen. As a mucosal layer, one of the roles of the gall bladder epithelial cells is to produce mucus, MUC5B representing one of the most abundant mucin (Kampf et al. 2014; van Klinken et al. 1998). Expectedly, its expression was detected in both the organ and the organoids (Figure II - 2 A, right column).

Traditional techniques of primary cells cultivation were frustrated by fibroblast outgrowth (Jones 2008). To exclude this possibility, organoids were probed via western blot for the epithelial marker E-cadherin and for the fibroblast marker vimentin at passage 1 and at passage 19 (Figure II - 2 B and C). The stability of E-cadherin and the absence of vimentin, even in the late passages, ensured the stability of epithelial identity. Most importantly, the stability

of the gall bladder-specific markers CK-19 and Cla-2(Figure II - 2 B) verified that the identity of the organoids did not change in time.

Once the murine organoids were established, the focus was moved to the human organoids, which are of central importance for this dissertation, as human gall bladder is the natural niche for chronic *Salmonella* carriage and eventually gall bladder cancer.

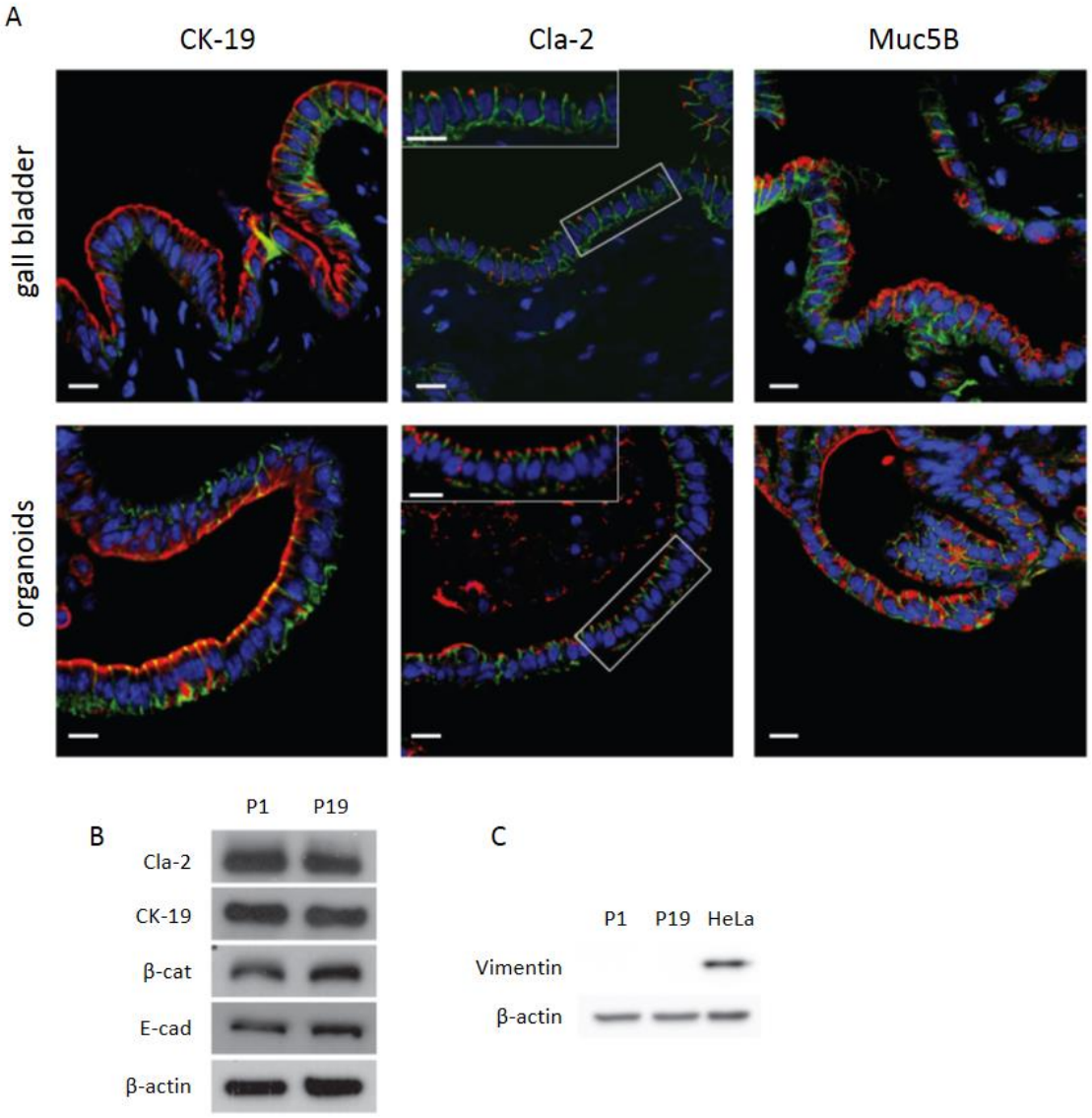

Figure II - 2 Characterization of murine gall bladder organoids. (A) Immunostainings of paraffinized sections of murine gall bladder and organoids (fixed 7 days post seeding). CK-19, Cla-2 and Muc5B in red, E-cadherin in green, DRAQ5 stains the nuclei in blue. Scale bar is 10um. (B) Western blots of the mentioned markers to verify the stability of the organoids. Proteins extracted at passage 1 and 19 (*i.e.* 6 months after isolation), 7 days post seeding. (C) Western blot to verify the absence at any time of the mesenchymal marker vimentin. HeLa cell extract used as positive control.

4.2 Establishment of human gall bladder organoids and their dependence on Wnt/β-catenin pathway activation

4.2.1 Establishment of human gall bladder organoids

Clinical sources of human material were cholecystectomies (surgical removal of the gall bladder) performed at the Charité Campus Virchow-Klinikum by Dr. Sascha Chopra and Dr. Sven Schmidt. The patients underwent the surgery due to presence of gall stones or gastric cancer. In case of gastric cancer the cholecystectomy was performed on a healthy gall bladder as a preventive measure.

Tissue samples were collected and kept in PBS on ice for up to 2 hours before processing (Figure II - 3 A). For each sample, four 0.5cm x 0.5cm pieces were cut and stored dry in liquid nitrogen; four 1cm x 0.5cm pieces were fixed in 3.5% PFA and paraffinized, and cells were isolated from the mucosa of the remaining tissue.

Five different techniques were tested for the isolation of cells. 1 - following a protocol based on collagenase IV incubation (30min, 37°C) and scraping of the tissue, slightly modified from Auth et al. (Auth et al. 1993); 2- trypsin incubation (30min, 37°C) and scraping the tissue, modified from Plevris et al (Plevris et al. 1993) who used it for isolation of gall bladder cells from bovine tissue; 3 - collagenase II incubation (30min, 37°C) and scraping; 4 – collagenase I incubation (30min, 37°C) and scraping; 5 – mincing the tissue, incubating with collagenase IV (30min, 37°C) and pipetting up/down to release the cells.

The protocol which gave the highest cell yield was using collagenase IV incubation and then scraping (2 to 5 x 10^6 cells/cm^2 of tissue. Described in detail in the methods section 3.10.1).

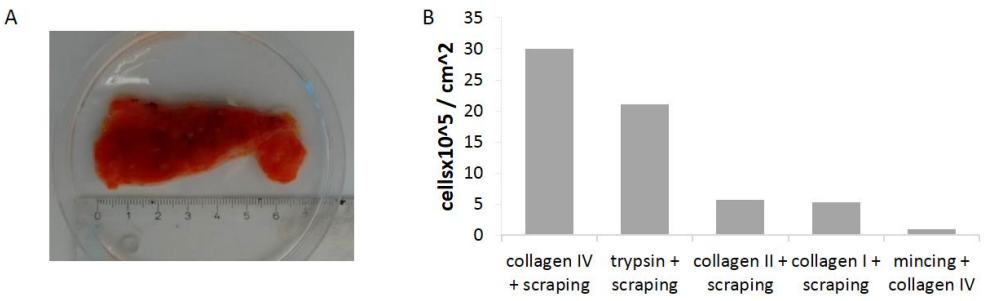

Figure II - 3 Isolation of cells from the human gall bladder. (A) Picture of a gall bladder tissue. (B) Cells were isolated from the tissue following different protocols and the yield was calculated as number of extracted cells/cm^2

1 to 3 x 10^6 isolated cells were seeded in a 50ul matrigel drop, and provided with a defined medium which was a modified version of the one described by Huch and colleagues (Huch, Dorrell, et al. 2013). The medium was based on DMEM-F12 and included 25% R-spondin 1 conditioned medium, B27, N2, noggin, human epidermal growth factor (EGF), fibroblast growth factor 10 (FGF-10), hepatocyte growth factor (HGF), forskolin (FSK), nicotinamide (NIC), A 83-01 (a TGF-β Type I receptor ALK-5 inhibitor) and Y-27632 (inhibitor of the kinase ROCK) for the first 4 days after seeding. In this medium organoids started to form within one week (Figure II - 4 A). The medium was changed twice per week, and every 10 to 14 days the culture was split. After re-seeding in matrigel and supplementing with the defined medium, organoids re-formed within 3 or 4 days. In this way it was possible to keep the culture for at least 6 months without any phenotypical change (Figure II - 4 A).

The immunostaining of paraffinized section with the proliferation marker Ki67 verified that both at an early and late time point (passage 2 and passage 10 respectively) cells comprising the organoids were actively proliferating (Figure II - 4 B).

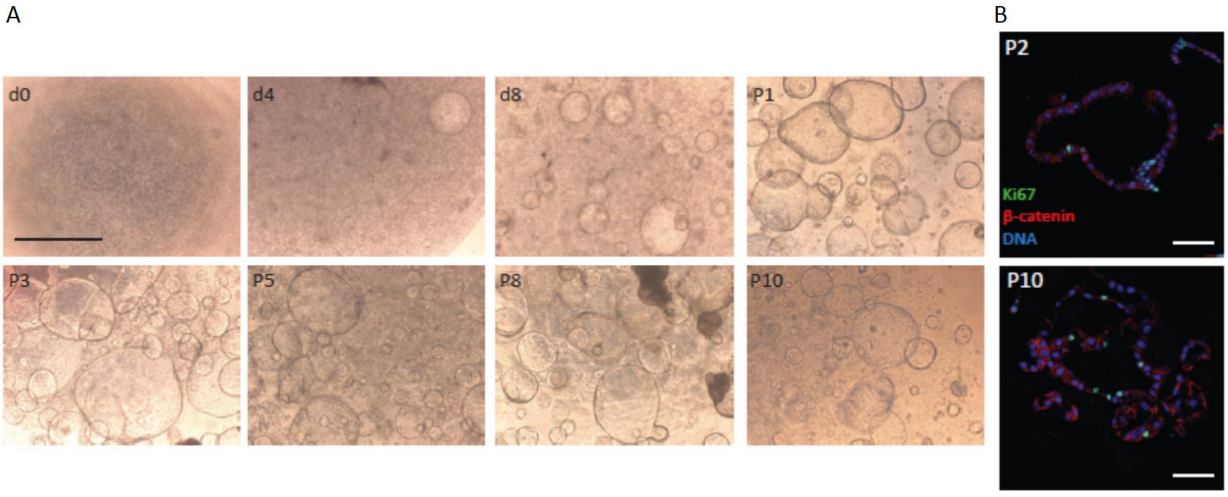

Figure II - 4 Generation of human gall bladder organoids. (A) Pictures taken at different days after seeding and at different passages. Scale bar is 1mm. (B) Paraffinized section of human organoids at passage 1 and 10 immunostained 7 days post seeding for Ki67 (green), β-catenin (red) and DRAQ5 to stain the DNA (blue). Scale bar is 50um.

4.2.2 Requirement of exogenous R-spondin and endogenous Wnt

The maintenance of gastrointestinal organoids usually requires the addition of the Wnt/β-catenin ligands Wnt and R-spondin. To test whether this was a requirement for human gall bladder organoids, primary cells were cultivated in different media with the addition of combinations of 25% Wnt3a and 25% R-spondin1 conditioned media. Organoids at passage 2 were split to single cells, 1000 to 2000 cells were seeded in matrigel, supplemented with the different media and the resulting organoids were counted after 7 days (Figure II - 5 A top row). Organoids were kept in cultivation in the different media for 8 more passages, and the counting was repeated to assess if the media are able to stably maintain the culture (Figure II - 5 A bottom row).

The quantification of organoid forming cells revealed that R-spondin is essential. Without it the organoid forming efficiency drops, and the primary cells stop proliferating after a few passages, even if Wnt is added. Wnt on the other hand seems dispensable, or even slightly deleterious (Figure II - 5 B).

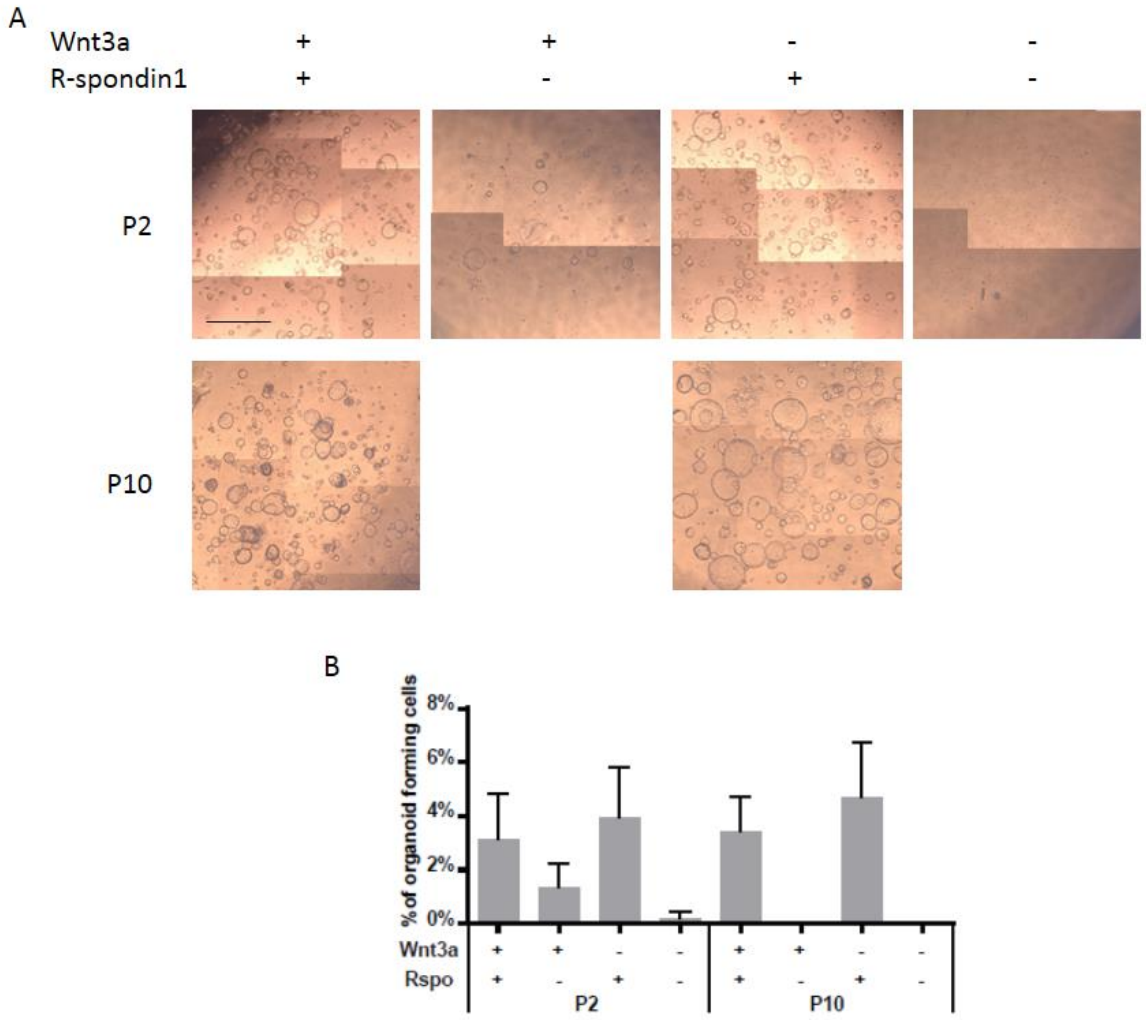

Figure II - 5 Requirement of the addition of R-spondin 1 and Wnt3a for the growth of gall bladder organoids. (A) Pictures of gall bladder organoids grown in media with different combinations of Wnt and Rspo taken 7 days post seeding. Scale bar is 1mm. (B) quantification of organoid forming cells in the different media at passage 2 and at passage 10. Bars are SD

4.2.3 Inhibition of Wnt secretion

Given that the addition of exogenous Wnt is not essential, I tested whether the growth of gall bladder epithelial cells was dependent on endogenously produced Wnt. This is the case, for example, of small intestinal organoids, in which Paneth cells produce enough Wnt to maintain the stem cell niche (Sato, van Es, et al. 2011). Given that gall bladder and small intestine share the same embryonic foregut origin, it was reasonable to speculate that also gall bladder epithelial cells could produce and secrete endogenous Wnt.

In order to test this, IWP2 was added to the medium. IWP2 is an inhibitor of Porcupine that prevents Wnt palmitoylation therefore its secretion. Organoids were split to single cells, 500 to 1000 were seeded in matrigel and provided with a medium containing Wnt and IWP2 in different combinations. After 7 days (Figure II - 6 A) the resulting organoids were counted and the ratio of organoid forming cells was calculated (Figure II - 6 B).

IWP completely abolished the growth of primary cells, pointing out a central role of Wnt. If exogenous Wnt3a (25% conditioned medium) was additionally added to the medium it was possible to partially recover the growth.

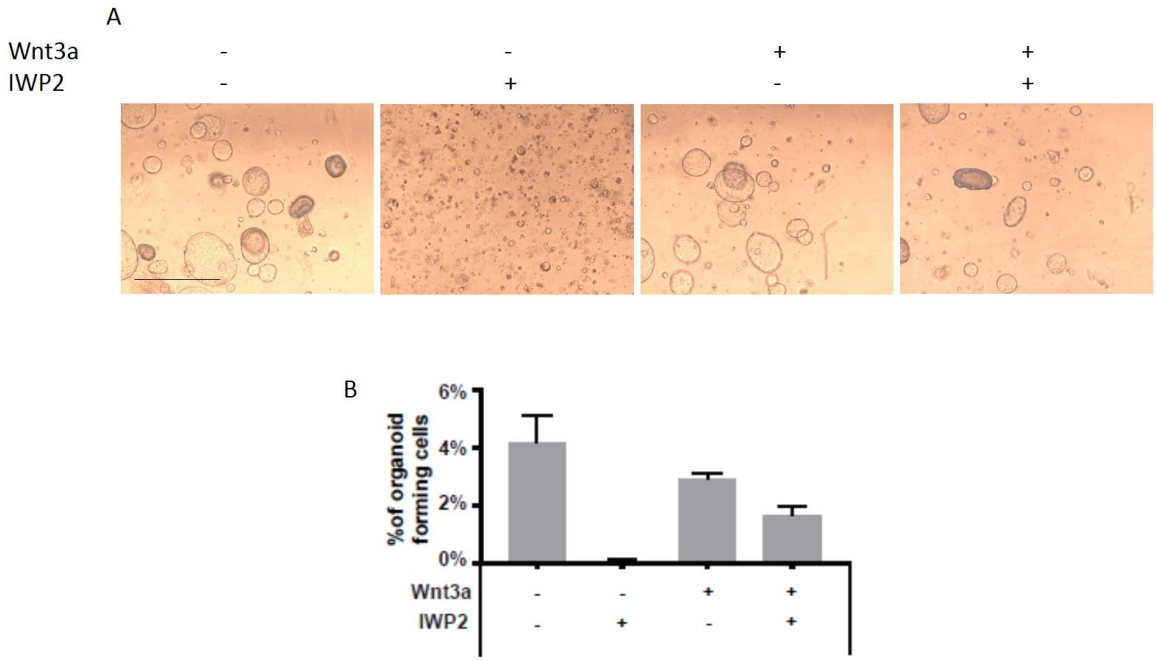

Figure II - 6 Inhibition of Wnt secretion. (A) Pictures of gall bladder organoids grown in media with different combinations of Wnt and IWP2 taken 7 days post seeding. Scale bar is 1mm. (B) Quantification of organoid forming cells in the different media. Bars are SD

4.2.4 Identification of the produced Wnts

To precisely identify the Wnts produced by the organoids, and to test whether particular Wnts were linked with stemness, a microarray was performed comparing early with late organoids. Early organoids were harvested at 4 days post seeding, and were considered to be enriched in stem cells, while late organoids were harvested at 14 days post seeding and were considered to be enriched in mature, differentiated cells (this hypothesis is verified in section 4.2.9). The list of Wnt family genes (HGNC ID 360 found here: http://www.genenames.org/cgi-bin/genefamilies/set/360) was compared with the results of the microarray.

The analysis (Figure II - 7 A) revealed that the most expressed Wnts are: Wnt7A, 7B, 4, 11 and 3. In particular Wnt 7a and Wnt7b, known activators of the canonical Wnt/β-catenin pathway (Davis et al. 2008), seemed to correlate with the adult stemness. Wnt4, on the other hand was found to be expressed only by differentiated organoids.

This partial switch in Wnt expression (Figure II - 7 B) indicates that different types of cells are secreting specific Wnt proteins. Wnt7a and b, due to their abundant expression in early organoids, might play specific role in stem cells self-maintenance.

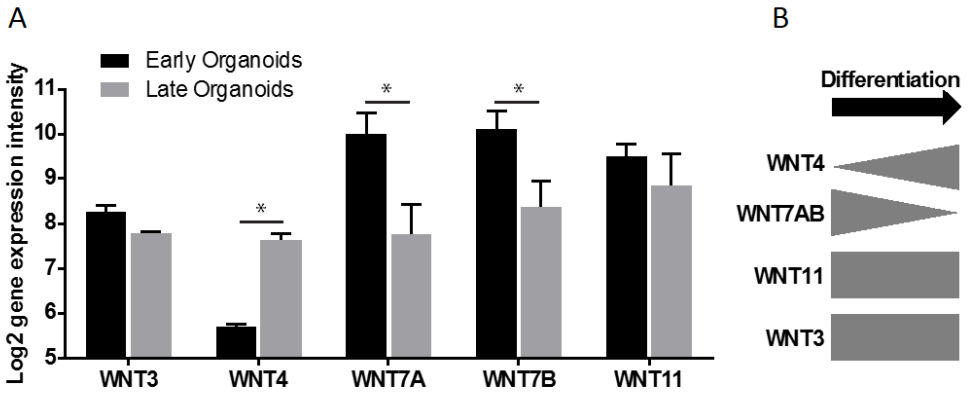

Figure II - 7 Wnt family proteins expressed by early and differentiated organoids. (A) Expression level of the Wnt family genes generated from the microarray analysis, filtered by average expression>6. The stars represent the genes which are differentially expressed between early and late organoids (p value<0.05). (B) Model of Wnt production during differentiation. Through differentiation from adult gall bladder stem cell to differentiated cell, the production of the Wnt family members changes. Wnt7a and b decrease, while Wnt4 starts to be produced. The expression of Wnt3 and Wnt11 is stable

4.2.5 *In vitro* activation and lineage tracing of the Wnt response gene Axin2

Axin2 is one of the few universal Wnt target genes (MacDonald et al. 2009) and its transcription is used to monitor the activation of the Wnt/β-catenin pathway (Jho et al. 2002; Ku et al. 2016).

To test the functionality of the produced Wnt, I temporarily turned to murine material in order to perform a lineage tracing experiment. Organoids were derived from an Axin2 reporter mouse: the cells of the mouse normally express mTomato, switching to mGFP in cells positive for Axin2, when 4-hydroxytamoxifen (HT) is added. Because the switch mTomato to mGFP takes place at a genome level, the GFP expression is inherited by progenitor cells.

Two days of *in vitro* HT induction led to the switch in colour of most of the cells of the organoids (Figure II - 8 A), pointing out a ubiquitous and homogeneous presence of secreted Wnt. As expected the mGFP expression was kept in progeny organoids (Figure II - 8 B and C)

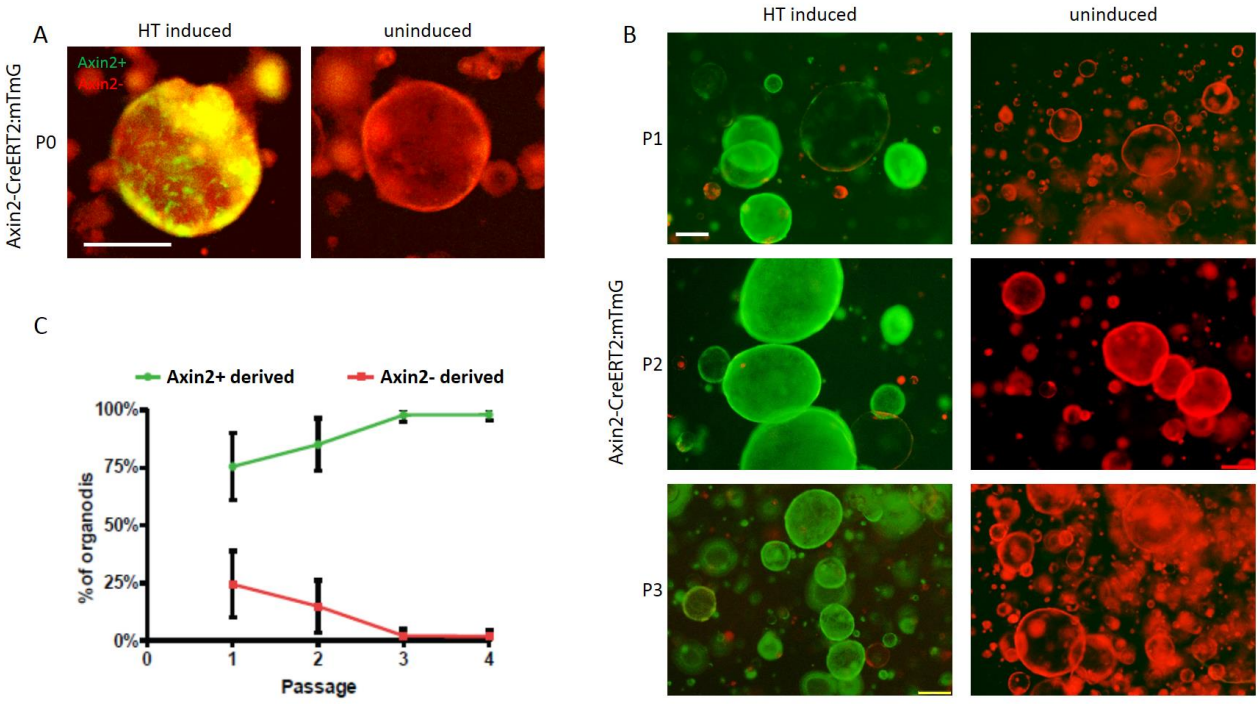

Figure II - 8 Lineage tracing of the Axin2 reporter mouse-derived organoids. (A) Pictures taken at the fluorescent microscope two days after HT induction of Axin2-CreERT2 / ROSA26 mTmG derived organoids. Cells Axin2 positive and derived from Axin2 positive cells (expressing mGFP) in green, cells derived from Axin2 negative cells (expressing mTomato) in red. Scale bar is 200um. (B) Pictures taken at different passages after HT induction. Scale bar is 200um. (C) Quantification of organoids derived from Axin2 positive or negative cells, bars are SD.

4.2.6 Expression of Wnt/β-catenin target genes in adult stem cells

The requirement for the of Wnt/β-catenin ligands R-spondin and Wnt for the growth and maintenance of human organoids strongly suggests that the Wnt/β-catenin pathway activation might play a major role in keeping the stemness potential.

To observe whether the pathway is active in adult stem cells, the expression pattern resulting from the microarray early versus late organoids was compared with the list of β-catenin target genes published by Herbst et al (Herbst et al. 2014).

The global gene enrichment analysis revealed a high correlation between the β-catenin target genes´ list and the expression profile of early organoids (Figure II - 9 A). At a more detailed look, following filtration for expression level and p value, it was possible to detect typical individual Wnt/β-catenin target genes (Figure II - 9 B). The most interesting transcripts enriched in early organoids were the secreted negative regulators of the pathway Dickkopf1 and 4 (DKK), the transcription factor binding to nuclear β-catenin LEF1, and the receptor of R-spondin Lgr5. The differentiated organoids, on the other hand, were enriched for the intracellular negative regulator Axin2 (Tan & Barker 2014).

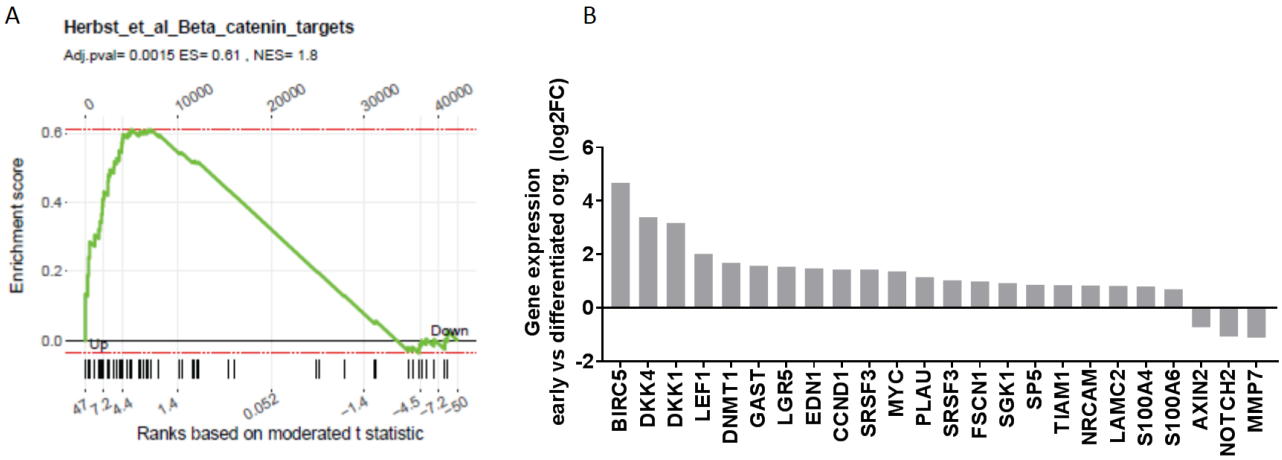

Figure II - 9 Correlation between microarray comparing early vs differentiated organoids and β-catenin target genes list. (A) Global comparison using gene set enrichment analysis between beta-catenin target genes (Herbst et al. 2014) and microarray result. Genes ranked by t-score. ES is the enrichment score, NES the normalized enrichment score. (B) Detailed analysis by filtering the genes for average expression>5, log2FC<-0.7 or >0.7, p value<0.05.

4.2.7 *In vitro* lineage tracing of Lgr5

Given the role of Wnt/β-catenin pathway in maintenance of the stemness of human gall bladder epithelial cells and given the fact that the stem cells are enriched in the upstream receptor Lgr5, I enquired whether Lgr5 could represent an adult stem cell marker of the gall bladder.

To investigate this I temporarily switched back to using murine material, and took advantage of an Lgr5 reporter mouse. The mouse expresses the HT-inducible Cre recombinase under the control of the Lgr5 promoter. After the induction with HT Cre is active and can excise the mTomato gene, leading to the expression of mGFP. In this way it is possible to follow the lineage of Lgr5+ derived cells.

After growing organoids from the Lgr5 reporter mouse and HT induction, rare switch from mTomato to mGFP was visible (Figure II - 10 A), meaning that the Lgr5 expressing cells represent a small portion of the total cells comprising an organoid. After splitting, it was possible to detect two separate populations of organoids: those deriving from Lgr5 negative cells, expressing mTomato, which were the vast majority, and those deriving from Lgr5 positive cells, fully expressing mGFP, which were only sporadically found (Figure II - 10 B top line and C). After an additional passage the population of Lgr5+ derived organoids however started to expand (Figure II - 10 B middle line and C), and after one more passage almost all the organoids were derived from Lgr5+ cells (Figure II - 10 B bottom line and C). I witnessed a slow but unrelenting expansion of organoids derived from Lgr5+ cells (Figure II - 10 C), meaning that only Lgr5 expressing cells could proliferate for a long term, an ability typical of stem cells.

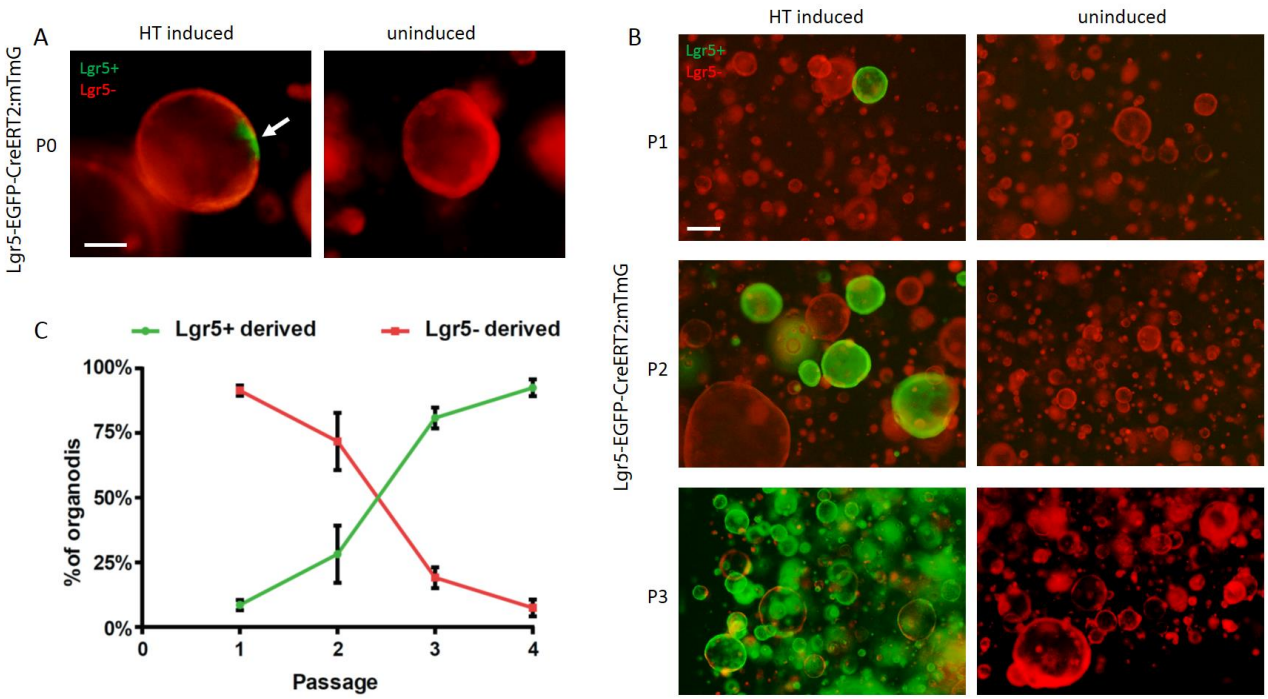

Figure II - 10 Lineage tracing of the Lgr5 reporter mouse-derived organoids. (A) Pictures taken at the fluorescent microscope two days after HT induction of Lgr5 EGFP-IRES-CreERT2:ROSA26 mTmG derived organoids. The arrow points to the Lgr5 positive cells (expressing mGFP) in green. Lgr5 negative cells (expressing mTomato) in red. Scale bar is 100um. (B) Pictures taken at different passages after HT induction. Scale bar is 200um. (C) Quantification of organoids derived from Lgr5 positive or negative cells. Bars are SD

4.2.8 *In vitro* lineage tracing of Sox2

Sox2 marks the adult stem cells of some gastrointestinal organs, like the pylorus and corpus regions of the stomach (Arnold et al. 2011). To test whether it was possible to detect Sox2 expression and tracing in gall bladder organoids, I performed an *in vitro* tracing experiment. Organoids were derived from a Sox2 reporter mouse (Sox2-EGFP-CreERT2:mTmG), and induced by treatment with HT. After induction, however, it was not possible to detect any Sox2 positive cell (Figure II - 11).

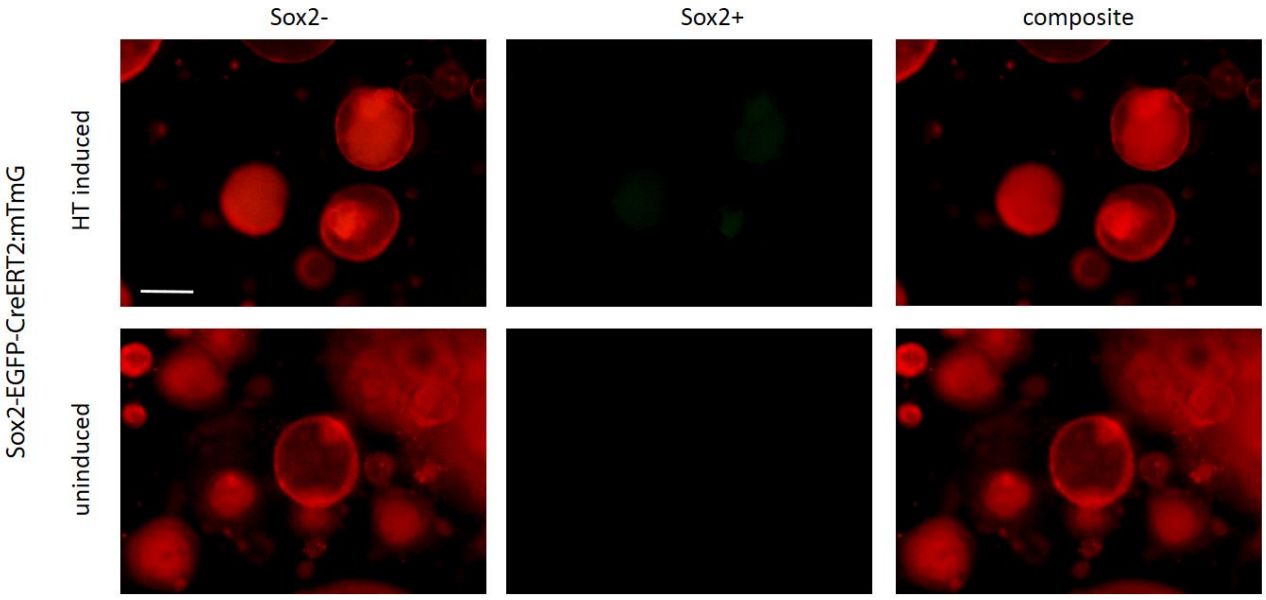

Figure II - 11 Lineage tracing of the Sox2 reporter mouse-derived organoids. Pictures taken at the fluorescent microscope one week after HT induction of Sox2 EGFP-IRES-CreERT2:ROSA26 mTmG derived organoids. It was not possible to detect Sox2 positive derived cells (expressing mGFP, in green). Sox2 negative derived cells in red

4.2.9 Global comparison between early and differentiated organoids

The already mentioned microarray comparing early and differentiated human organoids was also used as a tool to identify putative stem cell markers of the human adult gall bladder. Briefly, early organoids, considered to be enriched in stem cells, were harvested 4 days post seeding, while late organoids, considered to be enriched in differentiated cells and poor in stem cells, were harvested 14 days post seeding (Figure II - 12 A).

The global gene enrichment analysis revealed a high correlation between the general stem cell markers´ list published by Mallon et al (Mallon et al. 2013) and the expression profile of early organoids (Figure II - 12B). This verifies the enrichment of early organoids in stem cells.

In addition, some individual interesting hits were isolated. All the hits were filtered for average expression>5, log2 fold change larger than 0.7 or lower than -0.7, and p value<0.05 (Figure II - 12 C and D).

The top hit was the doublecortin-like kinase 1 (DCLK1), with a 52 fold change in early organoids compared to differentiated organoids. DCLK1 was reported to be both a tumor stem cell marker (Chandrakesan et al. 2017; Nakanishi et al. 2012) and a normal stem cell marker of the

intestine (May et al. 2009). The high expression in organoids enriched for stem cells candidates DCLK1 as an adult stem cell marker of the human gall bladder.

Also LGR5 was also found to be enriched in early organoids, as well as SOX17, an embryonic gall bladder marker (Uemura et al. 2010). During embryogenesis pancreatobiliary common progenitor cells positive for both Sox17 and Pdx1 differentiate into Sox17+/Pdx1- gallbladder progenitors and Sox17-/Pdx1+ ventral pancreatic progenitors (Saito et al. 2013). The microarray results suggest that the expression of Sox17 persists in adult gallbladder stem cell.

In addition another endodermal stem cell marker, PROX1, was found in early organoids, as well as Hepatocyte nuclear factor 4 alpha (HNF4A), a marker for hepatic progenitor cells (Battle et al. 2006), therefore confirming the enrichment in stem cells of early organoids.

To verify the differentiated nature of late-harvested organoids, mucin expression was analyzed. Mucin are large glycoprotein typical of, but not restricted to, differentiated cells. Mucins were identified by comparing the microarray results with the list found on the Hugo Gene Nomenclature Committee website (HGNC ID: 648 http://www.genenames.org/cgi-bin/genefamilies/set/648) and by filtering for average expression>5, log2 fold change larger than 0.7 or lower than -0.7, and p value<0.05. Not surprisingly all of the mucin transcripts were found to be upregulated in the differentiated organoids.

MOGAT1 (monoacylglycerol O-acyltransferase 1) is a gene highly expressed in the gallbladder compared to other organs (Kampf et al. 2014). In the microarray it was found to be upregulated in late organoids, further confirming that late organoids are enriched in mature-differentiated gall bladder cells.

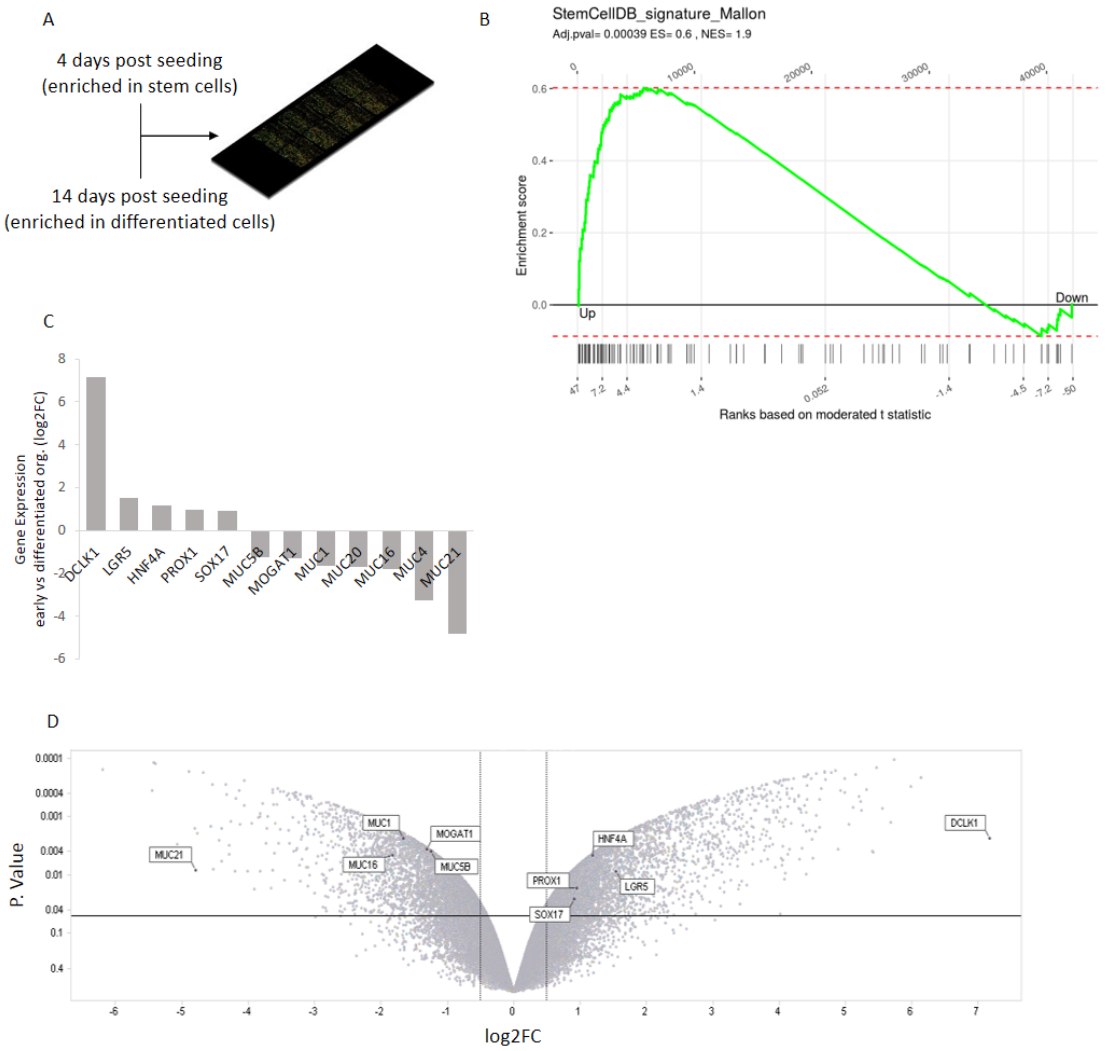

Figure II - 12 microarray results comparing early vs differentiated organoids. (A) Organoids were harvested 4 and 14 days after seeding and double colour microarray was performed. (B) Global comparison using gene set enrichment analysis between stem cell genes (Mallon et al. 2013) and microarray result. (C) Fold change expression of selected genes. Mucin genes were identified by comparing the microarray results with the list found on the Hugo Gene Nomenclature Committee website (HGNC ID: 648) http://www.genenames.org/cgi-bin/genefamilies/set/648. The transcripts were filtered for average expression>5, log2FC>0.7 or <-0.7, p value<0.05 (D) Volcano plot showing the global transcription change resulting from the microarray. Each dot represents one gene. Genes significatively enriched in early organoids are top right section, those significatively enriched in differentiated organoids are top left section. Genes selected for panel C are marked

4.3 Phenotypical characterization of human gall bladder organoids

4.3.1 Phenotypical characterization and stability of human gall bladder organoids

After successful establishment of a long term organoid culture from the human gallbladder, organoids were characterized in terms of protein markers by comparing the organoids with the tissue. The same proteins used to characterize the murine organoids (Figure II - 2 A) were chosen as immunofluorescence markers: Cytokeratin-19 (CK-19) (Kuver et al. 2007), the tight junction protein Claudin-2 (Cla-2) (Németh et al. 2009) and Mucin 5B (Muc5B) (Kampf et al. 2014; van Klinken et al. 1998).

First, it was verified that the organoids are composed entirely by epithelial cells, as seen by E-cadherin staining of all the cells. Like the organ, the cells of the organoids are polarized, shown by the eccentric nucleus and Cla-2 staining, delimiting an internal lumen (Figure II - 13 A). In the organoids the expression of all the gall bladder protein markers (CK-19, Cla-2 and Muc5B) reflects the one in the organ (Figure II - 13 A), confirming the gall bladder identity of organoids.

The stability in time of the epithelial identity was confirmed by comparing the protein level of the epithelial marker E-cadherin and fibroblast marker vimentin at an early and at a late passage (passage 1 and 10 respectively, *i.e.* ~6 months of culturing): while E-cadherin is always expressed at the same level, vimentin never appears (Figure II - 13 B and C). The maintenance of the gall bladder identity, on the other hand, was verified by observing that protein level of CK-19 and Cla-2 does not change between passage 1 and passage 10 (Figure II - 13 B)

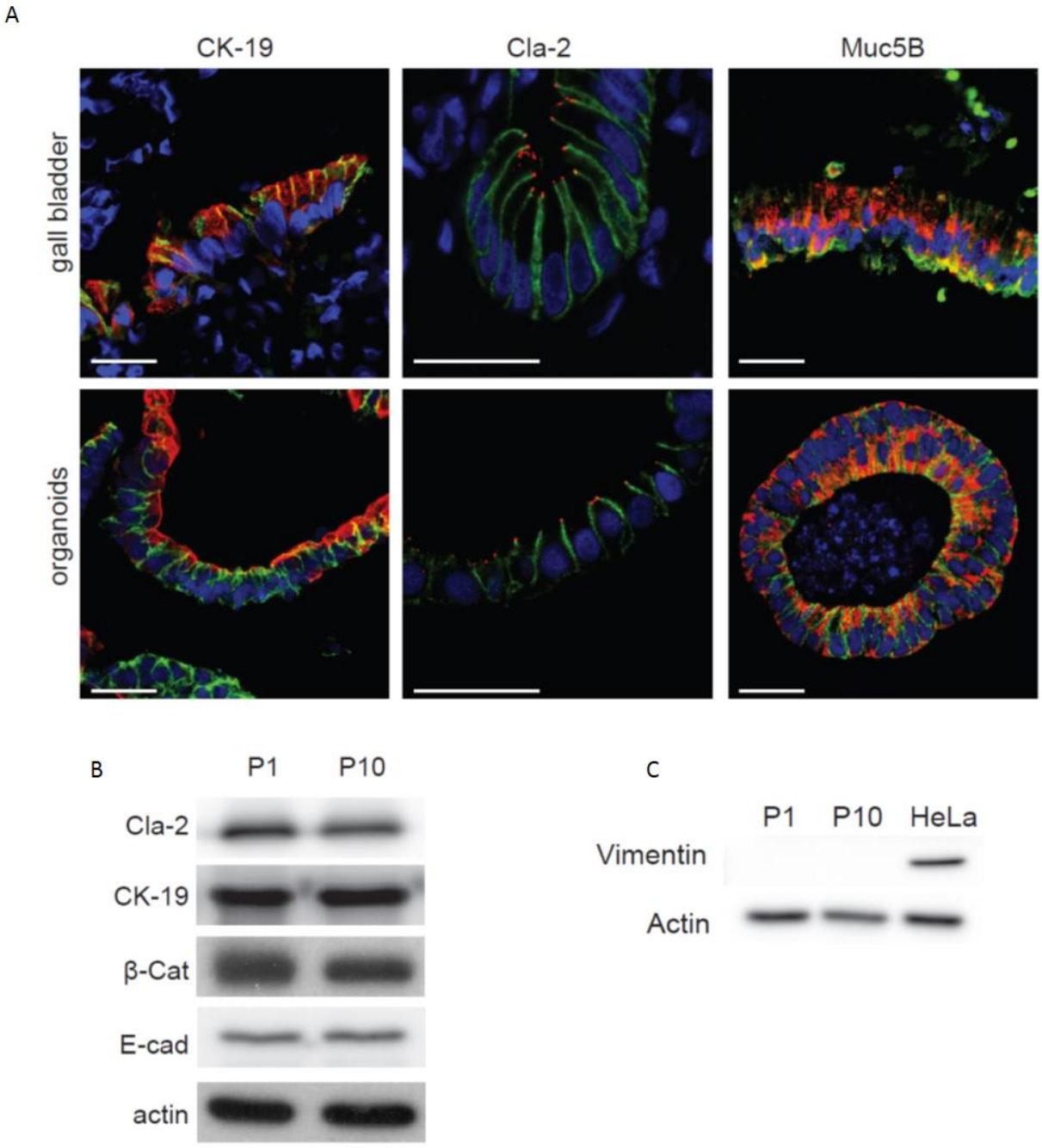

Figure II - 13 Characterization and stability of human gall bladder organoids. (A) Immunostainings of paraffinized sections of murine gall bladder and organoids (fixed 7 days post seeding). CK-19, Cla-2 and Muc5B in red, E-cadherin in green, DRAQ5 stains the nuclei in blue. Scale bar is 25um. (B) Western blots of the mentioned markers to verify the stability of the organoids. Proteins extracted at passage 1 and 10, 7 days post seeding. (C) Western blot to verify the absence at any time of the mesenchymal marker vimentin. HeLa cell extract used as positive control.

4.4 Functional characterization of human gall bladder organoids

4.4.1 Epithelial barrier functionality assay

As a tight epithelium, tight junction of gall bladder epithelial cells avoid the leakage of molecules and ions through adjacent cells.

After detecting the correct localization of Claudin-2 (Figure II - 2 A), to test the functionality of tight junctions, 4kDa FITC-Dextran was added to the medium for 1h. As expected, the dye was not able to penetrate the organoids (Figure II - 14 A first panel). Only after the addition of the chelating agent EGTA, the influx of dye in the lumen was observed (Figure II - 14 A and B), due to the sequestration of Ca^{++} normally used for the correct functionality of tight junction.

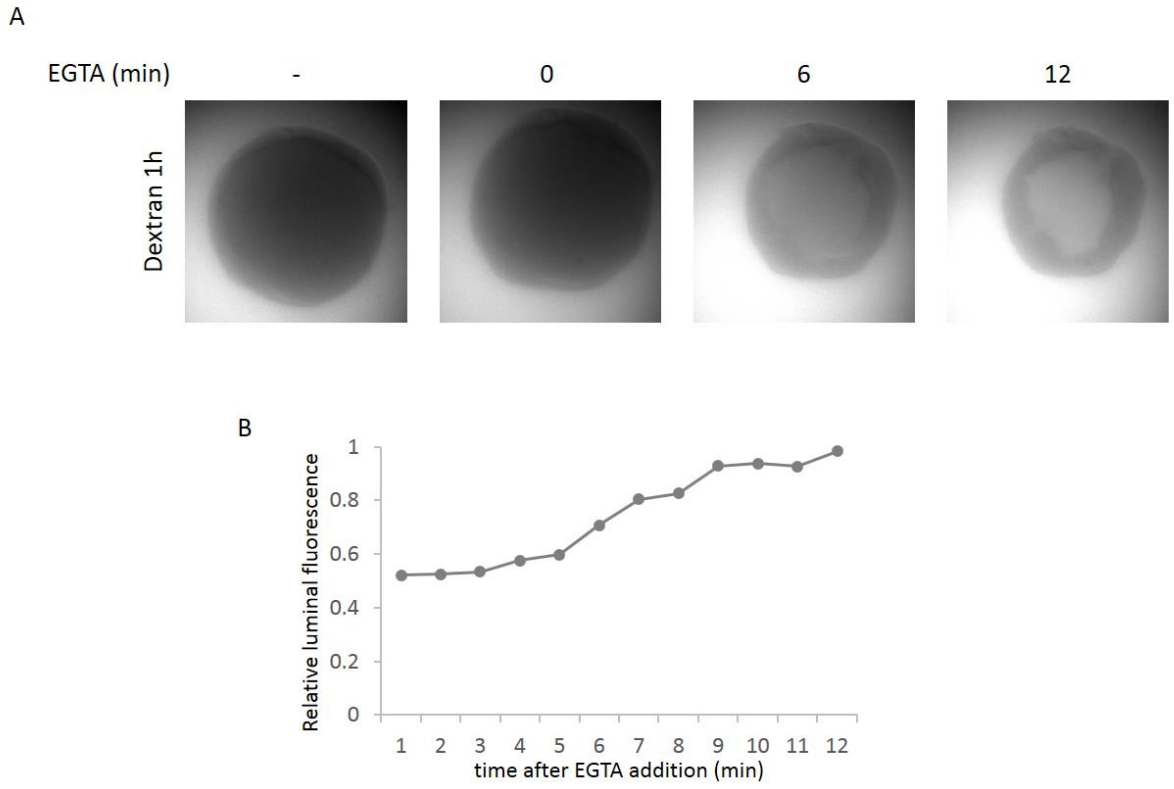

Figure II - 14 Influx of FITC-Dextran. (A) Pictures were taken 1h after FITC-Dextran incubation, and at several time points after EGTA addition. (B) Relative fluorescence (luminal/external) of the EGTA treated organoids in time.

4.4.2 Gall bladder functional assay

After ensuring the phenotypical resemblance between gall bladder organoids and the organ, I wondered whether the organoids were able to recapitulate also the functional feature of the organ: the transport from the basal to the luminal side of bile components.

Rhodamine-123 (Rho-123) is a fluorescent chemical compound often used to determine the functionality of bile transport (Tanimizu et al. 2007; Annaert & Brouwer 2004). The secretion of Rho-123 depends on mdr1, an ATP-dependent transport protein involved in the transport of bile components.

After the addition of Rho-123 in the medium (*i.e.* in the basal side of the cells), cells actively pump the dye in the lumen (Figure II - 15 top row), highlighting that the organoids conserved the functional feature of the organ.

To verify that the transport was due to mdr1, the assay was repeated after incubation with verapamil, an mdr1 inhibitor. As expected, in this condition the dye did not accumulate in the lumen (Figure II - 15 middle row). Gastric organoids, that lack mdr1, failed the assay (Figure II - 15 bottom row), emphasizing the uniqueness of gall bladder organoids.

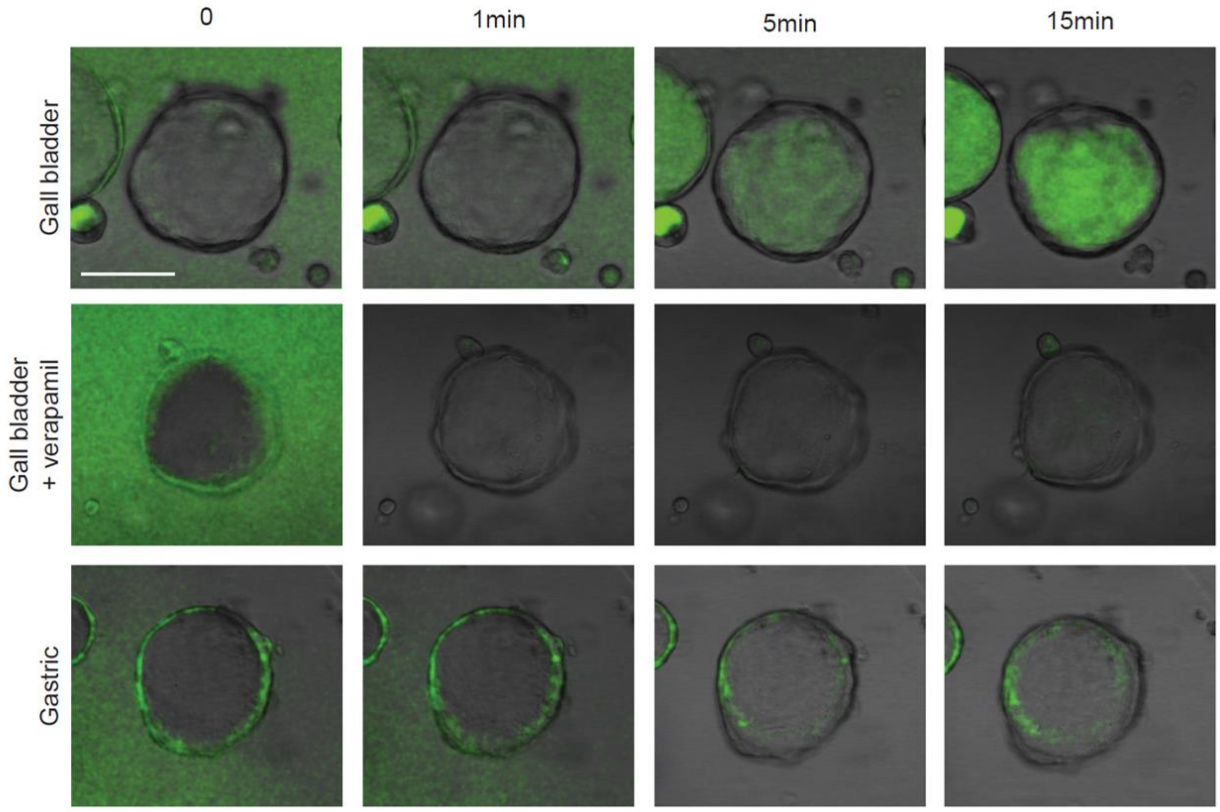

Figure II - 15 Functionality of gall bladder organoids. Time series of pictures taken after the addition of Rho-123. The top row shows a gall bladder organoid actively pumping the dye in the lumen. In the middle row the transport is blocked due to the inhibition of mdr1 by previous incubation with verapamil. The bottom row shows the same assay carried out with gastric organoids that lack mdr1

4.5 *Helicobacter hepaticus* infection of cell lines

4.5.1 Infection of cell lines with *Helicobacter hepaticus*

Before starting to work with *Salmonella*, an easy and straight forward proof of principle was needed to verify the genotoxic activity of CdtB.

For this purpose *Helicobacter hepaticus* was selected as a pathogen, as infection of cell lines is easily made and its CDT action results in a well-defined phenotype dependent on CdtB (Jinadasa et al. 2011) characterized by cells gaining a distended cytoplasm and nucleus. The use of this pathogen has also biological significance because *H. hepaticus* is sometimes found in human GBC samples (Pradhan & Dali 2004; Shimoyama et al. 2010).

Two cell lines commonly used for *Helicobacter in vitro* experiments (HeLa and CaCo-2) were therefore infected with *H. hepaticus*. The infection resulted in the expected outcome: distended cytoplasm and nucleus (Figure II - 16 A and C), DNA damage, as seen by the upregulation of the histone variant γH2AX on a western blot (Figure II - 16 B), and arrest in the cell cycle (Figure II - 16 D).

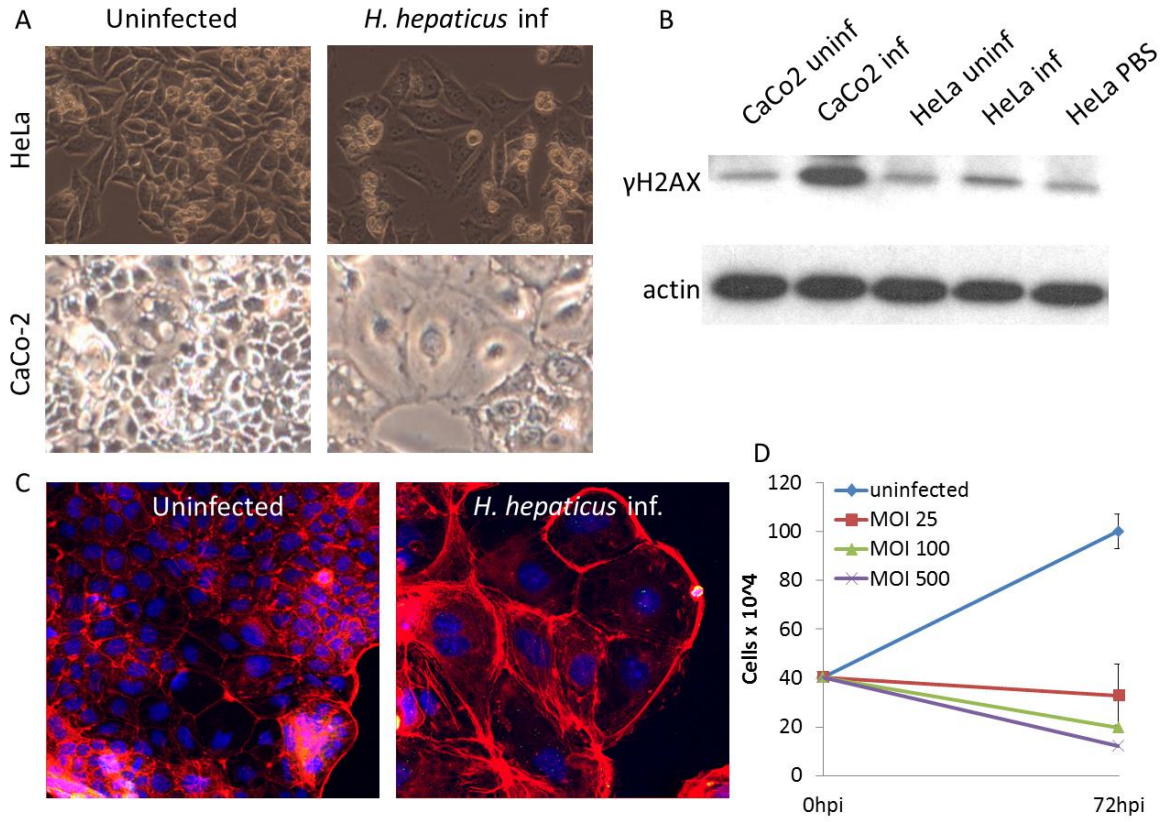

Figure II - 16 Infection of cell lines with *H. hepaticus* leads to distended phenotype coupled with DNA damage and arrest of the cell cycle. (A) HeLa and CaCo-2 cells were *in vitro* infected with *H. hepaticus* MOI 100 and pictures were taken 72hpi. (B) Proteins were harvested and a western blot was ran with the mentioned antibodies. (C) CaCo-2 cells were immunostained with antibodies anti *Helicobacter* urease (green), with phalloidin to visualize actin filaments (red) and DRAQ5 for DNA (blue). (D) 40x10^4 cells were seeded and cell number was counted at 72hpi, after infecting with different MOIs. Bars are SD

4.5.2 Generation and infection with *H. hepaticus ΔcdtB*

According to previous reports the cytopathic effect of *H. hepaticus* is due to the CdtB subunit of CDT (Jinadasa et al. 2011) . In order to verify its role, *cdtB* was knocked out of the genome by homologous recombination with a plasmid carrying the upstream and downstream regions of the gene interrupted with a chloramphenicol resistance cassette (Figure II - 17 A and B)

After knocking out of *cdtB*, CaCo-2 cells were infected with the w.t. and the *ΔcdtB* strains. Because CDT is supposed to be secreted in the medium, in addition to the infection cells were also treated with 10% bacteria supernatant. 72h after treatments, pictures were taken at the light microscope and confirmed that the cytopathic effect observed was due to the CdtB subunit of CDT (Figure II - 17 C). Interestingly the cytopathic phenotype appeared also in cells

treated with the bacteria supernatant (Figure II - 17 C bottom row), confirming that CDT is secreted in *H. hepaticus* medium. Additionally a western blot (Figure II - 17 D) verified that also the DNA damage was entirely due to CdtB, as seen by the impossibility for the *ΔcdtB* strain to upregulate γH2AX. The genotoxic effect is seen even when the bacteria are not in direct contact with the cells, after incubation with the filtered bacteria supernatant (Figure II - 17 E).

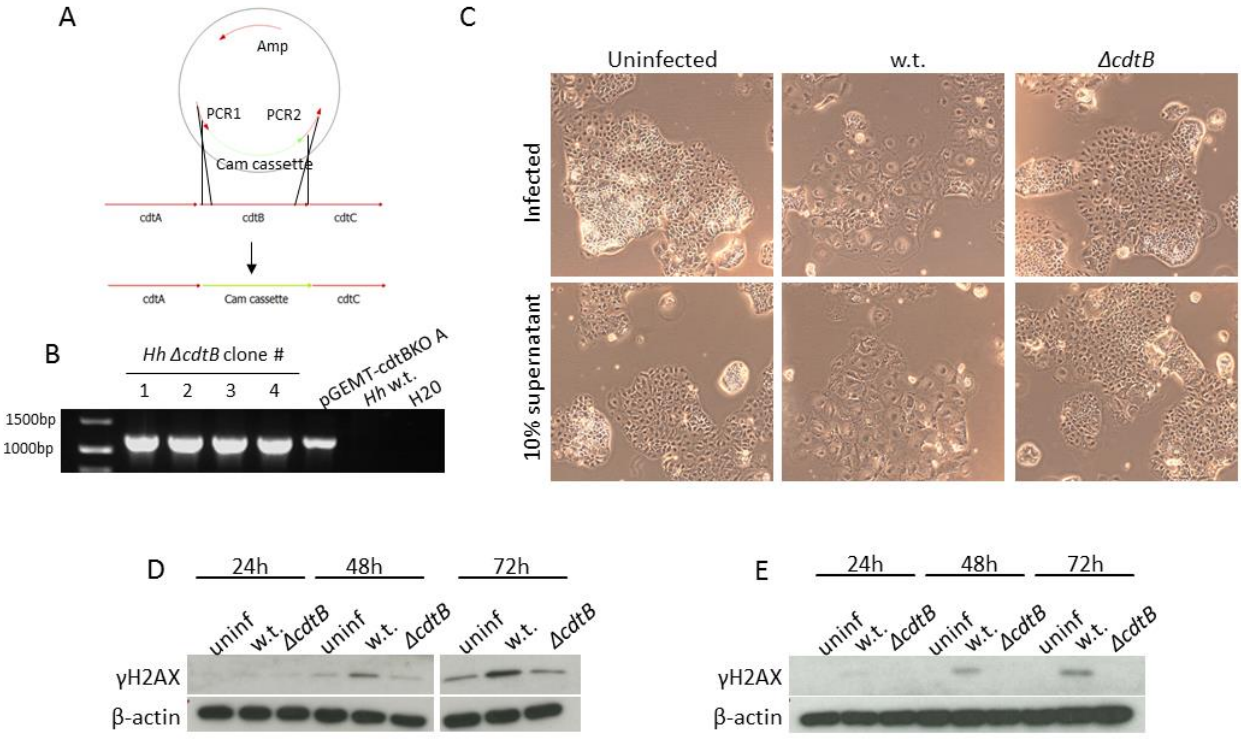

Figure II - 17 Infection and intoxication of CaCo-2 cells with *H. hepaticus* w.t. and ΔcdtB strains, and their supernatant. (A) A construct was generated, using pGEM-T easy as backbone, harboring two 500bp sequences upstream and downstream *cdtB* (called PCR1 and 2 in the picture), which were used as recombinant arms, interrupted by a chloramphenicol resistance cassette. It was electroporated into *Helicobacter*, and homologous recombination took place. (B) After checking for the sensitivity to the resistance cassette in the backbone (Amp), and the resistance to the cassette in the construct (Cam) a PCR was ran on 4 different clones to ensure the successful insertion. The forward primer is Cam-BamHI_01_F (internal to the cassette), the reverse Hh_cdtbKO_PCR2_R (common for *ΔcdtB* and wt). Expected band: 1200bp. pGEMT-cdtBKO A is the positive control. (C) Pictures taken 72h after infection (MOI100) or treatment with 10% bacteria supernatant. (D) Proteins were harvested every 24h after infection MOI100 and a western blot was performed with antibody anti γH2AX and β-actin. (E) Proteins were harvested every 24h after intoxication with 10% bacteria supernatant, and a western blot was performed with antibody anti γH2AX and β-actin.

4.6 *Salmonella* infection of organoids

4.6.1 Infection of murine organoids with *Salmonella* Paratyphi A

Murine primary cells were initially used to test the possibility of *Salmonella* infection of organoids. Organoids were derived from an mTmG mouse (whose cells stably express membrane Tomato) and infected with *Salmonella* Paratyphi A transformed with the plasmid pOR25, which expresses GFP (strain collection X568). Three days after infection the organoids were fixed, whole mount stained with DRAQ5 (which binds the DNA), mounted on a glass slide and pictures were taken at the confocal microscope (Figure II - 18 A and B). The digital reconstruction revealed intracellular bacteria infecting adjacent cells, therefore forming a defined focus of infection.

The proliferation of intracellular bacteria was proven by the increasing number of colony forming units recovered at different days post infection (Figure II - 18 C).

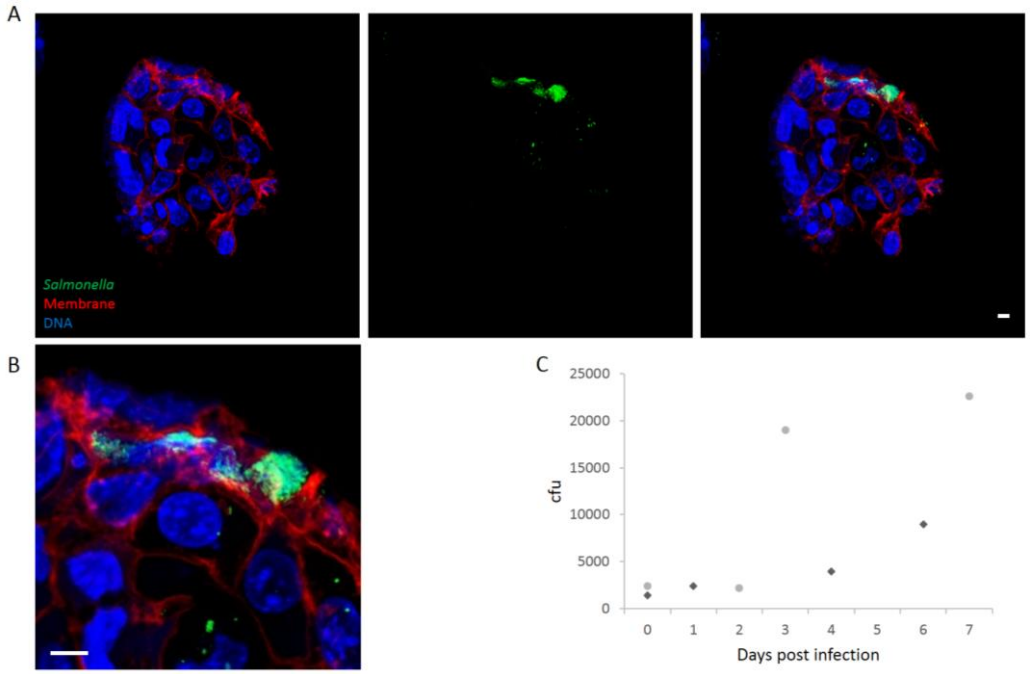

Figure II - 18 Infection of murine gall bladder organoids. (A) Pictures taken at the confocal microscope. 3 days post infection the organoids were fixed and stained for DRAQ5 to stain the DNA (blue). *Salmonella* expressing GFP (strain collection X568) in green, membrane in red. Organoids were then whole-mount imaged. A maximum projection of the z-stacks was digitally created with the software ImageJ. *Salmonella* in green, membrane in red, nuclei in blue. Scale bar is 10um. (B) Enlargement of the infection focus. Scale bar is 10um. (C) Growth curve of intracellular bacteria. At different time points intracellular *Salmonella* was recovered from the host cells by permeabilization, and different dilutions were plated on LB agar plates. The gray and black dots represent the result of two independent experiments.

4.6.2 Infection of human organoids with *Salmonella* Paratyphi A w.t. and *ΔcdtB*

Having demonstrated that in *Helicobacter hepaticus* CdtB is the leading cause of host DNA damage, I hypnotized a similar role for the CdtB subunit of the *Salmonella* produced typhoid toxin. To test this, *cdtB* was knocked out of the typhoid toxin genomic island by homologous recombination with a construct consisting of the upstream and downstream regions of the gene interrupted with a kanamycin resistance cassette (Figure II - 19 A and B).

Infection of murine organoids demonstrated that in principle it is possible to infect a 3D cell culture with *Salmonella* Paratyphi A. Having the availability of human primary cells, the bacterium was used to infect its natural host cells: the epithelial cells of the human gall bladder.

The infection appeared to be localized rather than homogenous: as in mouse, the bacteria infected only a fraction of cells and within 3 days they grew intracellularly forming distinct foci of infection (Figure II - 19 C). The *cdtB* mutation did not influence neither the internalization (Figure II - 19 D) nor the quantity of invading bacteria (Figure II - 19 E)

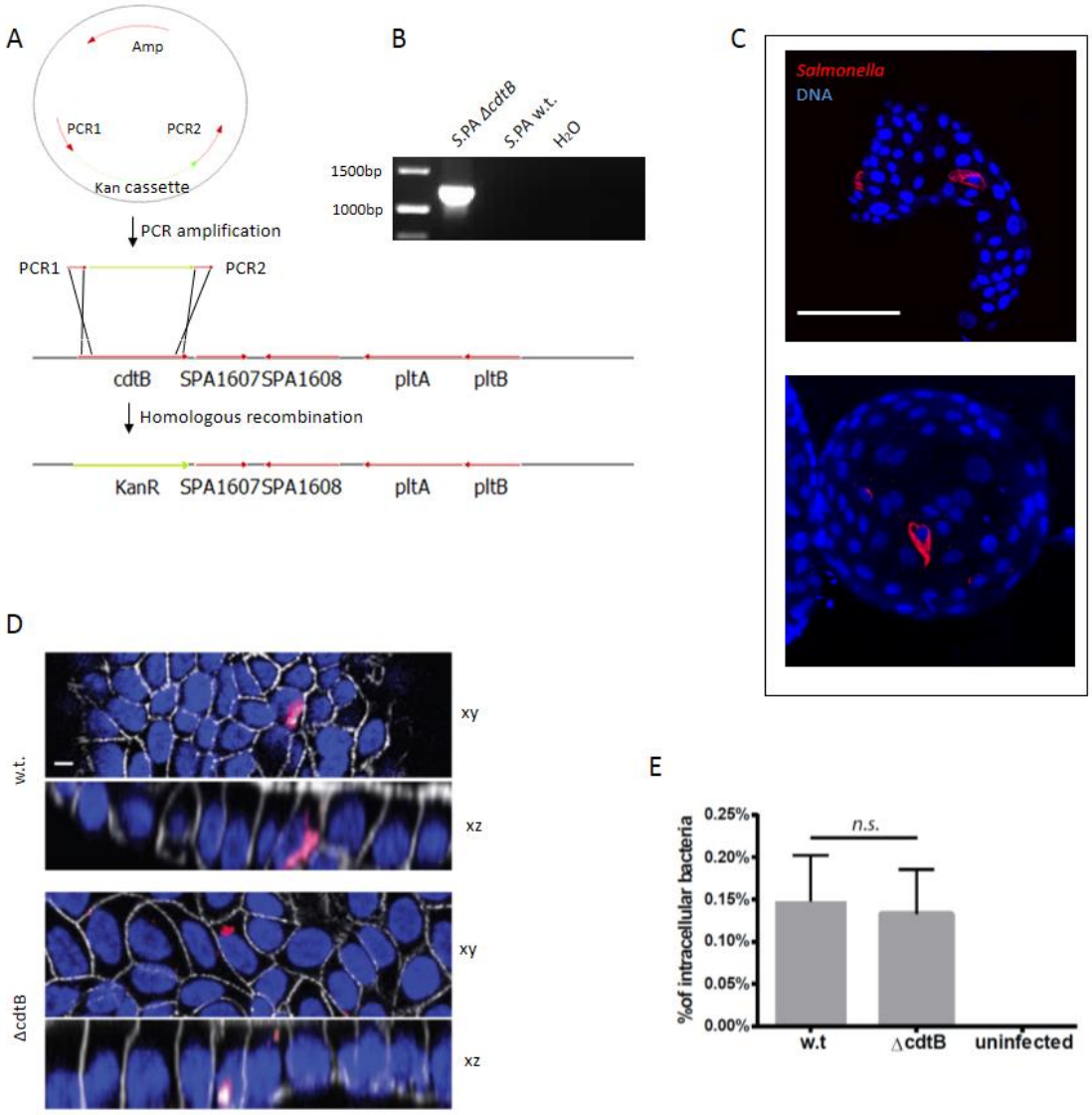

Figure II - 19 Generation of *Salmonella* Paratyphi A *ΔcdtB* and infection of human gall bladder organoids. (A) A construct was generated, using pGEM-T easy as backbone, harboring two 500bp sequences upstream and downstream *cdtB* (PCR1 and 2 in the picture), used as recombinant arms, interrupted by a kanamycin resistance cassette. After linearization of the construct by PCR, it was electroporated into *Salmonella* and homologous recombination was induced (Datsenko & Wanner 2000). (B) After checking for the sensitivity to the resistance cassette in the backbone (Amp) and the resistance to the cassette in the construct (Kan), a PCR was ran on the final clone to ensure successful insertion. The primers are listed in section 3.4.1, the forward primer is Check_cdtBKO_01F (common for *ΔcdtB* and wt), the reverse Check Kan_01R (internal to the Kan cassette). Expected band: 1255bp for the *ΔcdtB*, none for the w.t. (C) *Salmonella* Paratyphi A expressing mCherry was used to infect human organoids. 3 days after infection organoids were fixed, stained with DRAQ5 (to stain the nuclei) and whole mount pictures were taken at the confocal microscope. A maximum projection of the z-stacks was digitally generated with the software ImageJ. Scale bar is 100um. Salmonella in red, DNA in blue. (D) 3 days after infection with the w.t. or *ΔcdtB* bacterium organoids were fixed, stained with phalloidin and DRAQ5 (to stain the actin and the nuclei respectively) and whole mount pictures were taken at the confocal microscope (xy panel). A digital reconstruction of the z-stacks was created with the software ImageJ (xz panel). Scale bar is 10um. *Salmonella* in red, actin in grey, nuclei in blue (E) Invasion of *Salmonella* Paratyphi A w.t. and *ΔcdtB*. No difference in number of intracellular bacteria was noted between the strains. Bars are SD

4.6.3 Paracrine genotoxic effect of *Salmonella* Paratyphi A

In cell lines the infection with *S.* Typhi leads to DNA damage as seen by the phosphorylation of histone variant H2AX on Serine-139, γH2AX (Spanò et al. 2008), but the genotoxic effect of the human restricted serovars has never been proven on primary human gall bladder cells. In order to test this, *Salmonella* w.t. and *ΔcdtB* expressing mCherry were used to infect organoids for 3 days.

γH2AX foci appeared in cells infected with the w.t. bacterium, but rarely in absence of CdtB (Figure II - 20 A, arrow). At a closer look, it appeared that even cells close to the infected ones, but not directly infected, experienced a certain degree of DNA damage (Figure II - 20 A, arrowheads).

In order to quantify this paracrine genotoxic effect, a model was drawn which recapitulates the infected organoid (Figure II - 20 B). Each hexagon represents one cell. The infected cell, in red, is marked as “position 0”. The first three rings of non-infected cells, in orange, are marked as “position 1-3”, and the following three rings of non-infected cells, in green, are marked as “position 4-6”. The percentage of γH2AX positive cells was quantified in the infected and non-infected cells. A γH2AX positive cell was defined as a cell with > 3 foci, an infected cell was defined as a cell with > 5 bacteria, and a non-infected cell as a cell with no bacteria.

The quantification is shown in Figure II - 20 C. 17.2% of the cells in “position 0” (Figure II - 20 A arrow), which are directly infected with *Salmonella* Paratyphi A, experience DNA damage, while in an uninfected organoid the average rate is 1% (Figure II - 20 C dashed blue line). Surprisingly, 2.4% of the cells infected with the *ΔcdtB* strain are also positive for γH2AX. This very mild DNA damage might be due to typhoid toxin´s independent mechanisms, like the upregulation of ROS in infected cell (see section 4.6.7).

In the neighbouring rings of non-infected cells, “position 1-3” (Figure II - 20 A arrowhead), 3.5% of cells were still experiencing DNA damage, strictly dependent on the CdtB subunit of the typhoid toxin, highlighting a paracrine genotoxic effect of the infection. The outer rings of non-infected cells, “position 4-6” did not experience more damage than the cells in an organoid left uninfected.

Overall the paracrine effect of the toxin was observed to span 3 cells from the infected one.

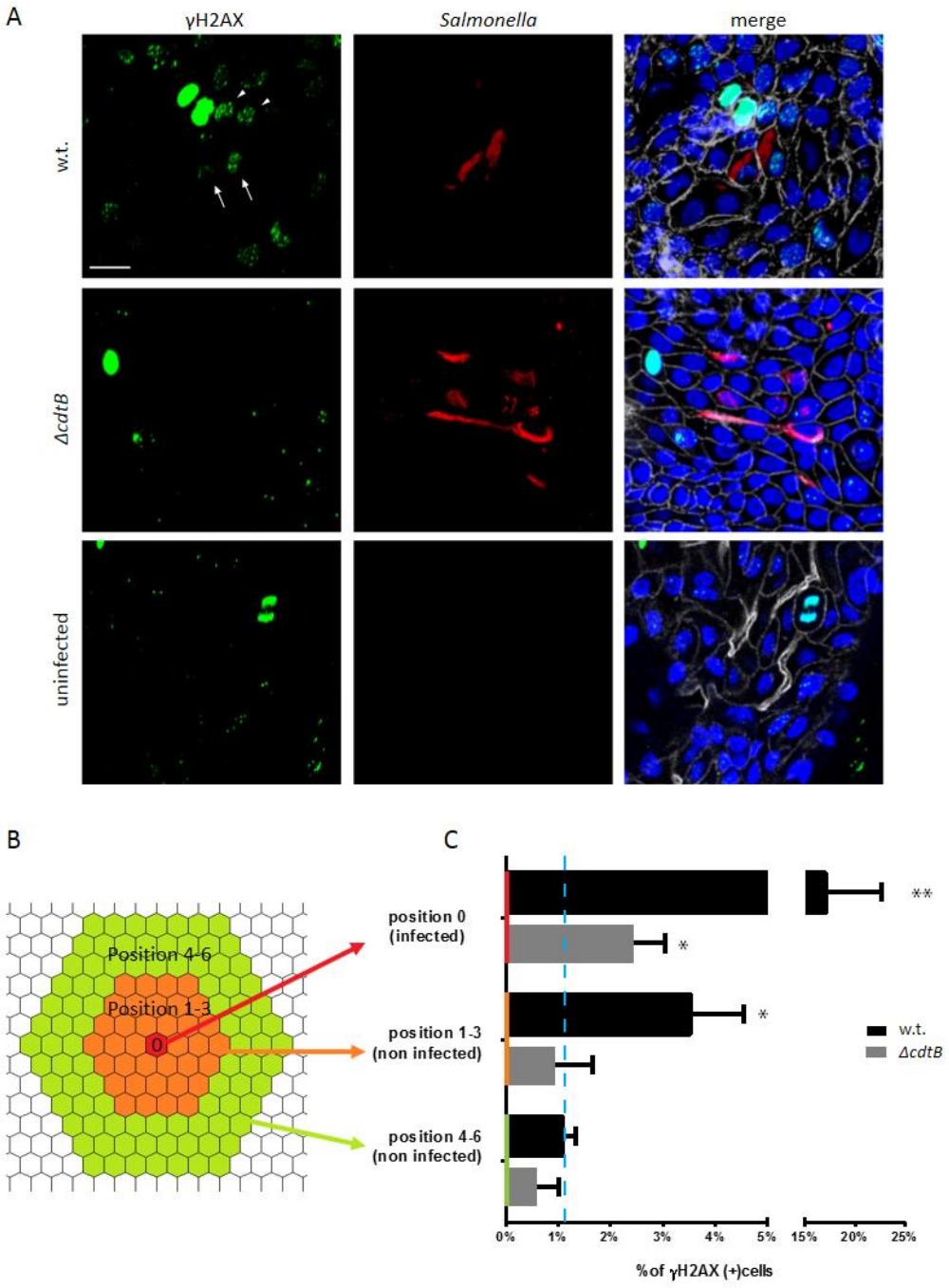

Figure II - 20 Genotoxic effect of CdtB. (A) Organoids were fixed 3 days post infection. They were whole mount stained with antibody anti-γH2AX FITCS conjugated (green), phalloidin to stain the actin (grey) and Hoechst for the DNA (blue). *Salmonella* expressing mCherry in red. Pictures of z-stacks were taken at the confocal microscope and the maximum projection was digitally created with the software ImageJ. Infected-damaged cells are marked with an arrow, neighboring non-infected-damaged cells are marked with arrowheads. (B) Model of infection to define the distance from the infected cell, which is coloured in red at "position 0". Orange represents the first three rings of non-infected cells, "position 1-3", while green represents the following three rings of non-infected cells, "position 4-5". (C) DNA damage based on position and infection status. Percentage of DNA damage experienced plotted by distance from the infected cell. The dashed blue line is the average of the γH2AX positive cells in an uninfected organoid (SD=0.97). p values were calculated comparing each condition to the uninfected. Infected cells are defined as cells with >5 bacteria, non-infected cells are bacteria free, and gH2AX positive are cells with >3 foci. Bars are SD

4.7 *Salmonella* infection of 2D gall bladder primary cells

4.7.1 Infection of 2D gall bladder cells

To achieve a more homogeneous infection, gall bladder primary cells were seeded in 2D on a collagen coated plastic dish and then infected. 2D cells lost their polarization, but could be infected simply by co-incubation with the bacteria, followed by gentamycin assay in order to get rid of the extracellular bacteria. The lack of *cdtB* did not influence the invasiveness of the bacteria, which overall proved to be 4 fold higher than the infection in 3D (compare Figure II - 26 B with Figure II - 19 E)

After 3 days of infection the *Salmonella* proliferated intracellularly forming large colonies in perinuclear position (Figure II - 26 A).

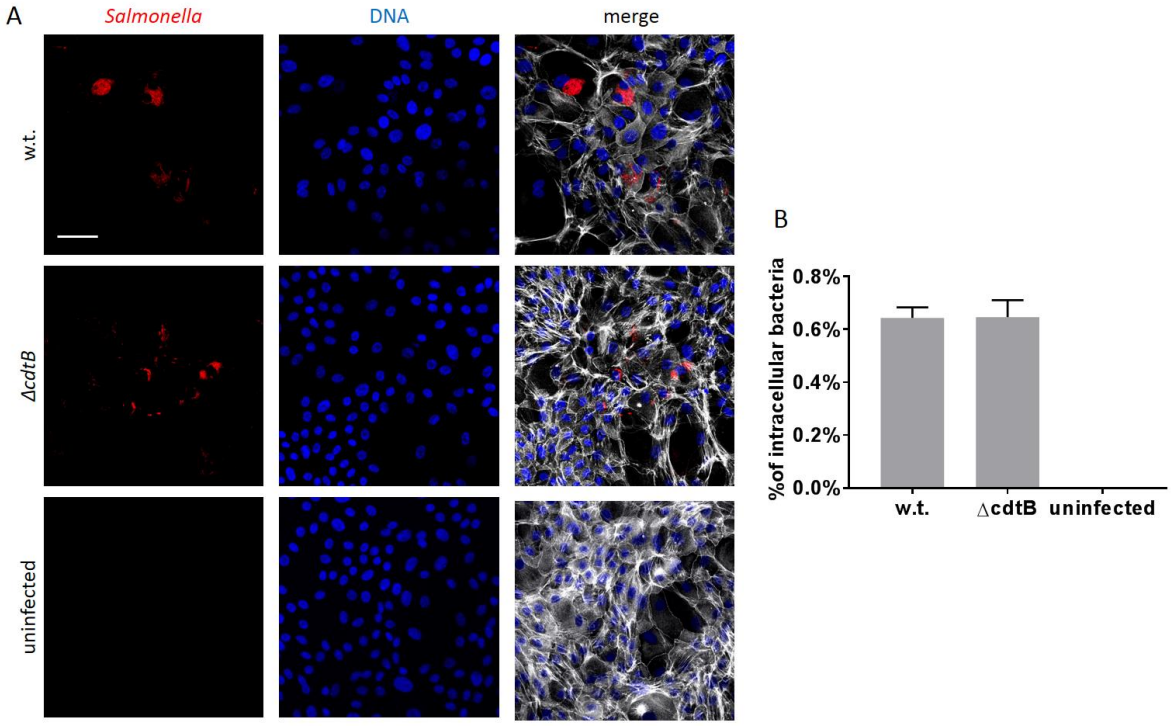

Figure II - 21 Infection of 2D primary gall bladder cells. (A) Cells were grown in 2D, then infected with *Salmonella* Paratyphi A w.t. or *ΔcdtB* expressing mCherry. 3 days after infection cells were fixed and stained with phalloidin to stain the actin (grey) and Hoechst for the DNA (blue). *Salmonella* expressing mCherry in red. Scale bar is 50um. (B) Invasion of *Salmonella* strains. No difference can be detected between w.t. and *ΔcdtB.* Bars are SD

4.7.2 Generation of FLAG tagged CdtB and its expression after infection

To study the expression of CdtB, a FLAG version of the protein was generated. The tag was in-frame fused to the C-terminal part of the protein as it is more accessible than the N-part. In addition the N-term might be cleaved following secretion. A 5Gly linker was interposed to avoid the destabilization of the structure (Figure II - 22 A). The construct was electroporated into *Salmonella* (Figure II - 22 B) and one positive clone was selected and tested by PCR and sequencing (Figure II - 22 C).

To ensure that the tagged form of CdtB was indeed expressed, *Salmonella* was grown in MM5.8, a medium known to stimulate the synthesis of the toxin (Guidi, Levi, et al. 2013), proteins were extracted and a western blot was run using antibodies anti FLAG (Figure II - 22 D). A band appeared at around 30kDa, which is the molecular weight of CdtB of other bacteria (Jinadasa et al. 2011), confirming the successful tagging of CdtB.

Upon infection of 2D gall bladder cells, CdtB-FLAG signal was observed only in heavily infected cells (Figure II - 22 E arrows), while the staining was absent in cells with just a few intracellular bacteria (Figure II - 22 E arrowheads). Only in cells which are infected by a lot of bacteria, therefore, *Salmonella* is able to produce the toxin, which is then reportedly secreted in the extracellular environment. It is therefore possible to conclude that it is the heavily infected cells that represent the source of the typhoid toxin.

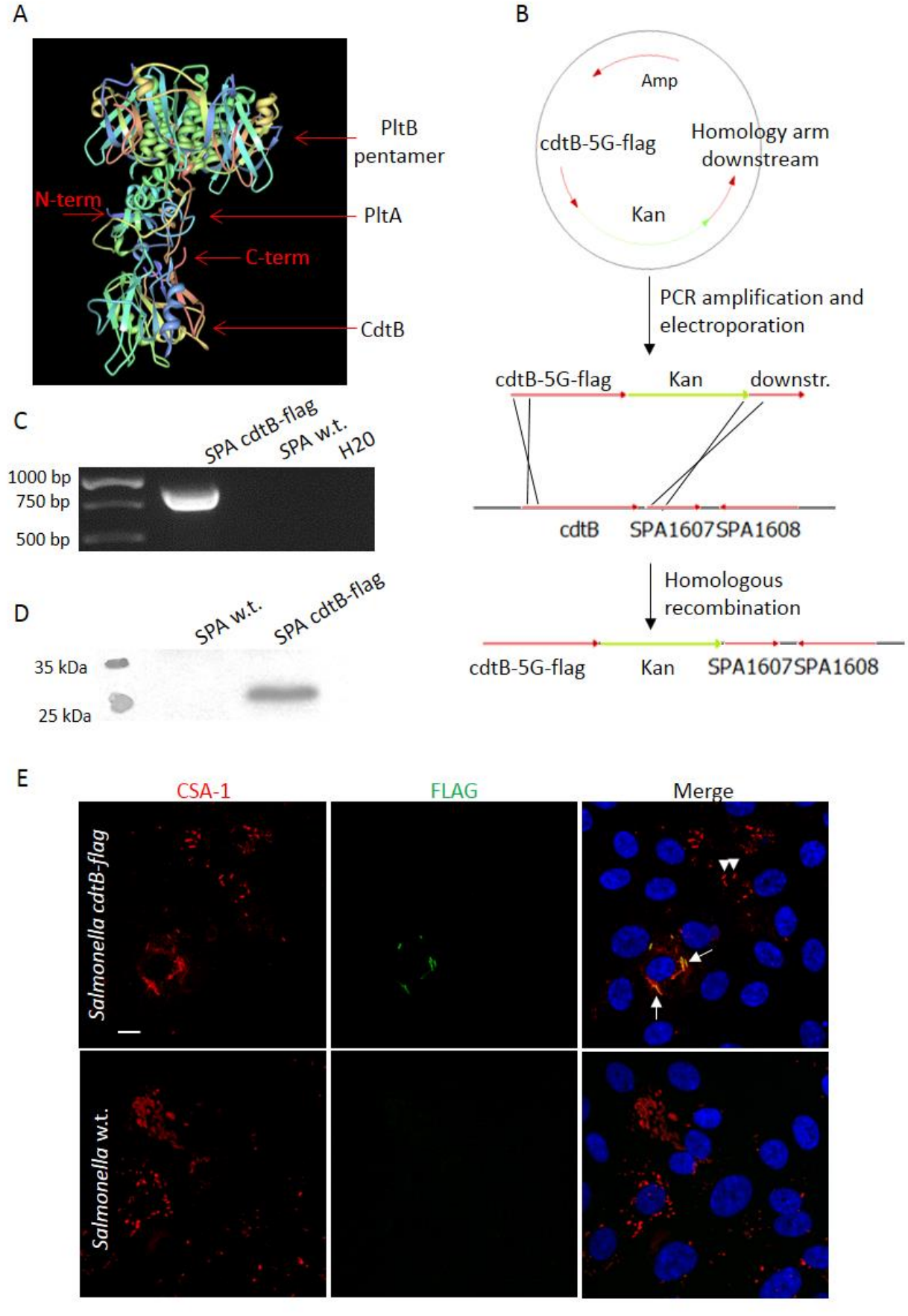
A
PltB
pentamer
N-term
PltA
C-term
CdtB
B
Amp
cdtB-5G-flag
Homology arm
downstream
Kan
PCR amplification and
electroporation
cdtB-5G-flag
Kan
downstr.
cdtB
SPA1607SPA1608
Homologous
recombination
cdtB-5G-flag
Kan
SPA1607SPA1608
C
SPA cdtB-flag
SPA w.t.
H20
1000 bp
750 bp
500 bp
D
SPA w.t.
SPA cdtB-flag
35 kDa
25 kDa
E
CSA-1
FLAG
Merge
Salmonella cdtB-flag
Salmonella w.t.

Figure II - 22 FLAG tag of CdtB. (A) Structure of the typhoid toxin. (B) Strategy of cloning. All the primer are listed in section 3.4.1. *cdtB* was cloned in a pGEMT-easy backbone and the linker+XhoI+BamHI sites were added on the reverse primer (primers are SPAcdtB-gfp_PCR1_F and SPAcdtB-gfp_PCR1_R). Subsequently the FLAG fragment was generated by running the PCR on the primers XhoI-flag_01_F and BamHI-flag_01_R (without a template because the primers bind to each other) and was inserted in the backbone. The sequence downstream of cdtB was amplified (primer SPAcdtB-gfp_PCR5 F and SPAcdtb-flag_PCR5_R) and inserted in the backbone. Finally the Kanamycin resistance cassette was inserted between cdtB-FLAG and the homology arm downstream (primers are SPAcdtB-gfp_PCR6F and SPAcdtB-gfp_PCR6R). After linearization of the construct, it was electroporated into *Salmonella* and homologous recombination was induced (Datsenko & Wanner 2000). (B) After checking for the sensitivity to the resistance cassette in the backbone (Amp), and the resistance to the cassette in the construct (Kan), a PCR was ran on the final clone to ensure the successful insertion. The primers are Check Kan_01F and Check Kan_01R. Expected band: 910bp for the *cdtB-flag*, none for the w.t. (D) Salmonella was grown in MM5.8 overnight, pelleted, proteins were extracted and a western blot was performed using antibodies anti flag. (E) 2D gall bladder cells were infected with *Salmonella cdtB-flag* or w.t. and immunostained with antibodies anti-common *Salmonella* antigen A (CSA-1) in red, anti-FLAG in green and Hoechst was used to stain the nuclei, in blue. Scale bar is 10um

4.7.3 FACS sorting of infected cells

Despite the increased invasiveness of bacteria infecting 2D cells, infected cells represented only a fraction of the total number of cells. In addition the typhoid toxin was produced only by cells heavily infected. In order to enrich for infected cells for further analyses, FACS sorting was performed based on the mCherry expression of intracellular bacteria.

2D cells were infected with *Salmonella* w.t. or *ΔcdtB* expressing mCherry. Control cells were left uninfected. As an additional control, cells were also infected with *Salmonella* not transformed with the mCherry plasmid. Because I was interested in a long term infection, cells were harvested only after 5 days. The gating on FACS data was set based on the lack of fluorescence of the uninfected cells and of cells infected with the non fluorescent bacteria. In both w.t. and *ΔcdtB* around 20% of the cells appeared to be infected (Figure II - 23).

After sorting, the RNA was extracted and used to run double colour microarrays comparing w.t. infected cells to uninfected cells, *ΔcdtB* infected to uninfected, and w.t. infected to *ΔcdtB* infected.

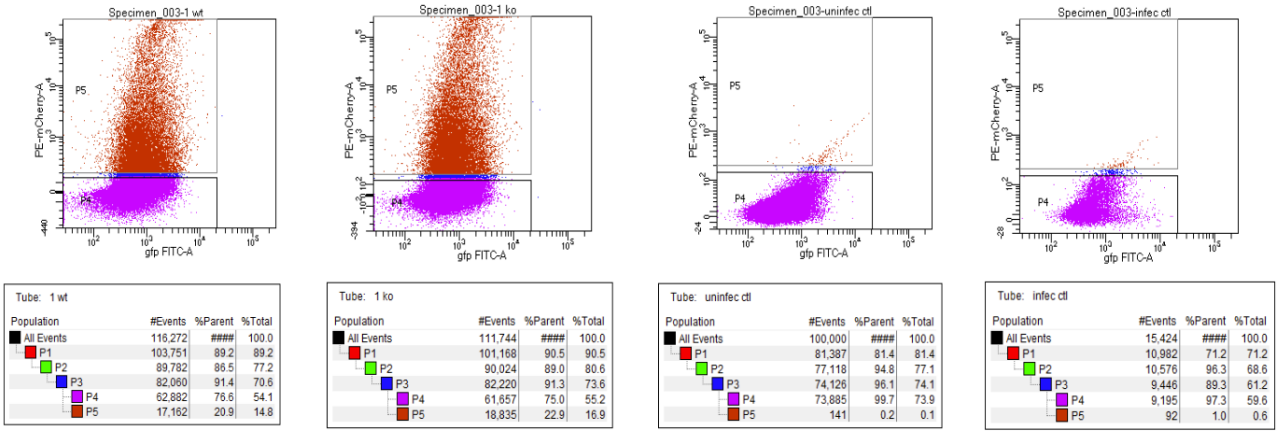

Figure II - 23 FACS sorting of infected cells. 2D gall bladder primary cells were infected for 5 days with the mentioned *Salmonella* strains. Cells were first sorted for Side-scattered light (SSC), forward scatter (FSC), then for mCherry fluorescence. mCherry negative population is named P4, while the positive population is named P5. Infection and the FACS sorting were done on 2 replicates.

4.7.4 Transcriptional response to infection with w.t. *Salmonella*

A microarray was ran comparing the sorted w.t. infected cells with the uninfected.

The top-4 differentially regulated genes were DEFB4A, SAA2, SAA4 and SAA1 (Figure II - 24 A and D). The human β-defensin 2 (DEFB4A) was the most upregulated gene, 22 folds, in infected organoids. The serum amyloid proteins SAA2, 4 and 1, upregulated 15, 12 and 9 folds respectively, are proteins produced in response to infection with strong opsonizing (Hari-Dass et al. 2005; Shah et al. 2006) and chemoattractant (Gouwy et al. 2015) proprieties. The chemoattractant potential was reflected by the upregulation of the chemokines CCL28, CCL2, CXCL6, CXCL3, CXCL14, CXCL1, CXCL2, CXCL8 (IL8), CXCL7 (PPBP) and CXCR4 (Figure II - 24 B).

To verify that the infection of primary cells was leading to an inflammatory response, the microarray results were compared to the gene set enrichment analysis list "GO_INFLAMMATORY_RESPONSE". Expectedly, the infection led to strong inflammatory response (Figure II - 24 C) as shown by the high enrichment for genes involved in the process.

In particular, it was possible to observe the upregulation of BCL2A1, IL1B, TNF, IL11, IL8 (CXCL8), which are transcripts already linked with *Salmonella* infection of intestinal organoids (Forbester et al. 2015), as well as IL17C and NOX1. (Figure II - 24 D). NOX1, which is the NADPH Oxidase 1, is an enzyme involved in the generation of superoxide or hydrogen peroxide, *i.e.* reactive oxygen species (ROS).

Uninfected cells, on the other hand, were mostly enriched for cell cycle transcripts: the fGSEA enrichment in hallmarks of mitotic spindle and G2M checkpoint was highly significant (p value 0.0005 for both)

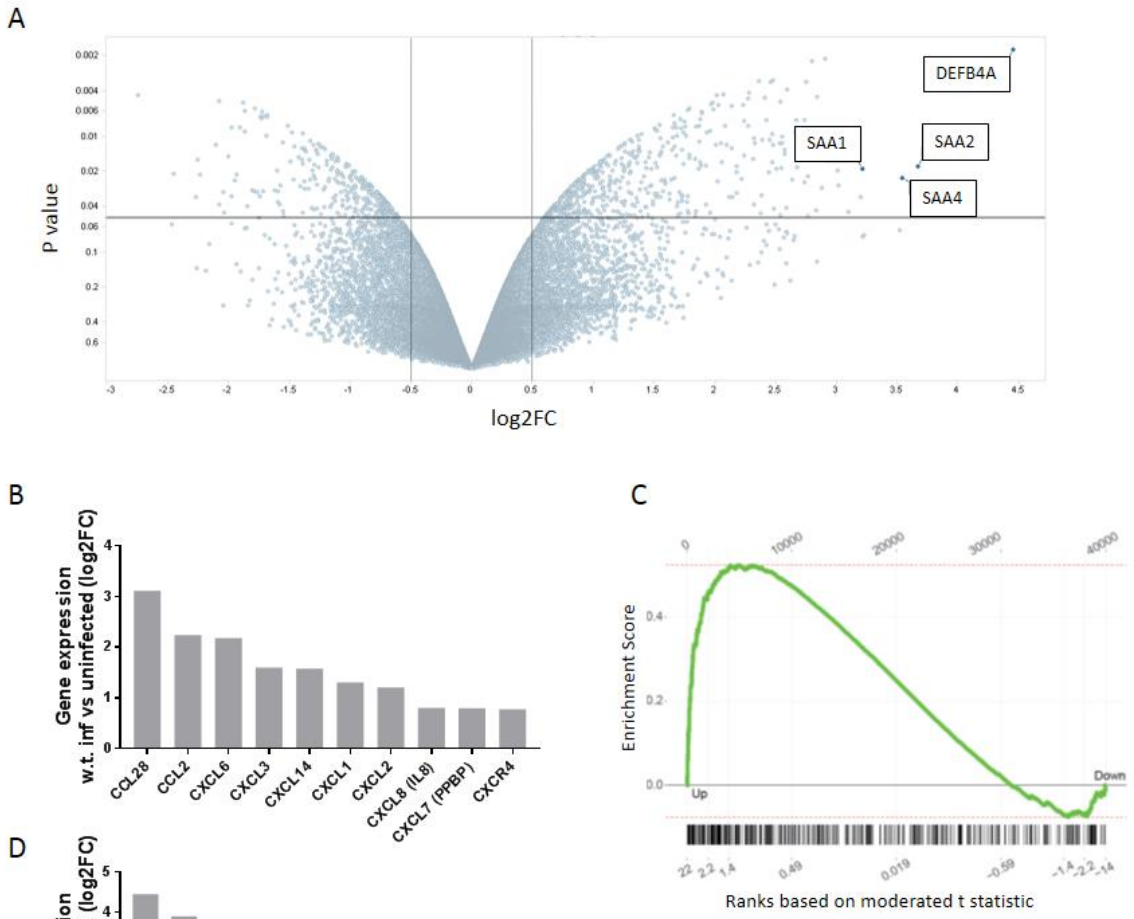

Figure II - 24 Analysis of microarray comparing w.t. infected vs uninfected 2D primary cells. (A) Volcano plot showing the global transcriptional change resulting from the microarray. Each dot represents one gene. Genes significatively enriched in infected cells are top right region. The top 4 hits are highlighted. (B) Expression change profile of chemokines. (C) Global comparison using gene set enrichment analysis. Microarray results were compared to the GO_INFLAMMATORY_RESPONSE list. Genes ranked by t-score. P valwe= 0.00029, ES= 0.52, NES= 2 (D) Expression change of selected genes involved in inflammatory response. In all the bar plots the genes were filtered for average expression>5, log2FC>0.7 or <-0.7, p value<0.05

4.7.5 Transcriptional response to infection with *ΔcdtB Salmonella* and comparison with w.t. infection

A microarray was ran comparing the sorted *ΔcdtB* infected cells with the uninfected.

The transcriptional response was very similar to the one induced by w.t. infection. The top 4 hits were human β-defensin 2 (DEFB4A) followed by SAA2, EGR2 and SAA4 (Figure II - 25 A. The expression of EGR2 was at a low level, therefore it was not taken into consideration for the analysis).

The gene set enrichment analysis list "GO_INFLAMMATORY_RESPONSE" was compared to the microarray results to verify the inflammatory response (Figure II - 25 B), and the same genes which were analyzed in the w.t. infection were examined, showing a similar upregulation (Figure II - 25 C).

Because of such similarities, the microarray comparing *ΔcdtB* infection with w.t. infection did not show striking differences (Figure II - 25 D). The most differentially expressed genes were CYP2C8, UBE2C, NADK2 and FSD1L, overexpressed in the *ΔcdtB* infected cells, and GOLGA8A, AMY1C, GOLGA6L10 and HIST2H2BE, overexpressed in the w.t. infection (Figure II - 25 E).

The two golgin proteins, GOLGA8A and GOLGA6L10, are probably involved in the transport of the typhoid toxin through the Golgi. The interpretation of the other differentially expressed transcripts is, however, not clear.

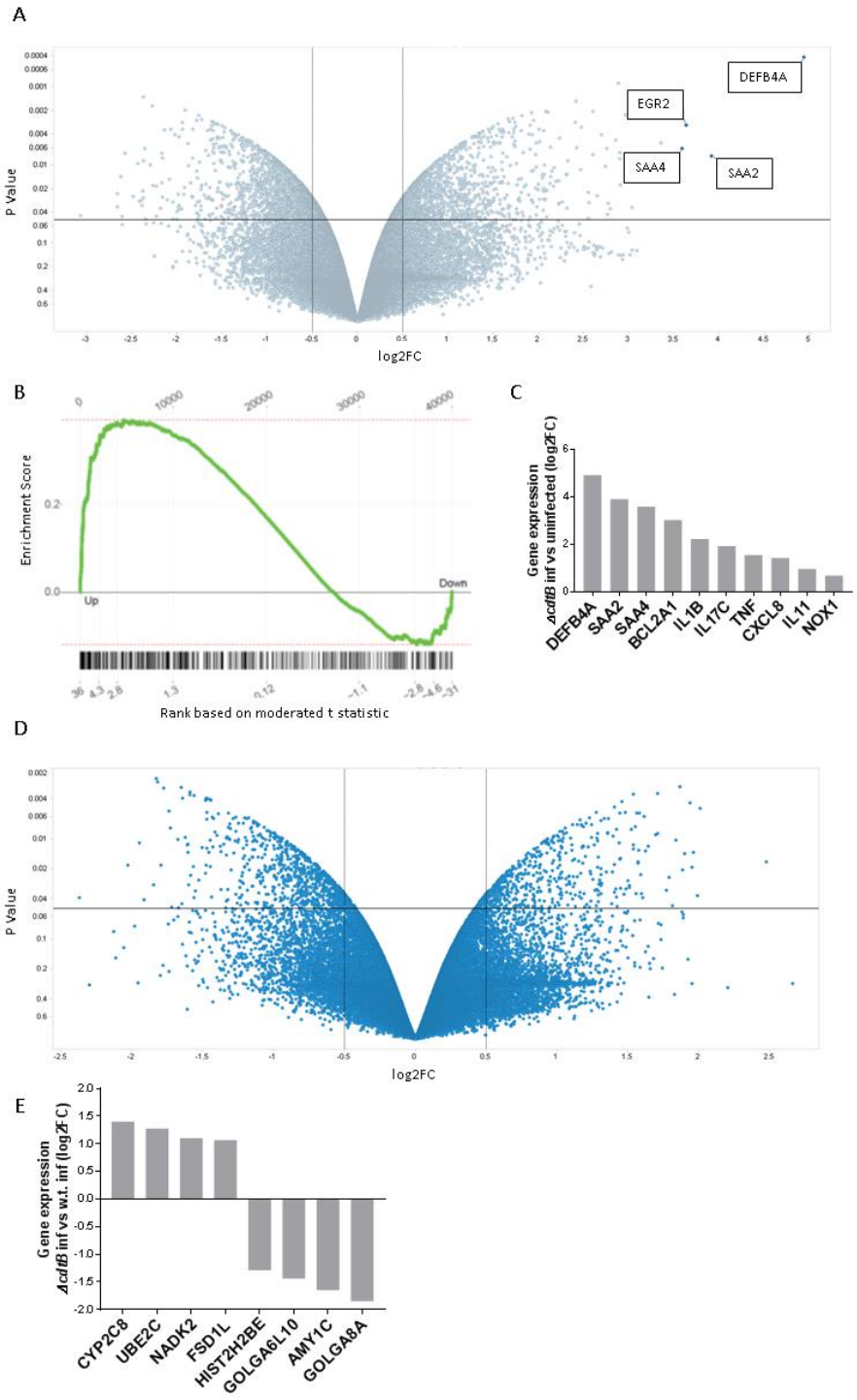

Figure II - 25 Analysis of microarray comparing *ΔcdtB* infected vs uninfected, and *ΔcdtB* vs w.t. infection. (A) Volcano plot showing the global transcription change resulting from the microarray comparing *ΔcdtB* infected vs uninfected cells. Each dot represents one gene. Genes significatively enriched in *ΔcdtB* infected cells are top right section. The top 4 hits are highlighted (B) Global comparison using gen set enrichment analysis. Microarray results were compared to the GO_INFLAMMATORY_RESPONSE list. Genes ranked by t-score. P value= 0.00046, ES= 0.39, NES= 1.6. (C) Expression change of selected genes involved in inflammatory response. (D) Volcano plot showing the global transcription change resulting from the microarray comparing *ΔcdtB* infected vs w.t. infected cells. Genes significatively enriched in *ΔcdtB* infected cells are top right section. (E) Expression change of the top 4 differentially expressed genes in *ΔcdtB* and w.t. infection. In all the bar plots the genes were filtered for average expression>5, log2FC>0.7 or <-0.7, p value<0.05.

4.7.6 DNA damage after infection of 2D gall bladder primary cells

The microarray analysis showed the global response of primary GB cells to the infection, however it did not prove to be optimal for the analysis of DNA damage. In order to study genotoxicity, an immunofluorescence approach was preferred.

Three days of infection of 2D primary cells led to DNA damage, seen by the appearance of γH2AX in the infected cells; this was dependent on the presence of CdtB (Figure II - 26 A). In these settings, however, it was not possible to reliably quantify the paracrine effect of the toxin, because of the heterogeneity in the shape of 2D cells and because cells lost the polarization, therefore not reassembling anymore the tissue of origin.

The DNA damage was also measured by western blot after harvesting the entire plate (Figure II - 26 C). It was not possible to see a global upregulation of γH2AX, most probably due to the fact that γH2AX upregulation in few intoxicated cells was masked by the general lower level in non-intoxicated cells. On the other hand, using an immunofluorescence approach, I observed a statistically significant increase in γH2AX when the intensity of the signal was measured specifically in the nuclei of infected cells (Figure II - 26 D).

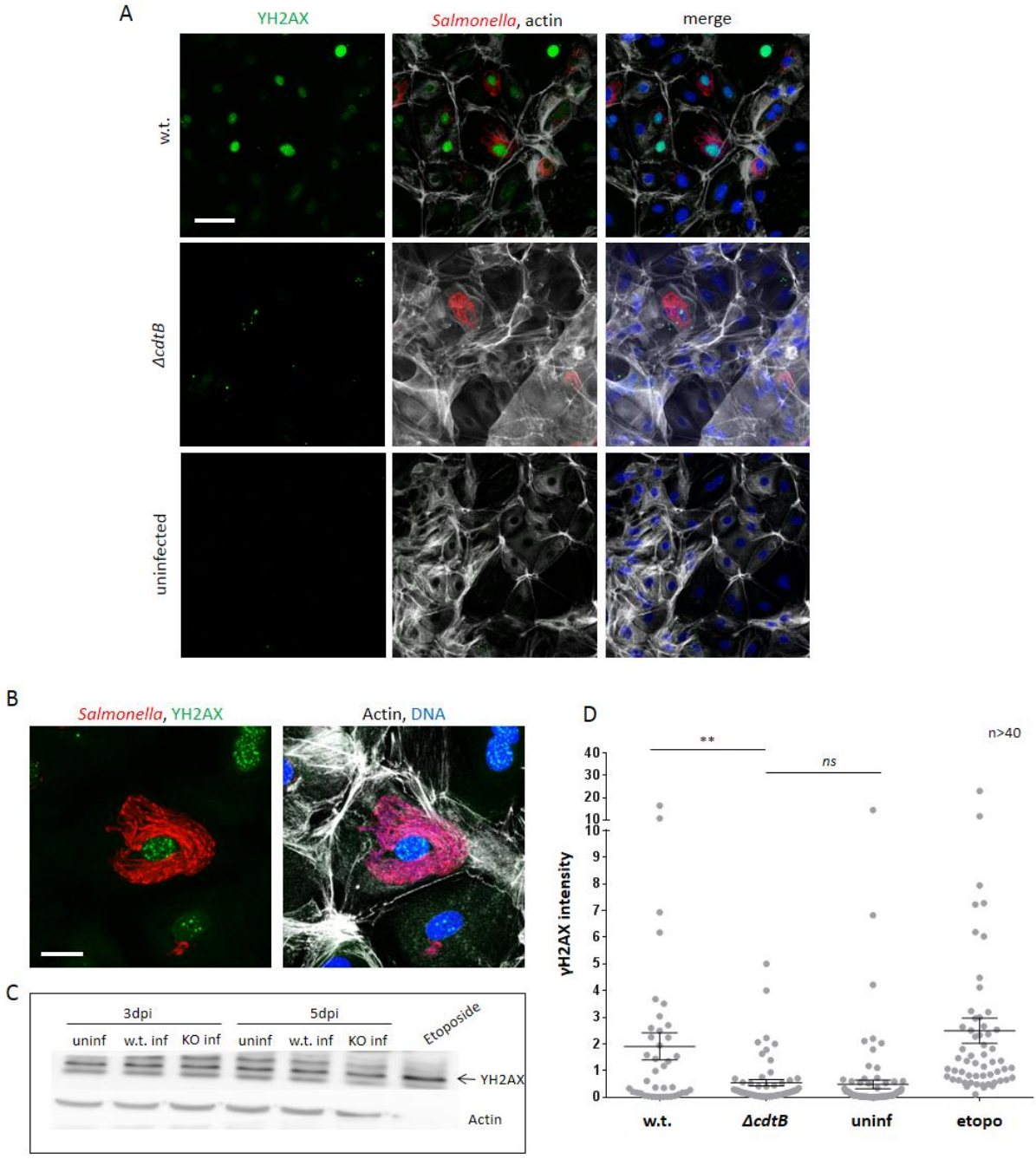

Figure II - 26 DNA damage in primary gall bladder cells grown in 2D. (A) Cells were grown in 2D, then infected with *Salmonella* Paratyphi A w.t. or *ΔcdtB*. 3 days after infection cells were fixed and immunostained with antibody anti-γH2AX FITCS conjugated (green), phalloidin to stain the actin (grey) and Hoechst for the DNA (blue). *Salmonella* expressing mCherry in red. Scale bar is 50um. (B) Magnification of a cell infected with the w.t. bacterium. Scale bar is 20um (C) Whole plate was harvested, SDS gel was ran and the membrane was blotted with antibodies against γH2AX and β-actin. (D) Confocal images were analyzed with the software ImageJ and the intensity of γH2AX was measured in the nuclei of infected cells. Each dot is one nucleus, bars are SEM

4.8 Intoxication of gall bladder primary cells

4.8.1 CdtB dependent DNA damage following intoxication

Because the typhoid toxin is expressed only in heavily infected cells, which are randomly distributed in the dish, I developed a method to more evenly intoxicate the cells. In the case of *H. hepaticus* CdtB, the toxin is secreted from the cultured bacteria, and the genotoxic effects are seen in cells treated with the bacteria supernatant (Figure II - 17 E). The typhoid toxin of *Salmonella*, however, is normally not expressed in bacteria grown in LB, but it is if bacteria are grown in the minimal medium MM5.8 (Guidi, Levi, et al. 2013).

Salmonella was therefore grown in MM5.8 overnight, filtered out, and 2D grown primary cells were incubated with the bacteria-conditioned medium for 24h (for the details see materials and methods section 3.13). A neutral comet assay was run to quantify DNA breaks. The method consists in the electrophoresis of nuclear DNA which, after the run, leaves a DNA tail if breaks are present. After treatment with the w.t. supernatant a statistically significant increase in tail-DNA was noticed. There was no difference between cells treated with the *ΔcdtB* strain supernatant and with sterile medium, while cells that received w.t. supernatant showed DNA breaks at a similar level than etoposide treated cells (Figure II - 27 A and B).

In order to confirm that the DNA damage was matched with increase in γH2AX level, whole protein extract was subjected to western blot after intoxication. While after infection it was not possible to see an upregulation of γH2AX on a western blot (Figure II - 26 C), using the intoxication method I could indeed observe higher level of γH2AX in cells treated with the w.t. supernatant or etoposide, but not in cells treated with *ΔcdtB* strain supernatant (Figure II - 27 C)

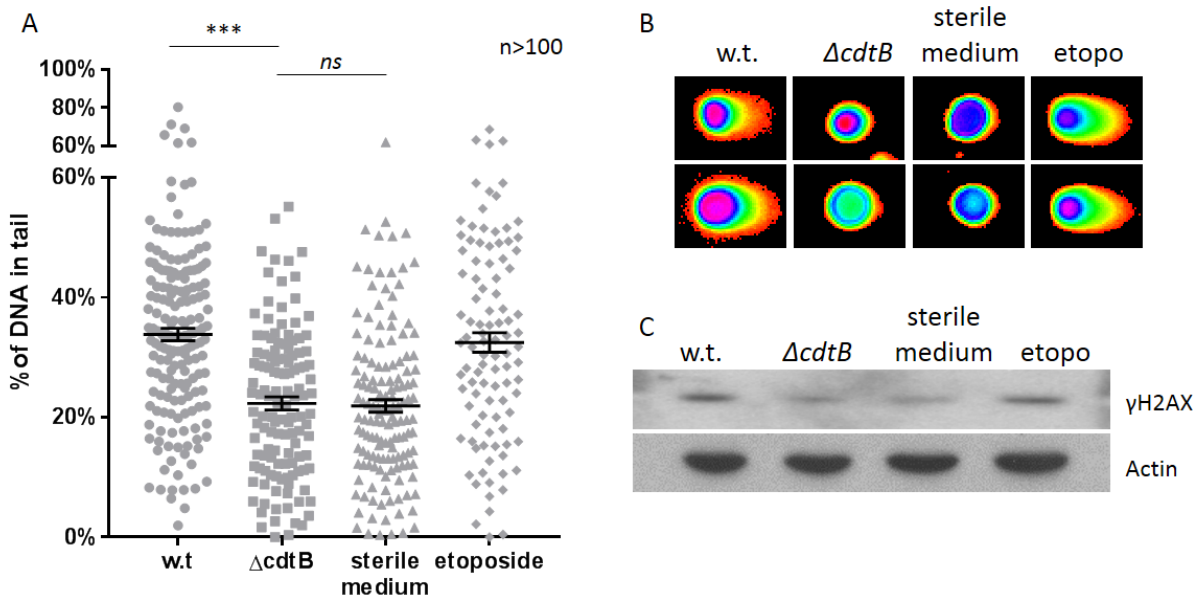

Figure II - 27 DNA damage of intoxicated cells. Cells were incubated for 24h with conditioned medium of *Salmonella* w.t. or *ΔcdtB* grown in MM5.8. As control the cells received the sterile medium or, as a positive control, etoposide (50uM for 24h). (A) A neutral comet assay was run (Trevigen ct.:4250-50-K), and the amount of DNA in tail of least 100 nuclei was measured. Each dot represents the measurement of one nucleus, bars are SEM. (B) Two nuclei per condition are shown after comet assay electrophoresis. (C) After intoxication, proteins from the whole plate were harvested, SDS gel was ran and the membrane was blotted with antibodies against γH2AX and β-actin.

4.8.2 Cell cycle progression after CdtB-induced genotoxicity

Normally cells respond to DNA damage by arresting the cell cycle. This is even the case of cells treated with genotoxins (Gagnaire et al. 2017). Because of the genotoxic action of CdtB, intoxicated cells were expected to arrest their cell cycle. In order to test this hypothesis, 2D gall bladder cells were incubated with w.t. supernatant, *ΔcdtB* supernatant, sterile medium, or etoposide. After 24h the cells were fixed and immunostained with antibodies detecting γH2AX and the proliferation marker Ki67 (Figure II - 28 A). Surprisingly cells that received w.t. supernatant kept cycling despite the DNA damage. The percentage of Ki67 positive cells in fact did not change between the conditions, except in the etoposide treated cells, where hardly any cell in active state of proliferation was found (Figure II - 28 B).

To investigate whether cycling cells bore DNA breaks, the intensity of γH2AX was measured in Ki67 positive and negative cell. It was remarkable to notice that cycling cells treated with the w.t. supernatant carried more DNA damage than cells treated with the *ΔcdtB* supernatant or sterile medium, and that most of the CdtB-induced DNA damage occurred in cycling cells (Figure II - 28 C).

These results highlight that, unexpectedly, human gall bladder primary cells intoxicated with the typhoid toxin continue to proliferate despite the DNA damage. Moreover cycling cells are harboring more DNA breaks than non-cycling cells. The importance of this finding in the light of *Salmonella*-induced carcinogenesis will be more deeply discussed in the discussion of this thesis (section 5)

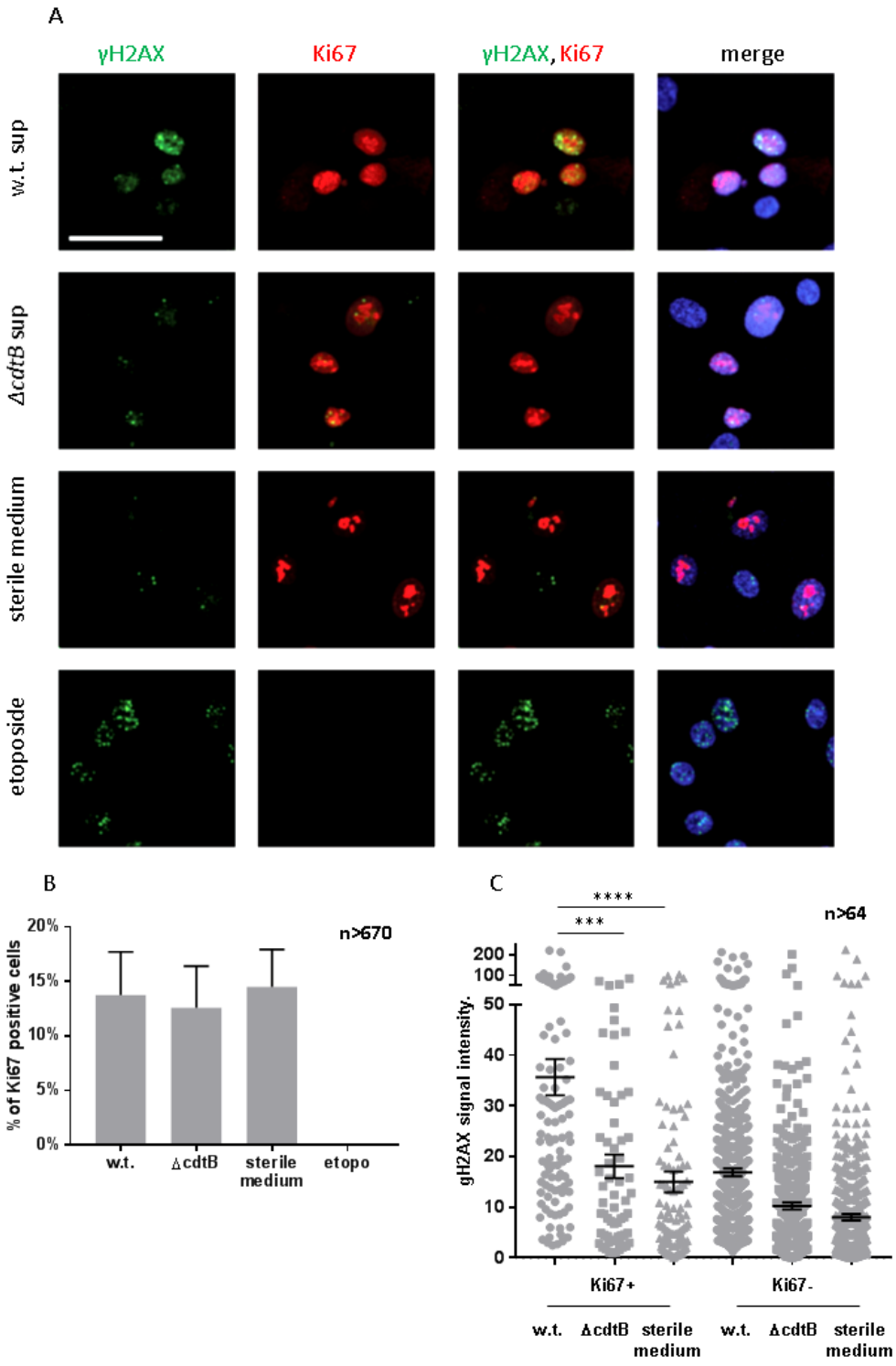

Figure II - 28 Immunostaining of intoxicated cells with DNA damage and proliferation markers. 2D gall bladder primary cells were fixed 24h after intoxication with the *Salmonella* supernatant or treatment with etoposide (50uM, 24h). Fixed cells were immunostained with antibodies anti γH2AX (green), Ki67 (red) and Hoechst was used to stain the nuclei (blue). Scale bar is 50um. (B) Quantification of Ki67 positive cells after intoxication. Bars are SD. (C) The intensity of γH2AX was measured with the software Imagej for each Ki67 positive and negative nucleus. Each dot represents one measurement, bars are SEM.

4.8.3 Cell cycle progression after infection induced genotoxicity

In Figure II - 28 I observed that cells intoxicated with the typhoid toxin keep proliferating despite the DNA breaks. To rule out that this unusual behavior was an artifact due to the intoxication method, 2D primary cells were infected with *Salmonella* and immunostained for γH2AX and Ki67 (Figure II - 29). Even under these conditions, sporadic triple positive cells were detectable (Figure II - 29 second row). Those cells were infected, bore γH2AX foci and at the same time were positive for Ki67, *i.e.* in active state of proliferation despite the DNA breaks.

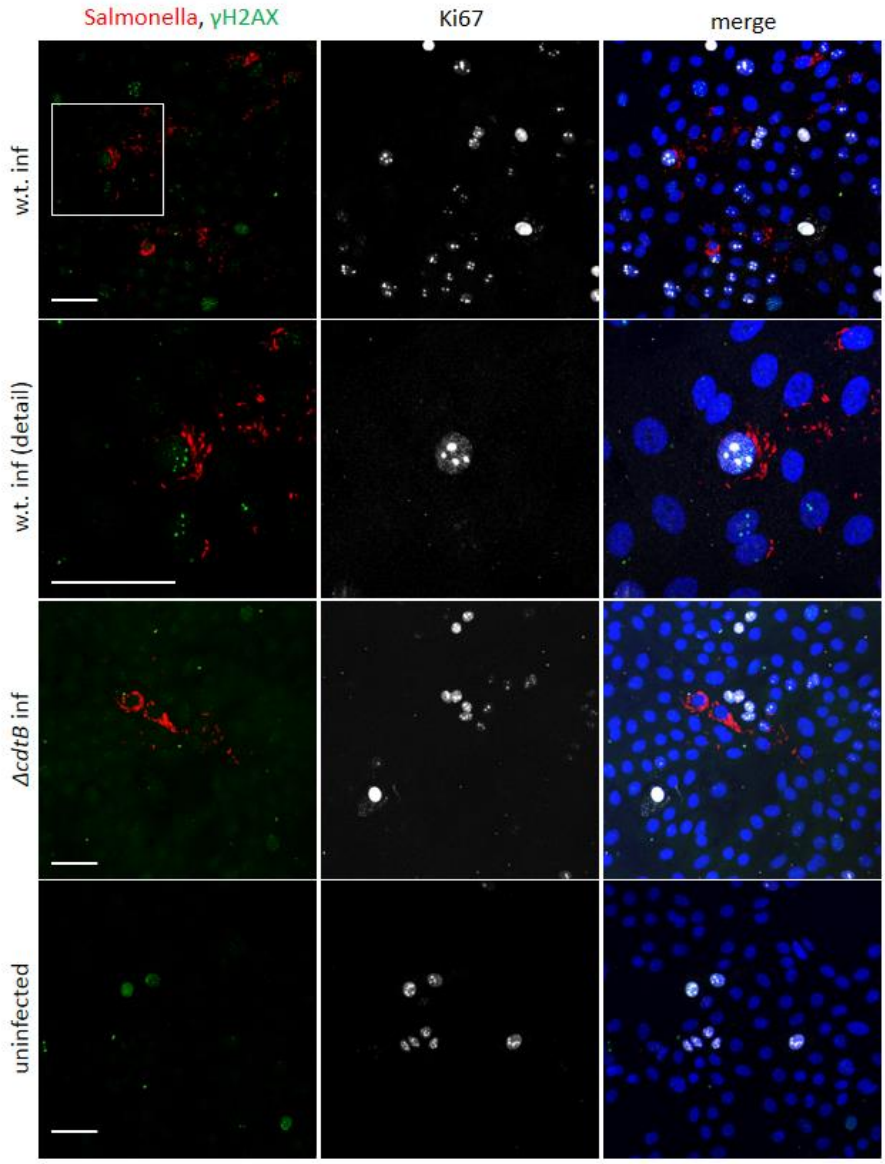

Figure II - 29 Immunostaining of infected cells with DNA damage and proliferation markers. 2D gall bladder primary cells were fixed 3 days after infection with *Salmonella* w.t. or *ΔcdtB* carrying mCherry plasmid. Fixed cells were immunostained with antibodies anti γH2AX (green), Ki67 (white) and Hoechst was used to stain the nuclei (blue). Fluorescent *Salmonella* in red. The second row is the magnification of the box highlighted in the w.t. infected cells. Scale bar is 50um.

5. DISCUSSION

5.1 Small gall bladders on a dish: the gall bladder organoids

Molecular biology in general, and cancer biology in particular, benefitted immensely from the use of cell lines. Cell lines, however, have certain limitations. They are derived from cancer or are otherwise genetically immortalized, making studies on transformation difficult to interpret. In addition different research institutes which supposedly work on the same cell line, might find themselves using different, highly heterogeneous clones, due to the fact that the culturing itself is enough to induce mutations (Marx 2014).

On the other hand the use of primary cells was traditionally complicated by fibroblast outgrowth, particularly when trying to cultivate epithelial cells (Jones 2008; Mitra et al. 2013), and by the entry of cells in irreversible senescence (Campisi & d'Adda di Fagagna 2007). Nevertheless, a number of attempts were made to cultivate primary gall bladder epithelial cells.

In 1980 Koyama and colleagues established a cell line from human gall bladder carcinoma (Koyama et al. 1980). A few years later, inspired by this work, but at the same time realizing that "it is not ideal to use carcinoma cells to examine GBEC [gall bladder epithelial cells] function because they may have lost some of their differentiated functions", Elhamady and colleagues were the first to cultivate primary GB cells originating from a guinea pig (Elhamady et al. 1983). Later, other groups succeeded in cultivating the gall bladder epithelium from different sources: dogs (Oda et al. 1991), cows (Plevris et al. 1993), humans (Auth et al. 1993), prairie dogs (Chapman et al. 1998) and mice (Kuver et al. 1997). Interestingly, while most of these papers lamented the limited life span of the primary culture, Kuvar and colleagues claimed a long-term culture of murine GB cells (more than 6 months and 20 passages) (Kuver et al. 1997). Unfortunately, the stability of such long-term culture was not confirmed by later publications.

Moreover, beside the limited life span of traditional primary cell cultures, another issue was that the morphology did not reflect the cellular architecture of the epithelial cell *in vivo*. Primary cells

grown on a plastic surface appeared flat, while the epithelium of the gall bladder consists of polarized columnar cells.

Pioneering work from the lab of Hans Clevers, however, managed to overcame the problems of both senescence and cell morphology of primary epithelial cells by the development of organoids (Sato & Clevers 2013). Thanks to this innovative 3D primary cell culture method, the adult stem cell potential is maintained *in vitro*, avoiding the cells to undergo senescence, and enabling the stable long term culture of primary epithelial cells. In addition the cell morphology of the organoids reflects the morphology of the organ *in vivo* (Fatehullah et al. 2016). Organoids, however, were not established for the human GB.

The initial aim of this thesis was therefore to develop an organoid model from the human GB. Initial attempts were carried out on murine material because of its easy availability. I managed to find the correct cocktail of growth factors involved in the maintenance of stemness and, together with the physical support given by the matrigel, I managed to keep and expand the culture for an indefinite time. The maintenance of stemness potential was verified by the stability in organoid-forming cells between an early and late time point (Figure II - 1). Moreover, the organoid model reassembled the organ of origin from the protein marker point of view, and its GB epithelium identity did not change in time (Figure II - 2).

The success using murine material demonstrated that in principle it is possible to grow primary GB cells as organoids. After adjustments in the cell isolation techniques and in the defined culture medium, I succeeded in establishing an organoid model from for the human tissue, overcoming recent struggles in cultivating GB epithelial cells (Imamura et al. n.d.). Again, the stem cell potential was maintained in time and the phenotype recapitulated the organ of origin (Figure II – 4 and 13): a polarized monolayer of epithelial cells expressing markers typical of the GB: Muc5B, CK19, and Cla-2.

I went deeper and tested also the functionality of the organoids. The transport functions of the GB were conserved in the organoids, as seen by the activity of the multidrug transported MDR1 (Figure II - 15). Thus, my GB organoid system reflects the organ of origin in terms of morphology, protein markers and even functionality, making it the ideal tool to study GB physiology *in vitro*.

Gallstone formation is the most common causes of inflammatory disease in the GB and defects in the phospholipids` constitution of bile or in transport mechanisms are associated with increased susceptibility to gallstone formation (Dowling 2000). My model thus provides an unprecedented opportunity for studying bile transport in authentic human GB. After ensuring the identity and stability of the model, I focused on investigating the mysterious stemness of the adult human gall bladder.

The Wnt/β-catenin pathway has been found to be essential for the homeostasis of several gastrointestinal epithelia, notably the intestinal crypts and gastric glands (Fevr et al. 2007; Schepers & Clevers 2012). Consequently the receptor of the pathway, Lgr5, was identified as the adult stem cell marker of many epithelia including those of the gastrointestinal tract, like the small intestine and the colon (Barker et al. 2007), but also of the liver intrahepatic ducts - though only after cellular damage (Huch, Boj, et al. 2013). Remarkably the organoids proved to be an unprecedented tool to study adult stemness, for example making use of them for lineage tracing experiments *in vitro*.

Contrarily to the stomach and intestine, which stem cell pathways and markers receive a lot of attention and are relatively well understood, there is no evidence of Wnt/β-catenin pathway activation in the stem cells of the gall bladder. One study, however, pointed out that the activation of Lgr5 is needed for the maintenance of murine gall bladder organoids (Lugli et al. 2016).

I have found human organoids to be strictly dependent on the activation of the Wnt/β-catenin pathway by their ligands Wnt and R-spondin. Interestingly, while R-spondin has to be provided to the culture exogenously, epithelial GB cells produce Wnt, which is sufficient for the long term propagation of the culture. If Wnt secretion is blocked with IWP2, an inhibitor of Porcupine, the organoids cannot form (Figure II - 6).

Wnt agonists may activate not just the canonical Wnt/β-catenin pathway, but even additional signaling pathways. At the same time Wnt family members have overlapping functions: different Wnts activate the analogous receptors, triggering the same cascade (Koch 2017). This redundancy is indeed seen in human GB organoids, in which epithelial cells produce Wnt7a, 7b, 4, 11 and 3. Interestingly, while the level of Wnt3 and Wnt11 remained the same, I observed a switch in Wnt

production, from Wnt7a/b to Wnt4, when stem cells undergo differentiation (Figure II - 7). The biological meaning of this switch will need further investigation to be elucidated.

In order to have a proof of Wnt functionality I looked at the activation of one of its most common target genes: Axin2. For this purpose I switched back to the mouse, taking advantage of an Axin2 reporter mouse (Figure II – 8), and could observe that in the organoids Wnt activation is homogenous, highlighting the fact that the produced Wnts are correctly functional and that there is no Wnt gradient, contrarily to what happens in the intestinal stem cell niche (Farin et al. 2016).

To study the expression of markers and pathways of human GB stem cells, I analyzed the transcriptional profile of organoids harvested at different times after seeding, via microarray. I hypothesized that early organoids are enriched in stem cells, while late organoids are enriched in differentiated cells, and could confirm this hypothesis by observing the different expression pattern of the endoderm stem cell markers SOX17 and PROX1, found to enrich early organoids. Sox 17 is an embryonic gall bladder marker (Uemura et al. 2010). During embryo development pancreatobiliary common progenitor cells positive for both Sox17 and Pdx1 differentiate into Sox17+/Pdx1- gallbladder progenitors and Sox17-/Pdx1+ ventral pancreatic progenitors (Saito et al. 2013). I found that Sox17 is still express in the adult gall bladder, and in these settings its expression correlates with the presence of stem cells.

Interestingly, the putative intestinal stem cell marker DCLK1 (May et al. 2009) was found to be the gene mostly upregulated in the early organoids, therefore it likely represents an important adult stem cell marker of the human GB.

The differentiated nature of late organoids was similarly confirmed observing that the transcription of all the mucins was upregulated in late organoids, as well as the adult gall bladder marker MOGAT1 (Kampf et al. 2014) (Figure II - 12). Using the same approach I detected β-catenin target genes to be upregulated in early-stem cell-enriched organoids (Figure II - 9). In particular early organoids were enriched in LEF1 (the transcription factor binding to nuclear β-catenin), in Lgr5 (the receptor of Rspo) and in the secreted negative regulators of the pathway Dickkopf1 and 4 (DKK). Interestingly late organoids were enriched in Axin2, the scaffold protein of the destruction complex, which inhibits the translocation of β-catenin in the nucleus. It is well

established that negative regulators of the Wnt/β-catenin pathway are transcriptional targets of the same pathway. This negative feedback allows a fine tuning of Wnt activity (Koch 2017). I could detect two different mechanisms by which the pathway is regulated, based on the differentiated status of the epithelial cells. In stem cells Wnt activates preferentially the secreted antagonist DKK, allowing the cells to maintain the activity of the Wnt/β-catenin pathway. Differentiated cells, on the other hand, express higher amount of the intracellular inhibitor Axin2, which results in the shutdown of the pathway.

The observation that Lgr5 is overexpressed in early organoids enriched in stem cells made me hypothesize that Lgr5 might indeed represent an adult stem cells marker of the GB. In order to test this hypothesis, I took advantage of a reporter mouse which normally expresses mTomato, switching to mGFP in Lgr5+ derived cells, after induction with HT. After growing organoids from the mouse and *in vitro* HT induction, I noticed that Lgr5+ cells represented a minority. While passaging the organoids, however, I observed a slow but unrelenting expansion of organoids derived from Lgr5+ cells (Figure II - 10), meaning that only Lgr5 expressing cells could proliferate for a long term, an ability typical of stem cells.

In conclusion my work describes for the first time the establishment of human GB organoids (a publication describing the generation of murine GB organoids was published while my work was in process (Lugli et al. 2016)). The organoids possess phenotypical and functional features typical of the organ of origin, and can be expanded for a long-term without loss of stemness potential or gall bladder epithelial identity. Furthermore I could prove that the Wnt/β-catenin pathway activation is needed for the maintenance of stemness via self-produced Wnt and exogenous R-spondin. I also identified Lgr5 as a stem cell marker of the adult GB and DCLK1 as another potential GB stem cell marker.

This model can therefore be taken advantage of for the investigation of GB epithelial physiology, pathology and adult stemness. Another unprecedented advantage of GB organoids it that they represent a unique tool to study the interaction between human-restricted *Salmonellae* and their host, focusing on potentially malignant consequences.

5.2 Infection of human primary gall bladder epithelial cells with *Salmonella enterica* serovar Paratyphi A

Despite strong epidemiological evidences linking the chronic carriage of *Salmonella* Typhi / Paratyphi A with the development of GBC, most of the *Salmonella* research focused on *Salmonella* Typhimurium, a murine serovar that causes self-limiting gastroenteritis and is not linked with the development of GBC. Mice are susceptible to Typhimurium, therefore an *in vivo* model exists, but *in vitro* infections relied on classical cell lines.

The most severe outcome for humans, typhoid and paratyphoid fever, results from Typhoidal *Salmonellae* infection, *i.e.* serovar Typhi and Paratyphi A. These serovars have a strict human host specificity: Mice are not susceptible, and the only existing mouse model relies on the use of an immunodeficient-humanized mouse (Song et al. 2010). Organoids represent therefore the logical solution to close the gap between human *Salmonellae* and their natural host.

Salmonella Typhimurium was already used as a pathogen to infect murine and human intestinal organoids by simple co-cultivation of the bacteria with the organoids (Zhang et al. 2014) or by microinjection (Wilson et al. 2014; Forbester et al. 2015).

Two methods are normally used for the bacterial infection of organoids; the first is the injection of pathogens in the lumen; the second is the seeding of organoids-derived cells in 2D, following co-cultivation with the bacteria (Bartfeld 2016; Schlaermann et al. 2014). The main problem with the microinjection lies in the technical difficulties of the method itself: microinjecting hundreds of organoids at the time is a tedious and not fully precise procedure. The infection of 2D grown primary cells is more controllable and reproducible, however host cells lose their polarity, therefore they not fully recapitulate any more the tissue of origin.

Pioneer work by Scanu and colleagues recently described the infection of primary fibroblast and murine GB organoids with *Salmonella* Typhimurium. The authors infected fibroblasts from a cancer-predisposed mouse harboring Arf deficiency (which inactivates TP53) and c-MYC overexpression, and found that the infection promoted anchorage independent growth *in vitro*, and solid tumour growth after xenotransplantation in mice. They then infected murine GB organoids, originating from a mouse lacking the Arf locus, with *S.* Typhimurium, and reported

organoids´ growth in a supplement-depleted medium. These events were mediated by the activation of the Akt and Map kinase pathway. Because of anchorage independent growth and growth in supplement deprived medium, the authors concluded that *Salmonella* might play a role in tumour development (Scanu et al. 2015).

For my work, I decided to use the human *Salmonella* Paratyphi A and to infect the human GB organoids that I previously generated. In order to expose the luminal side of the cells, the organoids were mechanically sheared and subsequently co-cultured with the bacteria. After re-seeding in matrigel, the organoids reconstituted an intact structure, and the bacteria grew intracellularly forming defined foci of infection (Figure II – 19). Alternatively organoids were used as a source of primary cells, which were then seeded in 2D on a plastic surface and then infected (Figure II – 21 and 25).

The first and most sticking outcome of the Infection with *Salmonella* Paratyphi A was the triggering of inflammatory response (Figure II - 23). I noticed the upregulation of chemokines, of inflammatory mediators like BCL2A1, IL1B, TNF, IL11, IL8 and IL 17C, of opsonizing proteins like SAA1, 2 and 4, and of defensins, in particular the human β-defensin 2 (DEFB4A).

Human β-defensin 2 represents a typical defensin of the GB (Fagerberg, Hallstrom et al., 2014). Its production was already found to be induced in cell lines following infection with various *Salmonella* strains (Ogushi, Wada et al., 2001), and it was also found to have bactericidal effect against the bacterium (Maiti, Patro et al., 2014).

The induction of inflammatory response might in part represent the answer to the question of how a chronic infection can induce malignant transformation (Boccellato & Meyer 2015; Espinoza et al. 2016). The inflamed environment resulting from chronic infection and cholelithiasis (Gonzalez-Escobedo et al. 2011) leads to a constant and prolonged release of mitogenic, pro survival and anti apoptotic signals (Saleh & Trinchieri 2011; Chatzinikolaou et al. 2014; Elinav et al. 2013; Borrello et al. 2008; Coussens & Werb 2002). In a normal scenario inflammation serves as a form of protection, eradicating the pathogens and the damaged cells and providing the signals for the replacement of the wounded tissue, but in the case of tumours the “wound does not heal” (Dvorak 1986). During chronic inflammation mitogenic and pro survival pathways are

excessively induced, some of which are remarkably in common with the cancerous tissue, like STAT3 and NFκB (Elinav et al. 2013). The link between inflammation and cancer development is in fact a well-accepted concept (Saleh & Trinchieri 2011).

Inflammatory mitogenic and anti-apoptotic stimuli however would not lead to malignant transformation in the presence of a correct response. Hypersusceptibility to proliferative signals, aberrant response to apoptotic signals and failure to activate a proper DNA damage response are required for a pre-malignant cell to gain selective clonal advantage over the healthy ones. Acquisition of these hallmarks depends on mutations and genomic instability (Hanahan & Weinberg 2011). Genotoxicity is therefore of central importance.

Genotoxicity could be due to the infection-induced reactive oxygen species (ROS) (Felmy et al. 2013; Hardbower et al.; Abdul-Sater et al. 2010) and reactive nitrogen species (RNS) production (Raffatellu et al. 2008; Henard & Vázquez-Torres 2011), already linked with the toumorigenesis (Hussain et al. 2003; Erdman et al. 2009). Indeed, infected primary cells upregulate the transcription of NADPH Oxidase 1 (NOX1), an enzyme involved in the generation of ROS (Figure II – 23 and 24). Induction of ROS, however, is triggered in response to most bacterial pathogens, even non-carcinogenic ones (Fang 2011), therefore it is unlikely to be the sole mutagenic agent.

In addition it was hypothesized, but never proven, that *Salmonella* can provoke genotoxicity though the metabolism of bile, producing genotoxic byproducts (Caygill et al. 1994). The most intriguing aspect, is that *Salmonella* Typhi / Paratyphi A can also provoke direct DNA damage by the action of the typhoid toxin. Following the infection of GB organoids with typhoid toxin-producing bacteria, I noticed autocrine as well as paracrine genotoxicity, which was strictly dependent on the CdtB subunit of the typhoid toxin. I observed that the genotoxic effect originated from the infected cell and spanned up to three rings of neighboring uninfected cells (Figure II - 20). This paracrine effect could easily be explained by the secretion mechanism of the typhoid toxin. Only invasive bacteria produce the toxin, which is then secreted from the infected cell in the extracellular environment. Neighboring cells then uptake the toxin independently from their infection status (Figueira & Holden 2012). The farther the toxin travels from the infected cell, the more it gets diluted, which is why the highest rate of genotoxicity is found in the infected cell itself. It then decreases, but is still evident, in the first three rings of surrounding, uninfected

cells, and then it completely fades farther away. Given the similarity between the organoids and the epithelium *in vivo*, this paracrine effect is most likely what *Salmonella* carriers experience for many years: a genotoxic environment that surrounds the infection focus (Figure III – 1).

In addition to typhoid toxin-dependent genotoxicity, another low-level DNA damaging effect restricted to the infected cell could be detected, which was 7 fold weaker than the genotoxic effect of CdtB (Figure II – 20). Given the fact that NOX1 is found upregulated in w.t as well as *ΔcdtB* infected cells, I concluded that it was most probably due to ROS production (Figure II – 23 and 24), however, because of its weak effect, it is unlikely to have a mutagenic role in the development of GBC.

Genotoxic stress on immune cells is hypothesized to cause local immunosuppression (Faïs et al. 2016), because immune cells, especially T cells, are highly sensitive to CDT (Shenker et al. 2004). Localized deficiency of immune response might have a double effect (Figure III – 1). (1) It might favor bacteria growth, therefore persistence. It has indeed been proven that the CdtB subunit of CDT is necessary for *Helicobacter hepaticus* persistent colonization (Ge et al. 2005), and that the typhoid toxin of *Salmonella* Typhi is essential for chronic infection of mice (Del Bel Belluz et al. 2016; Song et al. 2010). (2) The lack of immune surveillance that targets and lyses tumour cells, might promote tumour progression by allowing an uncontrolled growth of the tumoural mass.

Thanks to the organoids I was able to infect human gall bladder cells with its natural pathogen: *Salmonella* Paratyphi A, and I showed for the first time how the genotoxic environment appears and how far does it extend. Up to this point I assayed the DNA damage through the upregulation of γH2AX, a histone variant found on the site of DNA breaks. Recent evidences, however, suggest the possibility that γH2AX might also be induced during other cellular processes, like chromosome segregation (Turinetto & Giachino 2015). I needed therefore to confirm the genotoxic effect of CdtB without relying exclusively on γH2AX, but the patchy phenotype of infection in organoids represented an obstacle. In order to overcome this and to study the DNA damaging role of CdtB in cells more homogenously intoxicated, I decided to treat 2D grown primary cells with the toxin-containing supernatant of the bacteria. This intoxication method allowed me to detect direct DNA breaks via comet assay, which were reflected by the overexpression of γH2AX (Figure II - 27).

The most surprising observation was, however, that intoxicated cells did not arrest their cell cycle, despite the fact that cell cycle arrest, senescence, and in some cases apoptosis, are phenotypes normally triggered by genotoxin-induced DNA damage (Gagnaire et al. 2017). Not only cells intoxicated with the typhoid toxin continued to proliferate at the rate of the untreated cells, but proliferative cells intoxicated with the w.t. toxin harbored more DNA breaks than proliferative cells treated with a toxin lacking CdtB or left untreated (Figure II - 28). The observation that cells continue to proliferate despite being intoxicated by a genotoxin is remarkable, but not unprecedented. In 2010 Ramos and colleagues concluded that cells exposed to a low level of *E. coli* colibactin kept proliferating despite genomic aberrations (Cuevas-Ramos et al. 2010). Colibactin-producing *E. coli* is indeed epidemiologically linked with human colorectal cancer (Buc et al. 2013). A later study by Guidi and colleagues came to a similar conclusion by chronically intoxicating cells with doses of *H. hepaticus* CDT which were not sufficient to arrest the cell cycle, but enough to induce mutations and chromosomal aberrations (Guidi, Guerra, et al. 2013). CDT-producing *H. hepaticus* is a well-established murine carcinogenic bacterium (Ge et al. 2007).

My data show that human primary gall bladder cells are subjected to a low but persistent level of DNA damage caused by the CdtB subunit of the *S.* Paratyhi A-encoded typhoid toxin, and that damaged cells fail to arrest their cell cycle. In parallel to the genotoxicity it has been show that *Salmonella* is able to promote cell cycle trough the activation of AKT and MAPK pathway: in a xenograft model *S.* Typhimurium, which lacks the typhoid toxin, is in fact able to induce cancer formation of genetically predisposed primary fibroblast (Scanu et al. 2015). Mutations leading to such a predisposition can occur in chronic carriers that are subjected to low level of genotoxicity for years, resulting in DNA breaks, but without cell cycle arrest. Together with the reported anti-apoptotic effects of *Salmonella* on the host cells (Steele-Mortimer et al. 2000; Roppenser et al. 2013) and the persistent inflammation, this is likely to contribute to the increased risk of developing malignant mutations observed in chronic carriers (Boccellato & Meyer 2015). In addition to the cancer initiation events, *Salmonella* could also play a role in later events: the formation of a localized genotoxic environment, toxic to immune cells, might avoid immune detection and clearance of the tumour mass.

In conclusion my work describes the establishment of organoid model from the human and murine adult gall bladder. I have phenotypically and functionally characterized the organoids, and I have identified the adult stem cell markers. Subsequently I have infected the human gall bladder epithelial cells with their natural pathogen *Salmonella enterica* serovar Paratyphi A, and observed that the infection leads to genotoxicity dependent on the CdtB subunit of the typhoid toxin. Furthermore I have noticed that the genotoxic effect works in an autocrine as well as paracrine way, meaning that not just the infected cell, but also neighboring uninfected cell are subjected to DNA damage. I quantified the range of this paracrine genotoxic effect and, unexpectedly, observed that the DNA damage was not coupled with arrest in cell cycle. This low grade genotoxicity, enough to induce DNA damage but not arrest the cell cycle, might be the key mechanism by which human *Salmonellae* can induce mutations, therefore malignant transformation.

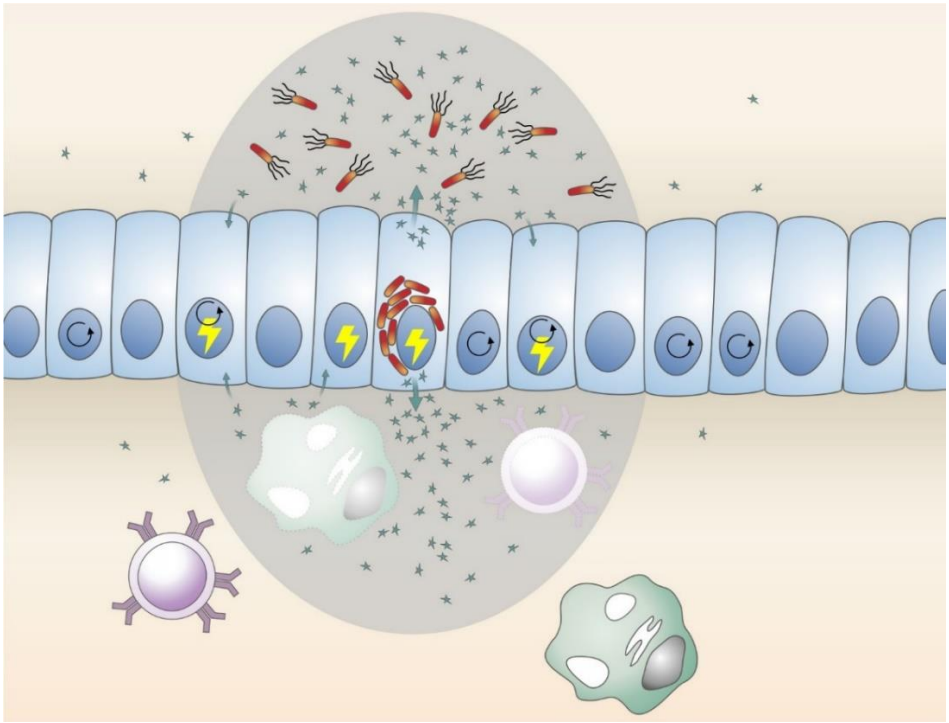

Figure III - 1 *Salmonella* genotoxicity in the gall bladder. The epithelial cell infected by *Salmonella* Typhi/Paratyphi A secretes the typhoid toxin, which affects the 3 neighboring uninfected cells (gray area) causing DNA damage (yellow bolt) without arresting the cell cycle (circular arrow). Chronic exposure to the toxin might eventually lead to malignant mutations.
The lethal effect of the toxin on immune cells (dead immune cells are dashed) prevents the detection and clearance of the transformed cells, facilitating the growth of the tumor mass. Furthermore, the lack of viable immune cells prevents the clearance of the infection, therefore supporting chronic carriage of *Salmonella*.

6. REFERENCES

Alouf, J.E. (Joseph E.., Ladant, D. & Popoff, M.R., 2015. *The comprehensive sourcebook of bacterial protein toxins*, Elsevier.

Andia, M.E. et al., 2008. Geographic variation of gallbladder cancer mortality and risk factors in Chile: a population-based ecologic study. *International journal of cancer. Journal international du cancer*, 123(6), pp.1411–6.

Annaert, P.P. & Brouwer, K.L.R., 2004. ASSESSMENT OF DRUG INTERACTIONS IN HEPATOBILIARY TRANSPORT USING RHODAMINE 123 IN SANDWICH-CULTURED RAT HEPATOCYTES. *Drug Metabolism and Disposition*, 33(3), pp.388–394.

Aoki-Yoshida, A. et al., 2016. Lactobacillus rhamnosus GG increases Toll-like receptor 3 gene expression in murine small intestine ex vivo and in vivo. *Beneficial microbes*, 7(3), pp.421–9.

Arnold, K. et al., 2011. Sox2+ Adult Stem and Progenitor Cells Are Important for Tissue Regeneration and Survival of Mice. *Cell Stem Cell*, 9(4), pp.317–329.

Auth, M.K. et al., 1993. Establishment and immunological characterization of cultured human gallbladder epithelial cells. *Hepatology (Baltimore, Md.)*, 18(3), pp.546–555.

Barker, N. et al., 2009. Crypt stem cells as the cells-of-origin of intestinal cancer. *Nature*, 457(7229), pp.608–611.

Barker, N. et al., 2007. Identification of stem cells in small intestine and colon by marker gene Lgr5. *Nature*, 449(7165), pp.1003–1007.

Bartfeld, S. et al., 2015. In Vitro Expansion of Human Gastric Epithelial Stem Cells and Their Responses to Bacterial Infection. *Gastroenterology*, 148(1), p.126–136.e6.

Bartfeld, S., 2016. Modeling infectious diseases and host-microbe interactions in gastrointestinal organoids. *Developmental Biology*, 420(2), pp.262–270.

Basak, F. et al., 2016. Incidental findings during routine pathological evaluation of gallbladder specimens: review of 1,747 elective laparoscopic cholecystectomy cases. *Annals of the Royal*

College of Surgeons of England, pp.1–4.

Battle, M.A. et al., 2006. Hepatocyte nuclear factor 4 orchestrates expression of cell adhesion proteins during the epithelial transformation of the developing liver. *Proceedings of the National Academy of Sciences*, 103(22), pp.8419–8424.

Behar, J. et al., 1989. Gallbladder contraction in patients with pigment and cholesterol stones. *Gastroenterology*, 97(6), pp.1479–84.

Behar, J., 2013. Physiology and Pathophysiology of the Biliary Tract: The Gallbladder and Sphincter of Oddi—A Review. *ISRN Physiology*, 2013, pp.1–15.

Del Bel Belluz, L. et al., 2016. The Typhoid Toxin Promotes Host Survival and the Establishment of a Persistent Asymptomatic Infection. *PLoS pathogens*, 12(4), p.e1005528.

Bezine, E. et al., 2016. Cell resistance to the Cytolethal Distending Toxin involves an association of DNA repair mechanisms. *Scientific Reports*, 6(1), p.36022.

Bezine, E., Vignard, J. & Mirey, G., 2014. The cytolethal distending toxin effects on Mammalian cells: a DNA damage perspective. *Cells*, 3(2), pp.592–615.

Blander, J.M. & Medzhitov, R., 2006. On regulation of phagosome maturation and antigen presentation. *Nature Immunology*, 7(10), pp.1029–1035.

Blaydon, D.C., Philpott, M.P. & Kelsell, D.P., 2007. R-Spondins in Cutaneous Biology: Nails and Cancer. *Cell Cycle*, 6(8), pp.895–897.

Boccellato, F. & Meyer, T.F., 2015. Bacteria Moving into Focus of Human Cancer. *Cell host & microbe*, 17(6), pp.728–30.

Brawn, L.C., Hayward, R.D. & Koronakis, V., 2007. Salmonella SPI1 effector SipA persists after entry and cooperates with a SPI2 effector to regulate phagosome maturation and intracellular replication. *Cell host & microbe*, 1(1), pp.63–75.

Brodie, J., Macqueen, I.A. & Livingstone, D., 1970. Effect of trimethoprim-sulphamethoxazole on typhoid and salmonella carriers. *British medical journal*, 3(5718), pp.318–9.

Buc, E. et al., 2013. High Prevalence of Mucosa-Associated E. coli Producing Cyclomodulin and Genotoxin in Colon Cancer J. R. Battista, ed. *PLoS ONE*, 8(2), p.e56964.

Campisi, J. & d'Adda di Fagagna, F., 2007. Cellular senescence: when bad things happen to good cells. *Nature Reviews Molecular Cell Biology*, 8(9), pp.729–740.

Carvajal-Restrepo, H. et al., 2017. Detection of Salmonella human carriers in Colombian outbreak areas. *Journal of infection in developing countries*, 11(3), pp.228–233.

Caygill, C.P.J. et al., 1994. Cancer mortality in chronic typhoid and paratyphoid carriers. *Lancet*, 343(8889), pp.83–84.

Caygill, C.P.J. & Hill, M.J., 2000. Salmonella typhi/paratyphi and gallbladder cancer.

Chandel, D. et al., 2000. Drug-Resistant Salmonella enterica Serotype Paratyphi A in India. *Emerging Infectious Diseases*, 6(4), pp.420–421.

Chandrakesan, P. et al., 2017. Dclk1, a tumor stem cell marker, regulates pro-survival signaling and self-renewal of intestinal tumor cells. *Molecular Cancer*, 16(1), p.30.

Chang, S.-J., Song, J. & Galán, J.E., 2016. Receptor-Mediated Sorting of Typhoid Toxin during Its Export from Salmonella Typhi-Infected Cells. *Cell Host & Microbe*, 20(5), pp.682–689.

Chapman, W.C. et al., 1998. Establishment and Characterization of Primary Gallbladder Epithelial Cell Cultures in the Prairie Dog. *Journal of Surgical Research*, 80(1), pp.35–43.

Charles, R.C. et al., 2013. Identification of Immunogenic Salmonella enterica Serotype Typhi Antigens Expressed in Chronic Biliary Carriers of S. Typhi in Kathmandu, Nepal J. M. Vinetz, ed. *PLoS Neglected Tropical Diseases*, 7(8), p.e2335.

Chen, Y., Kong, J. & Wu, S., 2015. Cholesterol gallstone disease: focusing on the role of gallbladder. *Laboratory Investigation*, 95(2), pp.124–131.

Chumduri, C. et al., 2013. Chlamydia infection promotes host DNA damage and proliferation but impairs the DNA damage response. *Cell Host and Microbe*, 13(6), pp.746–758.

Clevers, H. & Nusse, R., 2012. Wnt/?-Catenin Signaling and Disease. *Cell*, 149(6), pp.1192–1205.

Costerton, J.W., Stewart, P.S. & Greenberg, E.P., 1999. Bacterial biofilms: a common cause of persistent infections. *Science (New York, N.Y.)*, 284(5418), pp.1318–22.

Crump, J.A. & Mintz, E.D., 2010. Global trends in typhoid and paratyphoid Fever. *Clinical infectious diseases : an official publication of the Infectious Diseases Society of America*, 50(2), pp.241–6.

Crump, J., Luby, S. & Mintz, E., 2004. The global burden of typhoid fever. *Bulletin of the World Health Organization*, 2295(3), pp.346–353.

Cuevas-Ramos, G. et al., 2010. Escherichia coli induces DNA damage in vivo and triggers genomic instability in mammalian cells. *Proceedings of the National Academy of Sciences of the United States of America*, 107(25), pp.11537–42.

Datsenko, K. a & Wanner, B.L., 2000. One-step inactivation of chromosomal genes in Escherichia coli K-12 using PCR products. *Proceedings of the National Academy of Sciences of the United States of America*, 97(12), pp.6640–6645.

Dave, J. et al., 2017. What were the risk factors and trends in antimicrobial resistance for enteric fever in London 2005?2012? *Journal of Medical Microbiology*.

Davis, E.K., Zou, Y. & Ghosh, A., 2008. Wnts acting through canonical and noncanonical signaling pathways exert opposite effects on hippocampal synapse formation. *Neural Development*, 3(1), p.32.

Deng, L. et al., 2014. Host adaptation of a bacterial toxin from the human pathogen Salmonella Typhi. *Cell*, 159(6), pp.1290–9.

DiRienzo, J., 2014. Uptake and Processing of the Cytolethal Distending Toxin by Mammalian Cells. *Toxins*, 6(11), pp.3098–3116.

Dobinson, H.C. et al., 2017. Evaluation of the Clinical and Microbiological Response to Salmonella Paratyphi A Infection in the First Paratyphoid Human Challenge Model. *Clinical Infectious Diseases*, 64(8), pp.1066–1073.

Dougan, G. et al., 2011. Immunity to salmonellosis. *Immunological Reviews*, 240(1), pp.196–210.

Dowling, R.H., 2000. Review: pathogenesis of gallstones. *Alimentary pharmacology & therapeutics*, 14 Suppl 2, pp.39–47.

Drecktrah, D. et al., 2006. The Mechanism of Salmonella Entry Determines the Vacuolar Environment and Intracellular Gene Expression. *Traffic*, 7(1), pp.39–51.

Driehuis, E. & Clevers, H., 2017. CRISPR/Cas 9 genome editing and its applications in organoids. *American Journal of Physiology - Gastrointestinal and Liver Physiology*.

Drost, J. et al., 2015. Sequential cancer mutations in cultured human intestinal stem cells. *Nature*, 521(7550), pp.43–47.

Eastman, Q. & Grosschedl, R., 1999. Regulation of LEF-1/TCF transcription factors by Wnt and other signals. *Current Opinion in Cell Biology*, 11(2), pp.233–240.

el-Zayadi, A. et al., 1991. Bile duct carcinoma in Egypt: possible etiological factors. *Hepato-gastroenterology*, 38(4), pp.337–40.

Elamin, E. et al., 2013. Fatty Acid Ethyl Esters Induce Intestinal Epithelial Barrier Dysfunction via a Reactive Oxygen Species-Dependent Mechanism in a Three-Dimensional Cell Culture Model M. A. Deli, ed. *PLoS ONE*, 8(3), p.e58561.

Elhadad, D. et al., 2016. Differences in Host Cell Invasion and SPI-1 Expression between Salmonella enterica serovar Paratyphi A and the Non-Typhoidal Serovar Typhimurium. *Infection and immunity*.

Elhamady, M.S. et al., 1983. Tissue culture of guinea-pig gall-bladder epithelium. *The Journal of Pathology*, 140(3), pp.221–235.

Elwell, C.A. & Dreyfus, L.A., 2000. DNase I homologous residues in CdtB are critical for cytolethal distending toxin-mediated cell cycle arrest. *Molecular microbiology*, 37(4), pp.952–63.

Engevik, M.A. et al., 2013. Loss of NHE3 alters gut microbiota composition and influences Bacteroides thetaiotaomicron growth. *AJP: Gastrointestinal and Liver Physiology*, 305(10), pp.G697–G711.

Erdman, S.E. et al., 2003. CD4+ CD25+ Regulatory T Lymphocytes Inhibit Microbially Induced

Colon Cancer in Rag2-Deficient Mice. *The American Journal of Pathology*, 162(2), pp.691–702.

Fàbrega, A. & Vila, J., 2013. Salmonella enterica serovar Typhimurium skills to succeed in the host: virulence and regulation. *Clinical microbiology reviews*, 26(2), pp.308–41.

Faïs, T. et al., 2016. Impact of CDT Toxin on Human Diseases. *Toxins*, 8(7), p.220.

Faiz, O. & Moffat, D., 2002. *Anatomy At a Glance*, Blackwell Science.

Fang, F.C., 2011. Antimicrobial actions of reactive oxygen species. *mBio*, 2(5), pp.e00141-11.

Farin, H.F. et al., 2016. Visualization of a short-range Wnt gradient in the intestinal stem-cell niche. *Nature*, 530(7590), pp.340–343.

Fatehullah, A., Tan, S.H. & Barker, N., 2016. Organoids as an in vitro model of human development and disease. *Nature Cell Biology*, 18(3), pp.246–254.

Felix, A., 1938. DETECTION OF CHRONIC TYPHOID CARRIERS BY AGGLUTINATION TESTS. *The Lancet*, 232(6004), pp.738–741.

Ferlay, J. et al., 2013. Cancer incidence and mortality patterns in Europe: Estimates for 40 countries in 2012. *European Journal of Cancer*, 49(6), pp.1374–1403.

Fevr, T. et al., 2007. Wnt/beta-catenin is essential for intestinal homeostasis and maintenance of intestinal stem cells. *Molecular and cellular biology*, 27(21), pp.7551–9.

Figueira, R. & Holden, D.W., 2012. Functions of the Salmonella pathogenicity island 2 (SPI-2) type III secretion system effectors. *Microbiology*, 158(Pt_5), pp.1147–1161.

Fink, S.L. & Cookson, B.T., 2007. Pyroptosis and host cell death responses during Salmonella infection. *Cellular Microbiology*, 9(11), pp.2562–2570.

Forbester, J.L. et al., 2015. The interaction of *Salmonella enterica* Serovar Typhimurium with intestinal organoids derived from human induced pluripotent stem cells. *Infection and Immunity*, (May), p.IAI.00161-15.

Förster, C., 2008. Tight junctions and the modulation of barrier function in disease. *Histochemistry*

and cell biology, 130(1), pp.55–70.

Foster, J.W. & Hall, H.K., 1991. Inducible pH homeostasis and the acid tolerance response of Salmonella typhimurium. *Journal of bacteriology*, 173(16), pp.5129–35.

Fowler, C.C. et al., 2017. Emerging insights into the biology of typhoid toxin. *Current Opinion in Microbiology*, 35, pp.70–77.

Fox, J.G. et al., 2011. Helicobacter hepaticus infection in mice: models for understanding lower bowel inflammation and cancer. *Mucosal Immunology*, 4(1), pp.22–30.

Fox, J.G. et al., 1994. Helicobacter hepaticus sp. nov., a microaerophilic bacterium isolated from livers and intestinal mucosal scrapings from mice. *Journal of clinical microbiology*, 32(5), pp.1238–45.

Frisan, T., 2015. Bacterial genotoxins: The long journey to the nucleus of mammalian cells. *Biochimica et biophysica acta*.

Frizzell, R.A. & Heintze, K., 1980. Transport functions of the gallbladder. *International review of physiology*, 21, pp.221–47.

Fu, Y. & Galán, J.E., 1999. A salmonella protein antagonizes Rac-1 and Cdc42 to mediate host-cell recovery after bacterial invasion. *Nature*, 401(6750), pp.293–7.

Gagnaire, A. et al., 2017. Collateral damage: insights into bacterial mechanisms that predispose host cells to cancer. *Nature Reviews Microbiology*, 15(2), pp.109–128.

Gayet, R. et al., 2017. Vaccination against Salmonella Infection: the Mucosal Way. *Microbiology and molecular biology reviews : MMBR*, 81(3), pp.e00007-17.

Ge, Z. et al., 2007. Bacterial cytolethal distending toxin promotes the development of dysplasia in a model of microbially induced hepatocarcinogenesis. *Cellular Microbiology*, 9(8), pp.2070–2080.

Ge, Z. et al., 2005. Cytolethal distending toxin is essential for Helicobacter hepaticus colonization in outbred Swiss Webster mice. *Infection and Immunity*, 73(6), pp.3559–3567.

Gigliozzi, A. et al., 2000. Molecular identification and functional characterization of Mdr1a in rat cholangiocytes. *Gastroenterology*, 119(4), pp.1113–22.

Gonzalez-Escobedo, G. & Gunn, J.S., 2013. Gallbladder epithelium as a niche for chronic salmonella carriage. *Infection and Immunity*, 81(8), pp.2920–2930.

Gordon, M.A., 2008. Salmonella infections in immunocompromised adults. *Journal of Infection*, 56(6), pp.413–422.

Gouwy, M. et al., 2015. Serum amyloid A chemoattracts immature dendritic cells and indirectly provokes monocyte chemotaxis by induction of cooperating CC and CXC chemokines. *European Journal of Immunology*, 45(1), pp.101–112.

Grasso, F. & Frisan, T., 2015. Bacterial Genotoxins: Merging the DNA Damage Response into Infection Biology. *Biomolecules*, 5(3), pp.1762–82.

Guerra, L. et al., 2011. The biology of the cytolethal distending toxins. *Toxins*, 3(3), pp.172–190.

Guidi, R., Guerra, L., et al., 2013. Chronic exposure to the cytolethal distending toxins of Gram-negative bacteria promotes genomic instability and altered DNA damage response. *Cellular Microbiology*, 15(1), pp.98–113.

Guidi, R., Levi, L., et al., 2013. Salmonella enterica delivers its genotoxin through outer membrane vesicles secreted from infected cells. *Cellular Microbiology*, 15(12), pp.2034–2050.

Guidi, R., Belluz, L.D.B. & Frisan, T., 2016. Bacterial genotoxin functions as immune-modulator and promotes host survival. *Microbial Cell*, 3(8), pp.355–357.

Gunn, J.S. et al., 2014. Salmonella chronic carriage: epidemiology, diagnosis, and gallbladder persistence. *Trends in microbiology*, 22(11), pp.648–55.

Gupta, A. et al., 2006. Evaluation of community-based serologic screening for identification of chronic Salmonella Typhi carriers in Vietnam. *International Journal of Infectious Diseases*, 10(4), pp.309–314.

Guttman, J.A. & Finlay, B.B., 2009. Tight junctions as targets of infectious agents. *Biochimica et Biophysica Acta (BBA) - Biomembranes*, 1788(4), pp.832–841.

Haegebarth, A. & Clevers, H., 2009. Wnt signaling, lgr5, and stem cells in the intestine and skin. *The American journal of pathology*, 174(3), pp.715–721.

Haghjoo, E. & Galán, J.E., 2004. Salmonella typhi encodes a functional cytolethal distending toxin that is delivered into host cells by a bacterial-internalization pathway. *Proceedings of the National Academy of Sciences of the United States of America*, 101(13), pp.4614–4619.

Hari-Dass, R. et al., 2005. Serum Amyloid A Protein Binds to Outer Membrane Protein A of Gram-negative Bacteria. *Journal of Biological Chemistry*, 280(19), pp.18562–18567.

Herbst, A. et al., 2014. Comprehensive analysis of β-catenin target genes in colorectal carcinoma cell lines with deregulated Wnt/β-catenin signaling. *BMC Genomics*, 15(1), p.74.

Hodak, H. & Galán, J.E., 2013. A Salmonella Typhi homologue of bacteriophage muramidases controls typhoid toxin secretion. *EMBO reports*, 14(1), pp.95–102.

Huang, L. et al., 2015. Ductal pancreatic cancer modeling and drug screening using human pluripotent stem cell– and patient-derived tumor organoids. *Nature Medicine*, 21(11), pp.1364–1371.

Huch, M. et al., 2015. Article Long-Term Culture of Genome-Stable Bipotent Stem Cells from Adult Human Liver. *Cell*, 160(1–2), pp.299–312.

Huch, M., Dorrell, C., et al., 2013. In vitro expansion of single Lgr5+ liver stem cells induced by Wnt-driven regeneration. *Nature*, 494(7436), pp.247–50.

Huch, M., Boj, S.F. & Clevers, H., 2013. Lgr5(+) liver stem cells, hepatic organoids and regenerative medicine. *Regenerative medicine*, 8(4), pp.385–7.

Imamura, H. et al., A Modified Method for Purifying Gallbladder Epithelial Cells Using Fluorescence-activated Cell Sorting. *In vivo (Athens, Greece)*, 31(2), pp.169–173.

Inoue, H., Nojima, H. & Okayama, H., 1990. High efficiency transformation of Escherichia coli with plasmids. *Gene*, 96(1), pp.23–8.

Jepson, M.A. & Clark, M.A., 2001. The role of M cells in Salmonella infection. *Microbes and infection*, 3(14–15), pp.1183–90.

Jho, E. et al., 2002. Wnt/beta-catenin/Tcf signaling induces the transcription of Axin2, a negative regulator of the signaling pathway. *Molecular and cellular biology*, 22(4), pp.1172–83.

Jinadasa, R.N. et al., 2011. Cytolethal distending toxin: a conserved bacterial genotoxin that blocks cell cycle progression, leading to apoptosis of a broad range of mammalian cell lineages. *Microbiology (Reading, England)*, 157(Pt 7), pp.1851–75.

Johnson, W.M. & Lior, H., 1988a. A new heat-labile cytolethal distending toxin (CLDT) produced by Campylobacter spp. *Microbial pathogenesis*, 4(2), pp.115–26.

Johnson, W.M. & Lior, H., 1988b. A new heat-labile cytolethal distending toxin (CLDT) produced by Escherichia coli isolates from clinical material. *Microbial pathogenesis*, 4(2), pp.103–13.

Johnson, W.M. & Lior, H., 1987. Production of Shiga toxin and a cytolethal distending toxin (CLDT) by serogroups of *Shigella* spp. *FEMS Microbiology Letters*, 48(1–2), pp.235–238.

Jones, J.C.R., 2008. Reduction of contamination of epithelial cultures by fibroblasts. *CSH protocols*, 2008, p.pdb.prot4478.

Jones, R.M. et al., 2008. Salmonella AvrA Coordinates Suppression of Host Immune and Apoptotic Defenses via JNK Pathway Blockade. *Cell host & microbe*, 3(4), pp.233–44.

Jung, P. et al., 2011. Isolation and in vitro expansion of human colonic stem cells. *Nature Medicine*, 17(10), pp.1225–1227.

Kabiri, Z. et al., 2014. Stroma provides an intestinal stem cell niche in the absence of epithelial Wnts. *Development*, 141(11), pp.2206–2215.

Kampf, C. et al., 2014. Defining the human gallbladder proteome by transcriptomics and affinity proteomics. *Proteomics*, 14(21–22), pp.2498–2507.

Kanthan, R. et al., 2015. Gallbladder Cancer in the 21st Century. *Journal of oncology*, 2015, p.967472.

Keestra-Gounder, A.M., Tsolis, R.M. & Bäumler, A.J., 2015. Now you see me, now you don't: the interaction of Salmonella with innate immune receptors. *Nature Reviews Microbiology*, 13(4), pp.206–216.

Kessler, M. et al., 2015. The Notch and Wnt pathways regulate stemness and differentiation in human fallopian tube organoids. *Nature communications*, 6, p.8989.

Kimura, K. et al., 1985. Association of gallbladder carcinoma and anomalous pancreaticobiliary ductal union. *Gastroenterology*, 89(6), pp.1258–65.

van Klinken, B.J. et al., 1998. MUC5B is the prominent mucin in human gallbladder and is also expressed in a subset of colonic goblet cells. *The American journal of physiology*, 274(5 Pt 1), pp.G871-8.

Knodler, L.A. et al., 2010. Dissemination of invasive Salmonella via bacterial-induced extrusion of mucosal epithelia. *Proceedings of the National Academy of Sciences of the United States of America*, 107(41), pp.17733–8.

Knodler, L.A., Finlay, B.B. & Steele-Mortimer, O., 2005. The Salmonella Effector Protein SopB Protects Epithelial Cells from Apoptosis by Sustained Activation of Akt. *Journal of Biological Chemistry*, 280(10), pp.9058–9064.

Koch, S., 2017. Extrinsic control of Wnt signaling in the intestine. *Differentiation*, 97, pp.1–8.

Koeppel, M. et al., 2015. Helicobacter pylori Infection Causes Characteristic DNA Damage Patterns in Human Cells. *Cell reports*, 11(11), pp.1703–13.

Koshiol, J. et al., 2016. *Salmonella enterica* serovar Typhi and gallbladder cancer: a case-control study and meta-analysis. *Cancer Medicine*, 5(11), pp.3310–3235.

Koyama, S. et al., 1980. Establishment of a cell line (G-415) from a human gallbladder carcinoma. *Gan*, 71(4), pp.574–5.

Ku, A.T., Miao, Q. & Nguyen, H., 2016. Monitoring Wnt/β-Catenin Signaling in Skin. *Methods in molecular biology (Clifton, N.J.)*, 1481, pp.127–40.

Kuhle, V., Abrahams, G.L. & Hensel, M., 2006. Intracellular Salmonella enterica Redirect Exocytic Transport Processes in a Salmonella Pathogenicity Island 2-Dependent Manner. *Traffic*, 7(6), pp.716–730.

Kumar, A. et al., 2014. Proteomics-based identification of plasma proteins and their association

with the host–pathogen interaction in chronic typhoid carriers. *International Journal of Infectious Diseases*, 19, pp.59–66.

Kurita, A. et al., 2003. *Intracellular expression of the Salmonella plasmid virulence protein, SpvB, causes apoptotic cell death in eukaryotic cells*,

Kuver, R. et al., 1997. Isolation and long-term culture of gallbladder epithelial cells from wild-type and CF mice. *In Vitro Cellular & Developmental Biology - Animal*, 33(2), pp.104–109.

Kuver, R. et al., 2007. Murine gallbladder epithelial cells can differentiate into hepatocyte-like cells in vitro. *American journal of physiology. Gastrointestinal and liver physiology*, 293(5), pp.G944–G955.

Lara-Tejero, M. & Galán, J.E., 2000. A bacterial toxin that controls cell cycle progression as a deoxyribonuclease I-like protein. *Science (New York, N.Y.)*, 290(5490), pp.354–7.

de Lau, W.B.M., Snel, B. & Clevers, H.C., 2012. The R-spondin protein family. *Genome biology*, 13(3), p.242.

Lazcano-Ponce, E.C. et al., 2001. Epidemiology and molecular pathology of gallbladder cancer. *CA: a cancer journal for clinicians*, 51(6), pp.349–64.

Leslie, J.L. et al., 2015. Persistence and toxin production by Clostridium difficile within human intestinal organoids result in disruption of epithelial paracellular barrier function. *Infection and immunity*, 83(1), pp.138–45.

Li, V.S.W. et al., 2012. Wnt Signaling through Inhibition of β-Catenin Degradation in an Intact Axin1 Complex. *Cell*, 149(6), pp.1245–1256.

Liu, F. et al., 2016. Drug Discovery via Human-Derived Stem Cell Organoids. *Frontiers in pharmacology*, 7, p.334.

Lowenfels, A.B. & Maisonneuve, P., 1999. Pancreatico-biliary malignancy: prevalence and risk factors. *Annals of oncology : official journal of the European Society for Medical Oncology*, 10 Suppl 4, pp.1–3.

Lugli, N. et al., 2016. R-spondin 1 and noggin facilitate expansion of resident stem cells from non-

damaged gallbladders. *EMBO reports*.

Lukovac, S. et al., 2014. Differential modulation by Akkermansia muciniphila and Faecalibacterium prausnitzii of host peripheral lipid metabolism and histone acetylation in mouse gut organoids. *mBio*, 5(4), pp.e01438-14.

MacDonald, B.T., Tamai, K. & He, X., 2009. Wnt/beta-catenin signaling: components, mechanisms, and diseases. *Developmental cell*, 17(1), pp.9–26.

Maiti, S. et al., 2014. Effective Control of Salmonella Infections by Employing Combinations of Recombinant Antimicrobial Human -Defensins hBD-1 and hBD-2. *Antimicrobial Agents and Chemotherapy*, 58(11), pp.6896–6903.

Mallon, B.S. et al., 2013. StemCellDB: the human pluripotent stem cell database at the National Institutes of Health. *Stem cell research*, 10(1), pp.57–66.

Manohar, R. et al., 2015. Identification of a candidate stem cell in human gallbladder. *Stem Cell Research*, 14(3), pp.258–269.

Marx, V., 2014. Cell-line authentication demystified. *Nature Methods*, 11(5), pp.483–488.

Matano, M. et al., 2015. Modeling colorectal cancer using CRISPR-Cas9–mediated engineering of human intestinal organoids. *Nature Medicine*, 21(3), pp.256–262.

Matsukura, N. et al., 2002. Association between Helicobacter bilis in bile and biliary tract malignancies: H. bilis in bile from Japanese and Thai patients with benign and malignant diseases in the biliary tract. *Japanese journal of cancer research : Gann*, 93(7), pp.842–7.

May, R. et al., 2009. Doublecortin and CaM Kinase-like-1 and Leucine-Rich-Repeat-Containing G-Protein-Coupled Receptor Mark Quiescent and Cycling Intestinal Stem Cells, Respectively. *Stem Cells*, 27(10), pp.2571–2579.

Mellemgaard, A. & Gaarslev, K., 1988. Risk of hepatobiliary cancer in carriers of Salmonella typhi. *Journal of the National Cancer Institute*, 80(4), p.288.

Méresse, S. et al., 2001. Remodelling of the actin cytoskeleton is essential for replication of intravacuolar Salmonella. *Cellular microbiology*, 3(8), pp.567–77.

Miller, R. & Wiedmann, M., 2016. Dynamic Duo—The Salmonella Cytolethal Distending Toxin Combines ADP-Ribosyltransferase and Nuclease Activities in a Novel Form of the Cytolethal Distending Toxin. *Toxins*, 8(5), p.121.

Mitra, A., Mishra, L. & Li, S., 2013. Technologies for deriving primary tumor cells for use in personalized cancer therapy. *Trends in biotechnology*, 31(6), pp.347–54.

Miyoshi, H. & Stappenbeck, T.S., 2013. In vitro expansion and genetic modification of gastrointestinal stem cells in spheroid culture. *Nature protocols*, 8(12), pp.2471–82.

Müller, M. & Jansen, P.L., 1997. Molecular aspects of hepatobiliary transport. *The American journal of physiology*, 272(6 Pt 1), pp.G1285-303.

Murata, H. et al., 2004. Helicobacter bilis infection in biliary tract cancer. *Alimentary Pharmacology and Therapeutics*, 20(s1), pp.90–94.

Nagaraja, V. & Eslick, G.D., 2014. Systematic review with meta-analysis: The relationship between chronic Salmonella typhi carrier status and gall-bladder cancer. *Alimentary Pharmacology and Therapeutics*, 39(8), pp.745–750.

Nakanishi, Y. et al., 2012. Dclk1 distinguishes between tumor and normal stem cells in the intestine. *Nature Genetics*, 45(1), pp.98–103.

Nakanuma, Y. et al., 1997. Monolayer and three-dimensional cell culture and living tissue culture of gallbladder epithelium. *Microscopy Research and Technique*, 39(1), pp.71–84.

Nath, G. et al., 2011. Isolation of Salmonella typhi from apparently healthy liver. *Infection, Genetics and Evolution*, 11(8), pp.2103–2105.

Németh, Z. et al., 2009. Claudin-1, -2, -3, -4, -7, -8, and -10 protein expression in biliary tract cancers. *The journal of histochemistry and cytochemistry : official journal of the Histochemistry Society*, 57(2), pp.113–121.

Oda, D., Lee, S.P. & Hayashi, A., 1991. Long-term culture and partial characterization of dog gallbladder epithelial cells. *Laboratory investigation; a journal of technical methods and pathology*, 64(5), pp.682–92.

Pak, M. & Lindseth, G., 2016. Risk Factors for Cholelithiasis. *Gastroenterology Nursing*, 39(4), pp.297–309.

Parry, C.M. et al., 2002. Typhoid Fever. *New England Journal of Medicine*, 347(22), pp.1770–1782.

Petersen, C.P. & Reddien, P.W., 2009. Wnt Signaling and the Polarity of the Primary Body Axis. *Cell*, 139(6), pp.1056–1068.

Pilgrim, C.H.C. et al., 2013. Modern perspectives on factors predisposing to the development of gallbladder cancer. *HPB*, 15(11), pp.839–844.

Plevris, J.N. et al., 1993. Primary culture of bovine gall bladder epithelial cells. *Gut*, 34(11), pp.1612–1615.

Pradhan, S.B. & Dali, S., 2004. Relation between gallbladder neoplasm and Helicobacter hepaticus infection. *Kathmandu University medical journal (KUMJ)*, 2(4), pp.331–5.

Pratt, J.S. et al., 2006. Modulation of host immune responses by the cytolethal distending toxin of Helicobacter hepaticus. *Infection and Immunity*, 74(8), pp.4496–4504.

Pstrpw, J.D., 1967. Absorption of bile pigments by the gall bladder. *The Journal of clinical investigation*, 46(12), pp.2035–52.

Rabin, S.D.P., Flitton, J.G. & Demuth, D.R., 2009. Aggregatibacter actinomycetemcomitans cytolethal distending toxin induces apoptosis in nonproliferating macrophages by a phosphatase-independent mechanism. *Infection and immunity*, 77(8), pp.3161–9.

Ramos-Morales, F., 2012. Impact of Salmonella enterica Type III Secretion System Effectors on the Eukaryotic Host Cell. *ISRN Cell Biology*, 2012, pp.1–36.

Ramsden, A.E., Mota, L.J., et al., 2007. The SPI-2 type III secretion system restricts motility of Salmonella-containing vacuoles. *Cellular microbiology*, 9(10), pp.2517–29.

Ramsden, A.E., Holden, D.W. & Mota, L.J., 2007. Membrane dynamics and spatial distribution of Salmonella-containing vacuoles. *Trends in microbiology*, 15(11), pp.516–24.

Randi, G., Franceschi, S. & La Vecchia, C., 2006. Gallbladder cancer worldwide: Geographical

distribution and risk factors. *International Journal of Cancer*, 118(7), pp.1591–1602.

Ritchie, M.E. et al., 2015. limma powers differential expression analyses for RNA-sequencing and microarray studies. *Nucleic Acids Research*, 43(7), pp.e47–e47.

Roper, J. et al., 2017. In vivo genome editing and organoid transplantation models of colorectal cancer and metastasis. *Nature Biotechnology*, 35(6), pp.569–576.

Roppenser, B. et al., 2013. Multiple Host Kinases Contribute to Akt Activation during Salmonella Infection. *PLoS ONE*, 8(8), pp.1–10.

Roumagnac, P. et al., 2006. Evolutionary History of Salmonella Typhi. *Science*, 314(5803).

Ruiz-Albert, J. et al., 2002. Complementary activities of SseJ and SifA regulate dynamics of the Salmonella typhimurium vacuolar membrane. *Molecular microbiology*, 44(3), pp.645–61.

Ryu, S. et al., 2016. Gallstones and the Risk of Gallbladder Cancer Mortality: A Cohort Study. *The American journal of gastroenterology*.

Saito, Y., Kojima, T. & Takahashi, N., 2013. The septum transversum mesenchyme induces gall bladder development. *Biology open*, 2(8), pp.779–88.

Salzman, N.H. et al., 2003. Protection against enteric salmonellosis in transgenic mice expressing a human intestinal defensin. *Nature*, 422(6931), pp.522–526.

Sato, T., Stange, D.E., et al., 2011. Long-term expansion of epithelial organoids from human colon, adenoma, adenocarcinoma, and Barrett's epithelium. *Gastroenterology*, 141(5), pp.1762–1772.

Sato, T., van Es, J.H., et al., 2011. Paneth cells constitute the niche for Lgr5 stem cells in intestinal crypts. *Nature*, 469(7330), pp.415–418.

Sato, T. & Clevers, H., 2013. Growing self-organizing mini-guts from a single intestinal stem cell: mechanism and applications. *Science (New York, N.Y.)*, 340(6137), pp.1190–4.

Saul, A. et al., 2013. Stochastic Simulation of Endemic Salmonella enterica Serovar Typhi: The Importance of Long Lasting Immunity and the Carrier State C. V. Rao, ed. *PLoS ONE*, 8(9),

p.e74097.

Scanu, T. et al., 2015. Salmonella Manipulation of Host Signaling Pathways Provokes Cellular Transformation Associated with Gallbladder Carcinoma. *Cell host & microbe*, 17(6), pp.763–74.

Schepers, A. & Clevers, H., 2012. Wnt signaling, stem cells, and cancer of the gastrointestinal tract. *Cold Spring Harbor perspectives in biology*, 4(4), p.a007989.

Schlaermann, P. et al., 2014. A novel human gastric primary cell culture system for modelling Helicobacter pylori infection in vitro. *Gut*.

Schuijers, J. & Clevers, H., 2012. Adult mammalian stem cells: the role of Wnt, Lgr5 and R-spondins. *The EMBO Journal*, 31(13), pp.3031–3032.

Scoazec, J.Y. et al., 1997. The plasma membrane polarity of human biliary epithelial cells: in situ immunohistochemical analysis and functional implications. *Journal of hepatology*, 26(3), pp.543–53.

Sergushichev, A., 2016. An algorithm for fast preranked gene set enrichment analysis using cumulative statistic calculation. *bioRxiv*.

Shah, C., Hari-Dass, R. & Raynes, J.G., 2006. Serum amyloid A is an innate immune opsonin for Gram-negative bacteria. *Blood*, 108(5), pp.1751–1757.

Sharp, J.C.M., 1967. Typhoid Fever—30 Years On. *British Medical Journal*, 3(5559), p.240.

Shenker, B.J. et al., 2004. Actinobacillus actinomycetemcomitans cytolethal distending toxin (Cdt): evidence that the holotoxin is composed of three subunits: CdtA, CdtB, and CdtC. *Journal of immunology (Baltimore, Md. : 1950)*, 172(1), pp.410–417.

Shimoyama, T. et al., 2010. Serological analysis of Helicobacter hepaticus infection in patients with biliary and pancreatic diseases. *Journal of Gastroenterology and Hepatology*, 25, pp.S86–S89.

Skardal, A., Shupe, T. & Atala, A., 2016. Organoid-on-a-chip and body-on-a-chip systems for drug screening and disease modeling. *Drug Discovery Today*, 21(9), pp.1399–1411.

Smith, J.L. & Bayles, D.O., 2006. The Contribution of Cytolethal Distending Toxin to Bacterial Pathogenesis. *Critical Reviews in Microbiology*, 32(4), pp.227–248.

Song, J. et al., 2010. A Mouse Model for the Human Pathogen Salmonella Typhi. *Cell Host & Microbe*, 8(4), pp.369–376.

Song, J., Gao, X. & Galán, J.E., 2013. Structure and function of the Salmonella Typhi chimaeric A(2)B(5) typhoid toxin. *Nature*, 499(7458), pp.350–4.

Spanò, S. & Galán, J.E., 2008. A novel pathway for exotoxin delivery by an intracellular pathogen. *Current opinion in microbiology*, 11(1), pp.15–20.

Spanò, S., Ugalde, J.E. & Galán, J.E., 2008. Delivery of a Salmonella Typhi Exotoxin from a Host Intracellular Compartment. *Cell Host and Microbe*, 3(1), pp.30–38.

Steele-Mortimer, O. et al., 2000. Activation of Akt/Protein Kinase B in Epithelial Cells by the Salmonella typhimurium Effector SigD. *Journal of Biological Chemistry*, 275(48), pp.37718–37724.

Steele-Mortimer, O. et al., 1999. Biogenesis of Salmonella typhimurium-containing vacuoles in epithelial cells involves interactions with the early endocytic pathway. *Cellular microbiology*, 1(1), pp.33–49.

Steele-Mortimer, O., 2008. The Salmonella-containing vacuole: moving with the times. *Current opinion in microbiology*, 11(1), pp.38–45.

Stinton, L.M. & Shaffer, E.A., 2012. Epidemiology of gallbladder disease: cholelithiasis and cancer. *Gut and liver*, 6(2), pp.172–87.

Strom, B.L. et al., 1995. Risk factors for gallbladder cancer. An international collaborative case-control study. *Cancer*, 76(10), pp.1747–56.

Suez, J. et al., 2013. Virulence Gene Profiling and Pathogenicity Characterization of Non-Typhoidal Salmonella Accounted for Invasive Disease in Humans J. A. Chabalgoity, ed. *PLoS ONE*, 8(3), p.e58449.

Tan, S. & Barker, N., 2014. Epithelial stem cells and intestinal cancer. *Seminars in Cancer Biology*.

Tan, W. et al., 2015. Body Mass Index and Risk of Gallbladder Cancer: Systematic Review and Meta-Analysis of Observational Studies. *Nutrients*, 7(10), pp.8321–34.

Tanimizu, N., Miyajima, A. & Mostov, K.E., 2007. Liver progenitor cells develop cholangiocyte-type epithelial polarity in three-dimensional culture. *Molecular biology of the cell*, 18(4), pp.1472–9.

Terebiznik, M.R. et al., 2002. Elimination of host cell PtdIns(4,5)P2 by bacterial SigD promotes membrane fission during invasion by Salmonella. *Nature Cell Biology*, 4(10), pp.766–773.

Thompson, L.J. et al., 2009. Transcriptional response in the peripheral blood of patients infected with Salmonella enterica serovar Typhi. *Proceedings of the National Academy of Sciences*, 106(52), pp.22433–22438.

Turinetto, V. & Giachino, C., 2015. Multiple facets of histone variant H2AX: a DNA double-strand-break marker with several biological functions. *Nucleic acids research*, 43(5), pp.2489–98.

Uemura, M. et al., 2010. Expression and function of mouse Sox17 gene in the specification of gallbladder/bile-duct progenitors during early foregut morphogenesis. *Biochemical and Biophysical Research Communications*, 391(1), pp.357–363.

Vijay-Kumar, M. et al., 2006. Flagellin suppresses epithelial apoptosis and limits disease during enteric infection. *The American journal of pathology*, 169(5), pp.1686–700.

Ward, J.M. et al., 1994. Chronic active hepatitis and associated liver tumors in mice caused by a persistent bacterial infection with a novel Helicobacter species. *Journal of the National Cancer Institute*, 86(16), pp.1222–7.

Watson, C.L. et al., 2014. An in vivo model of human small intestine using pluripotent stem cells. *Nature Medicine*, 20(11), pp.1310–1314.

Welton, J.C., Marr, J.S. & Friedman, S.M., 1979. Association between hepatobiliary cancer and typhoid carrier state. *Lancet (London, England)*, 1(8120), pp.791–4.

Wilson, R.P. et al., 2008. The Vi-capsule prevents Toll-like receptor 4 recognition of Salmonella. *Cellular Microbiology*, 10(4), pp.876–890.

Wilson, S.S. et al., 2014. A small intestinal organoid model of non-invasive enteric pathogen-epithelial cell interactions. *Mucosal immunology*, 8(August), pp.1–10.

Wistuba, I.I. & Gazdar, A.F., 2004. Gallbladder cancer: lessons from a rare tumour. *Nature reviews. Cancer*, 4(9), pp.695–706.

Wood, J.R. & Svanvik, J., 1983. Gall-bladder water and electrolyte transport and its regulation. *Gut*, 24(6), pp.579–93.

Woods, C.W. et al., 2006. Emergence of Salmonella enterica serotype Paratyphi A as a major cause of enteric fever in Kathmandu, Nepal. *Transactions of the Royal Society of Tropical Medicine and Hygiene*, 100(11), pp.1063–1067.

Wu, H., Jones, R.M. & Neish, A.S., 2012. The Salmonella effector AvrA mediates bacterial intracellular survival during infection in vivo. *Cellular microbiology*, 14(1), pp.28–39.

Yin, X. et al., 2016. Engineering Stem Cell Organoids. *Cell Stem Cell*, 18(1), pp.25–38.

Yui, S. et al., 2012. Functional engraftment of colon epithelium expanded in vitro from a single adult Lgr5+ stem cell. *Nature Medicine*, 18(4), pp.618–623.

Zatonskí, W. et al., 1993. Descriptive epidemiology of gall-bladder cancer in Europe. *Journal of cancer research and clinical oncology*, 119(3), pp.165–71.

Zhang, Y.-G. et al., 2014. Salmonella-infected crypt-derived intestinal organoid culture system for host-bacterial interactions. *Physiological Reports*, 2(9), pp.e12147–e12147.

Zhou, D. et al., 2013. Infections of Helicobacter spp. in the biliary system are associated with biliary tract cancer. *European Journal of Gastroenterology & Hepatology*, 25(4), pp.447–454.

Zhu, A.X. et al., 2010. Current management of gallbladder carcinoma. *The oncologist*, 15(2), pp.168–81.

7. APPENDIX

7.1 List of figures

Introduction:

Results:

Discussion:

7.2 List of abbreviations

2D	2 dimension
3D	3 dimension
ADF	Advanced DMEM/Ham´s F12
APS	Ammonium persulfate
Amp	Ampicillin
BB	Brucella Broth
BHI	Brain Hearth infusion
b-cat	β-catenin
Cam	Chloramphenicol
Cat.	Catalogue number
CDT	Cytolehtal distending toxin
CdtA	Cytolehtal distending toxin subunit A
CdtB	Cytolehtal distending toxin subunit B
CdtC	Cytolehtal distending toxin subunit C
cfu	Colony forming units
Cla-2	Claudin-2
CK-19	Cytokeratin-19
DMEM	Dulbecco´s modified Eagle medium
DNA	deoxyribonucleic acid
dpi	Days post infection
dNTP	deoxynucleotide
e.g.	*Exempli gratia*, For example
Ecad	E-cadherin
ECL	Enhanced chemiluminescence
EGF	human epidermal growth factor
EGTA	ethylene glycol tetra acetic acid
ERT2	Mutated estrogen receptor, sensitive to HT (variant 2)
ES	Enrichment score
et al.	*et alia*, and others
FCS	Fetal calf serum
FGF	human fibroblast growth factor-10
Fig.	Figure
FITC	Fluorescein Isothiocyanate
FSK	Forskolin
GB	Gall bladder
GBC	Gall bladder cancer
GFP	Green fluorescent protein
h	hour
H_20	Double distilled water, if not stated otherwise
HGF	human hepatocyte growth factor
(HGNC	Hugo Gene Nomenclature Committee
Hh	*Helicobacter hepaticus*
hpi	Hours post infection
HRP	*Horseradish Peroxidase*
HT	4-Hydroxytamoxifen
i.e.	*id est*, that is
IFF	2D immunofluorescence buffer
IL	Interleukin, followed by a ndash and a number
IRES	Internal ribosome entry site

ITB	Inoue transformation buffer
Kan	Kanamycin
LB	Luria-Bertani medium
Lgr5	Leucine-rich repeat-containing G-protein coupled receptor 5
LPS	lipopolysaccharide
log	logarithmic
mCherry	Membrane cherry
mEGF	Murine epidermal growth factor
min	minutes
MM5.8	*Salmonella* minimal medium pH5.8
MOI	Multiplicity of infection
MPS	Max Planck Society
MUC5B	Mucin 5B
NES	Normalized enrichment score
NIC	Nicotinamide
no.	number
NOX1	NADPH Oxidase 1
NTS	non-typhoidal salmonellae
ON	Overnight
P/S	Penicillin/Streptomycin
PAMPs	pathogen associated molecular patterns
PFA	Paraformaldehyde
PIPES	piperazine-1,2-bis[2-ethanesulfonic acid]
PVDF	Polyvinylidene difluoride
pltA	Pertussis like toxin subunit A
pltB	Pertussis like toxin subunit B
R	Resistance, when put after an antibiotic
ROCK	Rho-associated protein kinase
RNS	Reactive nitrogen species
ROS	Reactive oxigen species
Rspo	R-spondin 1
RT	Room temperature
SCV	*Salmonella* containing vacuoles
SDS	sodium dodecyl sulphate
SDS-PAGE	SDS-polyacrylamide gel electrophoresis
SOB	Super optimal broth
SPA	Salmonella Paratyphi A
SPI-I	Salmonella pathogenicity island 1
SPI-II	Salmonella pathogenicity island 1
T3SS	type III secretion system
TBS	*Tris-buffered saline*
TBS-T	*Tris-buffered saline* 0.1% Tween 20
TLR	*Toll-like receptor*
Tm	*Melting temperature*
w.t.	Wild type

7.3 Curriculum vitae

For reasons of data protection, the curriculum vitae is not published in the electronic version

7.4 Acknowledgements

First I would like to thank Prof. Thomas Meyer for letting me work on such an exciting - although highly competitive - topic, and for his constant supervision. I especially appreciated our weekly meetings! I would also like to thank Prof. Lothar Wieler and Prof. Anton Aebischer for the discussion and the scientific advices that they gave me during my committee meetings. I am really sorry that you cannot be my supervisors anymore. A big thank to Prof. Rudolf Tauber that agreed to become my faculty supervisor on such a short notice. I am looking forward to discussing with you this thesis.

Paying the rent and being able to afford healthy food is as important as good scientific practice, therefore I shall acknowledge the GRK 1673 / BRIDGE study program and the MPS for financing this project.

I would like to thank Dr. Sascha Chopra and Dr. Sven Schmidt for providing the human material, and Kirstin Hoffmann for providing the murine gall bladders with such an unbelievable efficiency.

The microarrays were kindly ran by our core facility in a blink of an eye, thank you Dr. Hans Mollenkopf! I should also heartily thank Dr. Hilmar Berger for the microarray analyses and for his patience with my continuous questions.

The very last figure was created by Diane Schad. I really appreciated it, thank you!

Thanks also to Veronika Meier, for all the help with the many bureaucratic issues.

However, beside the scientific and technical assistance, I would not have reached the end of the doctoral project without the help of my coworkers. I cannot stress enough how crucial their support was in the darkest hours of this research. The first that I should mention is Francesco Boccellato, thank you for the long scientific discussions, for being always so positive and supportive, and mostly for the friendship beyond the lab. Thanks to Amina Iftekhar (I will miss our lunch breaks!), Piotr Zadora (let´s go for skiing!), Ana Costa (never stop the struggle!), Maria del Mar Reines (thanks for always caring about us, tiny phd students!), Kristin Fritsche (it was a pleasure sharing the office with you!), Pau Morey (✊), Konstantin Okonechnikov (our beloved Russian bioinformatics bear), Friderike Weege (it´s going to be fine!).

A special thanks to my parents and to my girlfriend, Giulia, for their unconditional support and for diverting my attention after a failed experiment.

7.5 Selbstständigkeitserklärung

Hiermit erkläre ich, dass ich die vorliegende Arbeit selbstständig und nur mit den angegebenen Hilfsmitteln erstellt habe.

Berlin, den _____ _____

Ludovico Sepe